5TH ARGA CONFERENCE

Australian Regolith Geoscientists Association

PROCEEDINGS

Editors: Carmen Krapf, John Keeling, Anna Petts

Australian Regolith Geoscientists Association

Fifth Australian Regolith Geoscientists Association Conference

---

Conference Proceedings

Wallaroo, SA
8-11th April 2018

Editors: Carmen Krapf, John Keeling, Anna Petts

Contents

Page number

About ARGA.....ii

How to join ARGA.....ii

What is regolith?.....iii

2018 conference program.....iv

Oral presentation abstracts 1

Poster presentation abstracts.....59

Authors list.....65

This publication is available online at: http://regolith.org.au/publications.html

Cover image credits: Carmen Krapf

Australian Regolith Geoscientists Association

About ARGA

The Australian Regolith Geoscientists Association Inc. (ARGA) is a not-for-profit learned association of regolith practitioners throughout Australia. The Association was set up to provide a mechanism through which people interested in regolith science could keep in touch and share their experiences via newsletters, email, the internet and an annual conference.

The objects of the association are to further the study of regolith geoscience and allied disciplines by:

- Facilitating the exchange of information among members of the association, and, in general, all those interested in regolith science;
- Stimulating interest in regolith geoscience;
- Encouraging the practical applications of regolith geoscience research.

How to join ARGA

All those having an interest in the objectives of the Association are eligible to become members. All who have attended a Biennial Conference of the Association become members for the next four years. Alternatively, you can join the Society by contacting the Secretary, explaining your interest and paying $1 per year.

ARGA 2016-2018 Committee

President: Leah Moore
Past President: Vanessa Wong
Secretary: Andrew McPherson, Carmen Krapf
Treasurer: John Keeling
Conference Organiser: Carmen Krapf
Student Representative: Margie Sweeney
Ian Roach (website manager)
Nadir De Souza Kovacs
Stephanie McLennan

Website: http://regolith.org.au

Panorama of the current quarry face at Clinton Quarry (Yorke Peninsula, SA) exposing fluvial palaeochannel deposits overlain by mottles Melton Limestone, separated by a distinctive thin clay layer.

Regolith is "the entire unconsolidated or secondarily recemented cover that overlies coherent bedrock, that has been formed by weathering, erosion, transport and/or deposition of older material. The regolith thus includes fractured and weathered basement rocks, saprolites, soils, organic accumulations, volcanic material, glacial deposits, colluvium, alluvium, evaporitic sediments, aeolian deposits and groundwater" (Eggleton 2001*).

Or, regolith is everything between fresh rock and fresh air!

**Eggleton R.A. ed. 2001. The Regolith Glossary: surficial geology, soils and landscapes. Cooperative Research Centre for Landscape Environments and Mineral Exploration (CRC LEME).*

ARGA 2018 Program

Sunday 8th April 2018: Pre-conference Field Trip
Clare Valley Rocks – the earth beneath our vines Field trip leaders: Mick Roche (Stewardship Matters) and Mario Werner (GSSA) Departure: **8.00 am** Adelaide Hindmarsh Square in front of Mantra Hotel Arrival: approx. **5.30 pm** Wallaroo **7 pm – 9 pm: Icebreaker** at KEG Room, Coopers Alehouse, Wallaroo

Monday 9th April: Conference (KEG Room, Coopers Alehouse, Wallaroo)			
9 am	**Registration**		
Chair: Carmen Krapf			
9.10	Carmen Krapf	Welcome and opening	Page
9.15	**Keynote:** Ignacio González-Álvarez	Insights on the paradigms applied for mineral exploration in deeply weathered landscapes	1
10.00	Caroline Tiddy	Geochemical sampling of cover sequence materials throughout the Gawler Craton	5
10.20	Ken McQueen	Cretes and 'chemical' landscapes, South Australia	7
10.40 am	**Morning tea**		
Chair: Nadir de Souza Kovacs			
11.10	Anna Petts	Covering the bases - baseline geochemistry of South Australian's cover and new efforts to characterise it	12
11.30	Adrian Fabris	Could rapid XRF analysis techniques provide a step change in our ability to map geochemical dispersion patterns through cover and deliver future mineral discoveries?	15
11.50	Ian Roach	Correlations between spectral mineralogy and borehole rock properties in the Eromanga basin	16
12.10	Sara Jakica	Using passive seismic to estimate the thickness of Leonora Breakaways, WA	17
12.30 pm	**Lunch**		

Chair: Lisa Worrall			
1.30	Leah Moore	Evaluating geomorphic and subsurface controls on surface water-groundwater interactions to contextualize a floodplain rehydration project at Mulloon Creek, NSW Southern Tablelands	21
1.50	Alie Cowood	The influence of regolith configuration on hydrology and hydrogeology in the Ginini Flats Ramsar Wetland Complex, Namadgi National Park, ACT	21
2.10	Mark Keppel	Modelling initial carbonate platform formation in groundwater upwelling zones, Lake Eyre south region, South Australia	22
2.30	Poster session	Poster session with short talks	59
3.00 pm	**Afternoon Tea**		
Chair: John Keeling			
3.20	Brad Pillans	Seeing red: a history of redness in Australian landscapes	23
3.40	Nadir de Souza Kovacs	Beneath the sand of the Tanami Desert	27
4.00	Richard Greene	Loess materials in vineyard soils in Australia and New Zealand: how their properties can influence wine composition	31
4.20	Carmen Krapf	The complex story of regolith material distribution along the Skeleton Coast of Namibia	35
4.40	Caroline Tiddy & Ignacio González-Álvarez	GSA info	
5.00 pm	Day 1 close		

Tuesday 10th April: Mid-Conference Field Trip and Conference Dinner

Some aspects of the geology and regolith of the northern Yorke Peninsula

Field trip leaders: Gus Harvey, Carmen Krapf, John Keeling (all GSSA)
Departure: **8.00 am** Cooper's Alehouse, Wallaroo. Bring hat, raincoat, backpack, camera, etc.
4.00 pm afternoon winery tour and tasting at Barley Stack Winery
Arrival: approx. **5.45 pm** Wallaroo

7.00 pm CONFERENCE DINNER @ dining room Cooper's Alehouse, Wallaroo

- with short talks about CRCLEME1, CRCLEME2 and ARGA – re-living the past!

Wednesday 11th April: KEG room, Cooper's Alehouse, Wallaroo			
Chair: Anna Petts			
9.00 am	**Welcome to Day 3**		
9.15	**Keynote:** Allan Chivas	Oxygen isotope dating the Australian regolith	37
10.00	Tony Eggleton	Mineralogy modifies Snowy Mountains too	39
10.20	John Keeling	Atypical alteration of biotite to celadonite and nontronite, southern Eyre Peninsula: timing and environmental factors	43
10.40 am	**Morning Tea**		
Chair: Brad Pillans			
11.10	Lisa Worrall	Are critical zone observatories materially advancing regolith science?	47
11.30	Sabine Pernreiter	Landscape evolution in the Albany-Fraser Orogen and South Yilgarn Craton, Western Australia	48
11.50	Savannah McGuirk	Sand dunes of the Northern Himalaya	52
12.10	Ian Roach	Cover and UNCOVER: an update on Geoscience Australia's work on regolith and under-cover mapping	56
12.30 pm	**Lunch**		
Chair: Ian Roach			
1.30	Awards	Student Prize Presentation: Keith Scott Memorial Award Best Presentation: GA book prize	
1.35	AGM	Board elections Welcome to new ARGA board Vote on future direction of ARGA	
3.30 pm	Day 3 close	End of proceedings	
4.00 pm Guided Heritage Tour through Wallaroo (approx. 1 hour)			

Thursday 12th April: POST-Conference Field Trip
Roll fronts, calcrete and limestones – more geology and regolith of the northern Yorke Peninsula Field trip leader: Steve Hill (GSSA) Departure: **8.00 am** Cooper's Alehouse, Wallaroo. Bring hat, raincoat, backpack, camera, etc. Arrival: **approx. 5.00 pm** Adelaide Hindmarsh Square in front of Mantra Hotel (potential drop of at airport could be arranged)

Insights on the paradigms applied for mineral exploration in deeply weathered landscapes

I . González-Álvarez[1,2], A.R. King[1], J. Klump[1], G. Smith[1], M. Brønner[3], S. Pernreiter[1,4] and T. Ibrahimi[1]

[1]CSIRO, Mineral Resources, Discovery Program, Kensington 6151, Western Australia,
[2]Centre for Exploration Targeting, University of Western Australia, Crawley, Western Australia
[3]NGU, Norwegian Geological Survey, Trondheim, Norway
[4]Institute of Geology, University of Innsbruck, Innrain 52, A-6020 Innsbruck, Austria

Nearly 25% of Earth's continental surface area currently has a humid tropical climate (Fig. 1). This figure increases when considering regions that have experienced such conditions in the geological past. This is shown by the occurrence of abundant nickel laterite and bauxite deposits within now cooler high-latitude regions (Fig.1). Landscapes dominated by deep weathering and transported cover are commonly found on major stable geological features such as cratons, continental lowlands and plateaus. In parts of Australia, Africa and China these features are currently experiencing arid conditions, and are blanketed by deeply and intensely weathered profiles, that are made of local basement and sedimentary packages up to hundreds of metres deep. These regions evolved through significantly different dynamic from that of their glaciated counterparts, due to pervasive and recurrent weathering-overprinting, weathering processes, age span and tectonic settings (Ollier & Pain 1996; Twidale 2017; Pain *et al.* 2012; González-Álvarez *et al.* 2016; Butt *et al.* 2017).

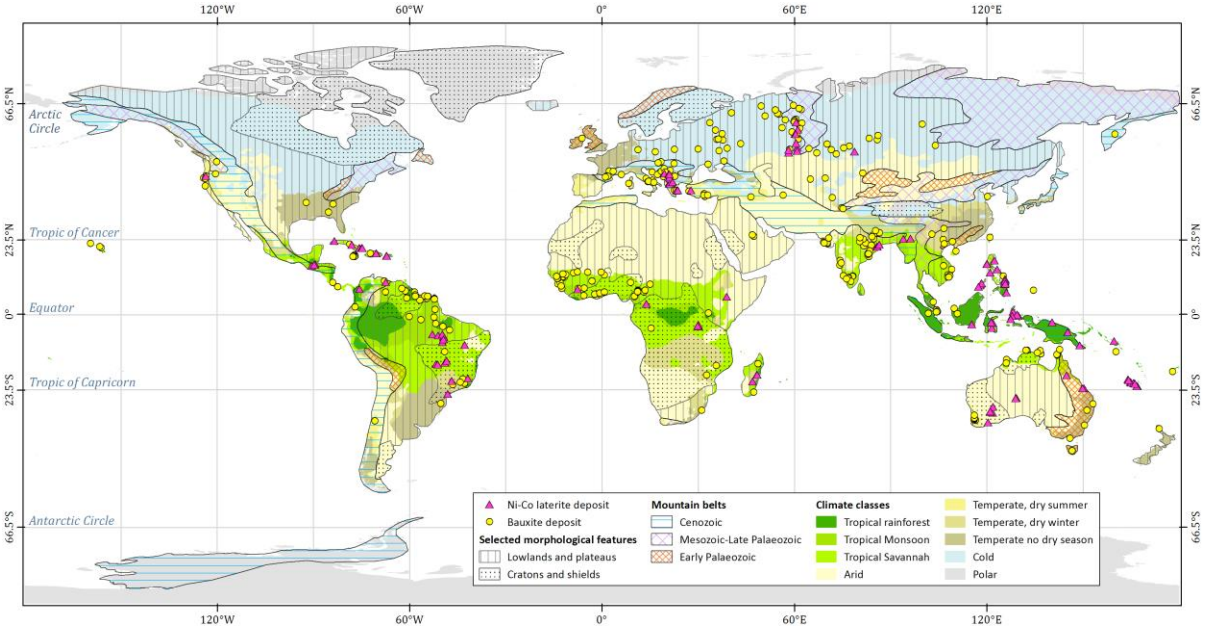

Figure 1: Main global climatic domains and major selected morphological continental features showing the location of the principal Ni-Co laterite and bauxite deposits (from González-Álvarez *et al.* 2016a).

Classifying landscape domains at regional or continental scales can be challenging. However, satellite-derived data such as Digital Elevation Models can image diverse geomorphological surface patterns at scales that would be impracticable for detailed field observations and mapping. By using machine-learning algorithms and a knowledge-based approach, different landscape types can be mapped and their features quantified at regional and continental scales (Fig. 2; Pernreiter *et al.* 2018). Quantifying geomorphological elements can have a substantial impact on the understanding of surface geochemical surveys, since it allows the evaluation of the best sample media for capturing vertical and lateral geochemical dispersion within the cover associated with basement and regolith geochemical footprints (e.g. Anand 2015).

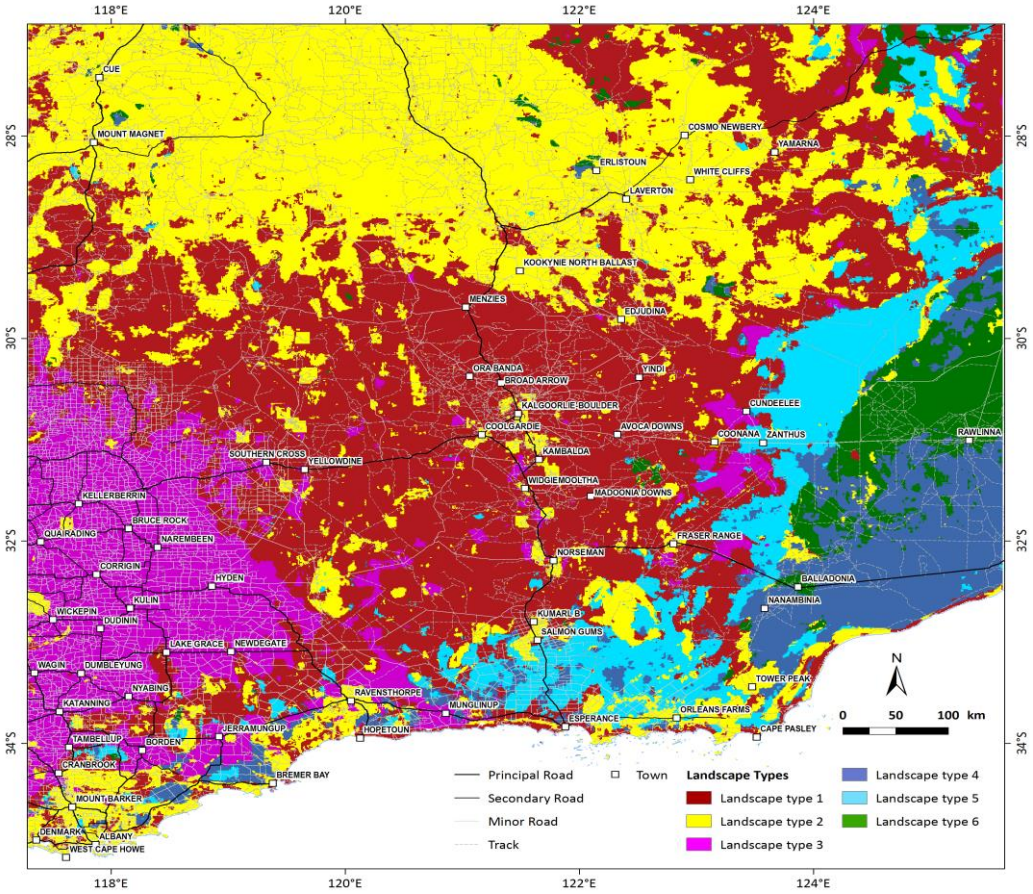

Figure 2: Preliminary map of different landscape types in the Albany-Fraser and Yilgarn Craton, derived from machine learning (González-Álvarez *et al.,* in progress).

Diverse landscapes that have a thick weathered profile are widespread throughout Europe, where they form blankets often >50 m thick, such as in the Scandinavian Mountains, Fennoscandian Shield, British Isles, and the central European mountain and upland belts. All of these are characterized by abundance of Mesozoic and Cenozoic geology weathered to kaolinite-rich saprolite (Migoń & LidmarBergström 2001). Remnants of deeply-weathered basement rocks in Norway occur along structurally-defined zones of crustal weakness, where locally-continuous saprolite layers can be up to 100 m in thickness (Fig. 3). This likely had a substantial impact on the geomorphological evolution of the topography of Norway, since erosion of the sedimentary succession does not seem sufficient to explain the observed immature Alpine-type topography.

The Norwegian arctic landscape displays pockets of deeply-weathered profiles, which likely represent the remnants of a formerly-extensive weathered blanket. These weathered profiles could have been preserved in areas where glacial erosion did not occur or was stagnant. These saprolitic pockets could be the result of grusification of coarse-grained rocks developed on specific palaeolandscape features (Fig. 3). Their relationship to weathering processes and climatic changes is still uncertain.

Due to the complexity of deeply-weathered landscapes and transported sedimentary packages, further strategies need to be in place to expand the use of predictive and descriptive geochemical models from the surface to depth and specifically to unravel the architecture of the cover. This can be attained at local scale by hydrogeochemical sampling and the integration of stratigraphic and mineral drilling datasets. Geophysics, especially airborne electromagnetics (AEM), becomes a powerful tool when combined with the previous approaches, since its interpretation may contribute enough information to infer geological features in between available drillholes. For this an understanding of the petrophysics of lithological units, and how they relate to geochemical processes, is required. The integration of geomorphology, geochemistry and petrophysics allows a better understanding of landscape geochemistry, and therefore of the surface element dispersion processes.

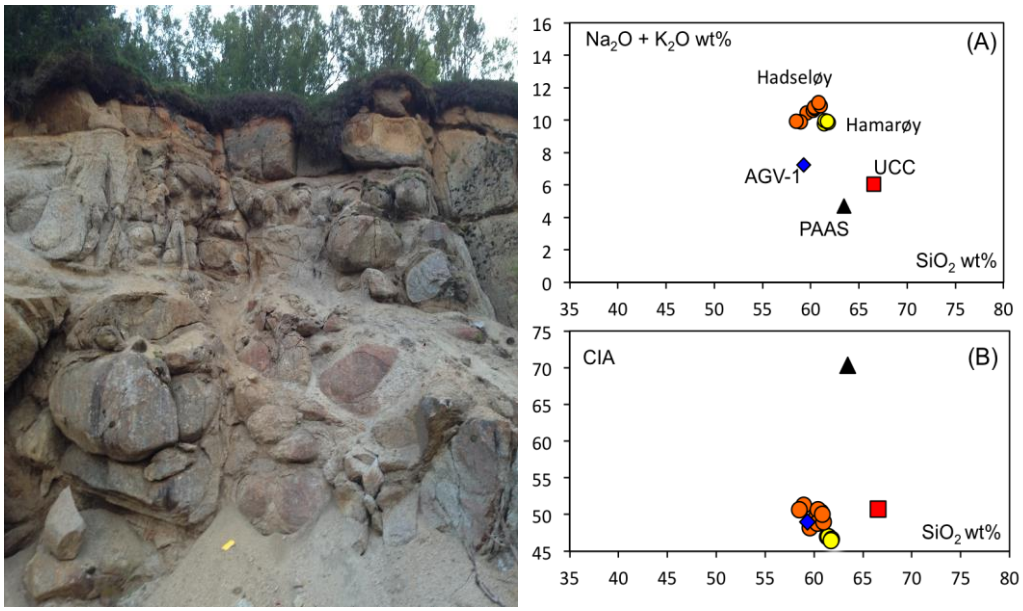

Figure 3: Left panel: an example of deep weathered profiles at Hadseløy and Hamarøy. Right panel (A) Major oxide variability in the sample sets. (B) Chemical Index of Alteration (CIA; Nesbit & Young 1984) clustering at ~50 CIA which is equivalent to unweathered rock (from González-Álvarez & Brønner 2016).

In deeply-weathered landscapes, the use of geophysical datasets such as magnetics and gravimetrics has dominated the mapping of basement geology prior to drilling. In addition, subject to data density and the depth of ground penetration (>400 m), airborne electromagnetics can be a powerful tool to correlate the geology between known stratigraphic profiles. This has the potential to significantly improve the cover architecture reconstruction in 3D, which has important implications for describing landscape and regolith evolution and, therefore, for interpreting landscape geochemistry, since geochemical signatures from the basement will tend to be concentrated in certain stratigraphic units, or associated with particular paleo-landscape features. The ability to map stratigraphic units, unconformities, and structures within the regolith provides key information about its geochemical evolution.

Knowledge of the general structure and composition of the regolith allows to explicitly specify the stratigraphic units which will be present, and to invert AEM data for layer boundaries rather than for a more general conductivity distribution. It makes sense to allow the conductivities to vary laterally within a layer, but only within a range characteristic of that stratigraphy. Understanding which layers are homogeneous, and which are heterogeneous, allows to specify a geostatistical-type spatial covariance structure for each layer, which further constrains the possible solutions. The resulting inversion is then a direct estimate of the parameters of interest to a geologist, namely the depths to the various horizons, along with estimates of their uncertainties (Fig. 4).

Within the Western Australian landscape, paleochannels are one of the most extensive features (Fig. 5). Their fill-in architecture and hydrogeochemistry are key elements for exploration through cover. However, in most regions of Australia there is an important gap in the understanding of groundwater systems and groundwater flow directions, which directly affect metal dispersion within the cover. Paleodrainage and its relationship to geochemical dispersion at depth is a fundamental piece of information for mineral exploration in areas where the landscape is dominated by paleochannel and paleovalley sequences. This is of key importance in the understanding of landscape geochemical anomalies that relate to the basement or to secondary weathering processes within the cover itself.

Landscape geochemistry in deeply weathered regions still has a long way to go regarding predictive and descriptive geochemical models at large scale. This is an essential building block for a more efficient greenfields mineral exploration in these regions. The merging of multiple datasets (geophysics, geology, geochemistry and landscape evolution etc.) requires a shift in paradigm and a change in the way we understand weathering processes at continental and long-time scales.

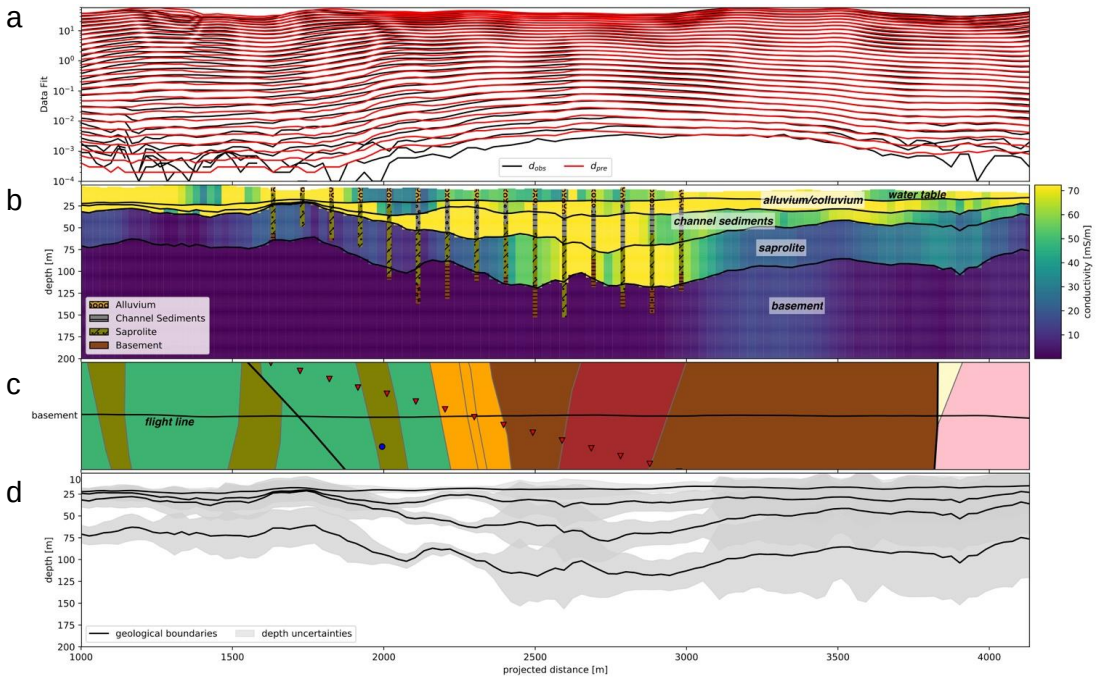

Figure 4: An example inverted section. (a) Observed and best-fit-predicted EM data. (b) Inverted section, with nearby boreholes overlaid. (c) Plan view of interpreted basement geology, along with locations of nearby boreholes. (d) Uncertainty estimates of layer boundaries (from King & González-Álvarez, 2018).

Figure 5: General view of a deeply weathered landscape within a paleochannel system feature in the south of the Yilgarn Craton and Albany-Fraser Orogen region.

References

Anand R.R. 2015. Importance of 3-D regolith-landform control in areas of transported cover: implications for geochemical exploration. *Geochemistry: Exploration, Environment, Analyses,* **16**, 14-26.

Butt C.R.M., Anand R.R. and Smith R.S. 2017. Geology of the Australian regolith. *In:* Phillips N. ed. *Australian Ore Deposits.* AusIMM The Minerals Institute, Monograph **32**, 27-34.

González-Álvarez I., Boni M. and Anand R.R. 2016. Mineral Exploration in Regolith-Dominated Terrains. Global considerations and challenges. *Ore Geology Reviews Special Issue*, **73**, 375-379.

González-Álvarez I. and Brønner M. 2016. Putative deep weathering profiles in the Arctic. Geological Society of America Abstracts with Programs. Vol. 48, No. 7. doi: 10.1130/abs/2016AM-282152. Denver, USA.

King A. and González-Álvarez I. 2018. Constraining airborne electromagnetic interpretation with regolith stratigraphy and landscape evolution processes. Technical Program Expanded Abstracts, AEGC, Australasian Exploration Geoscience Conference, 18-21 Feb 2018, Sydney, Australia.

Migoń P. and LidmarBergström K. 2001.Weathering mantles and their significance for geomorphological evolution of central and northern Europe since the Mesozoic. *Earth Science Reviews*, **56**, 285–324.

Nesbitt H.W. and Young G.M. 1984. Prediction of some weathering trends of plutonic and volcanic rocks based on thermodynamic and kinetic considerations. *Geochmicia et Cosmochimica Acta*, **48**, 1523-1534.

Ollier C. and Pain C. 1996. *Regolith, Soils and Landforms*. John Wiley & Sons, Chichester, 316pp.

Pernreiter S., González-Álvarez I., Klump J., Smith G. and Ibrahimi T. 2018. Landscape evolution in the Albany-Fraser Orogen and South Yilgarn Craton, Western Australia. ARGA, Australian Regolith Geologists Association Annual meeting, 8-11 April, Wallaroo, South Australia.

Pain C., Pillans B., Worrall L. and Roach I. 2012. Old, flat and red: Australia's distinctive landscape. *In*: Blewett R. ed. *Shaping a Nation: Geology of Australia*. ANU ePress, Canberra, 228-275.

Twidale C.R. 2007. *Ancient Australian Landscapes*. Rosenberg, NSW, 144pp.

Geochemical sampling of cover sequence materials throughout the Gawler Craton

C. J. Tiddy[1,2], D. Giles[1,2], S. Hill[3], E. Baudet[1,2,4], A. Brotodewo[2,4], K. M. Custance[1,5], R. L. Hill[1,5], V. Normington[1,5]*, D. Plavsa[2], B. van der Hoek[1,2], K. Wolff[1,5]

[1]Deep Exploration Technologies Cooperative Research Centre (DET CRC)
[2]Future Industries Institute, University of South Australia, Mawson Lakes Campus, Mawson Lakes, 5095
[3]Geological Survey of South Australia, 101 Grenfell St, Adelaide SA 5005
[4]School of Natural and Built Environments, University of South Australia
[5]Department of Earth Sciences, University of Adelaide, Adelaide, South Australia
*Now at Northern Territory Geological Survey, Alice Springs

Over the last eight years there has been a concerted effort within the Deep Exploration Technologies Cooperative Research Centre (DET CRC) and associated collaborative projects to assess how cover sequence materials can be used in mineral exploration throughout the Gawler Craton. The motivation behind this is in addressing the global issue of decreasing rates of ore deposit discovery and consequent metal inventory coupled with increasing exploration costs and risk (e.g. Schodde 2017). The work presented here is a brief overview of results that have come from the significant efforts of numerous researchers and is intended to be ongoing as DET CRC winds up and future projects come online.

The Gawler Craton is a particularly challenging terrane in mineral exploration as highly prospective Archean to Proterozoic basement rocks are extensively overlain by Cambrian and younger cover sequence materials. Basement rocks include Paleo- to Meso-Proterozoic rock packages of the Olympic Domain in the eastern Gawler Craton, which host the Olympic Dam, Prominent Hill, Carrapateena and Hillside and historic Moonta-Wallaroo iron-oxide-copper-gold (IOCG) deposits and districts.

Improving our understanding of mechanical dispersion of geochemical signatures within transported cover has been the subject of ongoing of research within the Gawler Craton. This requires linking element deportment within commonly occurring resistate mineral phases that can withstand alteration during weathering and transport processes back to the chemical signature of ore deposits themselves. Forbes *et al*. (2015) demonstrated that the resistate phase monazite can preserve light rare earth element (LREE) signatures related to IOCG mineralisation at Prominent Hill. The monazite is preserved within Permian glacial sequences of the Boorthanna Formation within the Arckaringa Basin directly overlying the Prominent Hill IOCG deposit. These glacial sequences have demonstrably transported monazite-bearing mineralised basement rocks that were exposed at the time of glaciation northwards, resulting in dispersion of a LREE geochemical signature that can be related back to Prominent Hill mineralisation (Forbes *et al*. 2015). Deportment of elements within other resistate phases including zircon (Brotodewo *et al*. 2018) and rutile (e.g. Plavsa *et al*. 2018) are currently under investigation.

Investigation into signatures of element dispersion by phreatic or vadose processes (Anand *et al*. 2015) has been more widely undertaken (e.g. van der Hoek & Forbes 2013). Normington (2017) conducted a broad study and showed that geochemical analysis of the Permian glacial sequences and overlying Paleozoic glacigene sequences from the Arckaringa and Troubridge basins may be used to identify localised commodity element enrichment so long as the geochemical signals related to provenance, depositional and weathering processes are understood and accounted for. Custance (2015) and Hill (2015) showed that geochemical indicators that vector towards known IOCG mineralisation are preserved within drillhole samples taken from the base of cover across the Yorke Peninsula, and correspond to samples taken from immediately underlying basement rocks. Younger sequences of the Early Cretaceous Cadna-owie Formation and Bulldog Shale that also overlie the Prominent Hill IOCG deposit and are extensive throughout the Eromanga Basin are shown to preserve elevated chemical signatures that may be related to mineralisation. However, this sample media must be used with caution due to effects of chemical dispersion during intense and deep weathering (e.g. Baudet *et al*. 2017; pers. comm.).

Surface sampling of calcrete material was shown to be successful in highlighting the location of the Tunkillia Au-prospect, where Au mineralisation is at depths exceeding 40 m (Fabris & Keeling 2010). Calcrete sampling was also integral in the discovery of the Challenger Au deposit (Poustie &

Abbot 2006). However, it has been recognised that calcrete sampling needs to be undertaken with caution, and that it is critical to sample pedogenically-derived rather than marine-derived calcrete as the latter does not have the potential to preserve signatures of underlying mineralisation (e.g. Chen *et al*. 2002). This led Wolff *et al*. (2017) to investigate how Ca/Sr ratios may be used to discriminate between pedogenic- and marine-carbonates across the Yorke Peninsula. In general, Ca/Sr ratios <650 are considered indicative of pedogenic carbonate, Ca/Sr ratios >1260 indicate marine carbonate and values of 650-1260 are potentially of mixed source.

Van der Hoek *et al*. (2012) also demonstrated inter-relationships between calcrete and vegetation chemistry over the Tunkillia Au prospect in the central Gawler Craton where there is limited spatial association between elevated Au concentrations in dominant plant species (*Casurina pauper* and *Eucalyptus concinna*) and in calcrete. The application of regional biogeochemistry to map out prospective areas of IOCG mineralisation on the Yorke Peninsula was demonstrated by Wolff *et al*. (2018), who successfully used locally occurring *Eucalypt* species of mallee form to highlight areas of known mineralisation. An additional area of elevated Cu within the eucalypt leaves was also identified in the southern Yorke Peninsula, but is yet to be investigated.

The key factor in success of using all types of sample media (cover sequence materials, surface sampling, biogeochemistry and element deportment within specific mineral phases), and critical step has been in defining background chemistry. Without understanding background, the ability to positively identify true elevated or anomalous concentrations is compromised to the point where false anomalies may appear to be an attractive target.

References

Anand R.R., Aspandiar M.F. and Noble R.R.P. 2015. A review of metal transfer mechanisms through transported cover with emphasis on the vadose zone within the Australian regolith. *Ore Geology Reviews* **73**, 394-416.

Baudet E., Tiddy C., Giles D. and Hill S. 2017. Use of cover sequence geochemistry from regional and mineralisation-associated datasets to understand element transport mechanisms. *Goldschmidt 2018*, Paris.

Brotodewo A., Tiddy C., Giles D., Fabris A. and Plavsa D. 2018. Establishment of geochemical exploration criteria in mineral phases within basement and cover sequences. *ARGA Conference 2018* (this volume).

Chen X.Y., Lintern M.J. and Roach I.C. 2002. *Calcrete: Characteristics, distribution and use in mineral exploration*. Cooperative Research Centre for Landscape Environments and Mineral Exploration (CRC *LEME),* Perth.

Custance K.M. 2015. Identifying and characterising potential pathfinder elements to IOCG style mineralisation on central-northern Yorke Peninsula. Hons thesis, University of Adelaide (unpub.).

Fabris A.J. and Keeling J.L. 2010. Soil geochemistry to explore through aeolian cover: results from the Tunkillia gold prospect, Great Victoria Desert. *MESA Journal* **57**, 16-21.

Forbes C., Giles D., Freeman H., Sawyer M. and Normington V. 2015. Glacial dispersion of hydrothermal monazite in the Prominent Hill deposit: An exploration tool. *Journal of Geochemical Exploration* **156**, 10-33.

Hill R.L. 2015. Lithogeochemical characterisation of cover sequence on Yorke Peninsula, South Australia, and identification fo pathfinder elements for IOCG exploration. Hons thesis, University of Adelaide (unpub.).

Normington V.J. 2017. Characterisation of Late Palaeozoic glacigene sedimentary rocks of the Troubridge and Arckaringa basins and implications for palaeogeographic reconstructions of late Palaeozoic South Australia. PhD thesis (under examination).

Plavsa D., Reddy S.M., Agangi A., Clark C., Kylander-Clark A. and Tiddy C. 2018. Microstructural, trace element and geochronological characterization of TiO_2 polymorphs and implications for mineral exploration. *Chemical Geology*, **476**, 130-149.

Poustie T. and Abbot P. 2006. Challenger gold mine – looking at a long term future. *MESA Journal* **40**, 4-7.

Schodde R. 2017. The national state of exploration. *Copper to the World Conference*, June 2017, Adelaide.

Van der Hoek B., Hill S.M. and Dart R.C. 2012. Calcrete and plant inter-relationships for the expression of concealed mineralization at the Tunkillia gold prospect, central Gawler Craton, Australia. *Geochemistry: Exploration, Environment, Analysis* **12**, 361-372.

Van der Hoek B.and Forbes C. 2013. Project 3.3: Geochemical sampling of deep cover. Geological and hydrological atlas of the Gawler Craton, South Austraila. DET CRC Report 2013/326.

Wolff K., Tiddy C., Giles D, Hill S.M. and Gordon G. 2017. Distinguishing pedogenic carbonates from weathered carbonates on the Yorke Peninsula, South Australia: Implications for mineral exploration. *Journal of Geochemical Exploration* **181**, 81-98.

Wolff K., Hill S.M., Tiddy C., Giles D. and Smernik R.J. 2018. Biogeochemcial expression of buried iron-oxide-copper-gold (IOCG) mineral systems in mallee eucalypts on the Yorke Peninsula, southern Olympic Domain; South Australia. *Journal of Geochemical Exploration* **185**, 139-152.

Cretes and 'chemical' landscapes, South Australia

K.G. McQueen

IAE, Faculty of Science and Technology, University of Canberra, ACT, 2601

With abundant silcrete, ferricrete calcrete and gypcrete, the arid and semi-arid areas of South Australia can be fairly described as the 'home of the crete'. These regolith cretes commonly define what could be termed a 'chemical' landscape. Geomorphology tends to stress the physical processes of landscape formation, even though landscapes are the result of both physical and chemical processes. Landscapes can be considered within a spectrum between two end members, largely reflecting the abundance and behaviour of water and biota. The end members are:

- 'physical' landscapes – dominated by erosion, transport, deposition;
- 'chemical' landscapes – dominated by solution, transport, precipitation.

The significance of chemical mass transfer (CMT) has been greatly underestimated in most landscape evolution models, because the transport is harder to see and quantify than physical mass transfer. Clearly CMT can occur on a large scale, as evidenced by the chemistry of river, ground and ocean waters (e.g. Drever 1997), significantly dissolved karst landscapes and large areas of precipitated cretes. Chemical mass transfer is a potentially important process in surface levelling and may help explain the enigma of why much of the Australian landscape is so flat.

Precipitation and/or residual concentration of chemically and physically resistate minerals following solution and transport is commonly revealed by subsequent erosion, and in the defined physical landscape features. Many landscapes in Australia are a combination of 'chemical' landscapes formed under previous wet conditions and superimposed 'physical' landscapes formed under more recent arid conditions (e.g. Twidale 2002, 2007).

Some observations on the shore of Lake Eyre

A small example of the interplay between 'physical' and 'chemical' landscapes can be observed in the area between Lake Eyre (indigenous *Kati Thanda*) and William Creek (Fig. 1). The larger Lake Eyre catchment forms a closed basin, the Lake Eyre Basin, and has done so for a significant time (e.g. Habeck-Fardy & Nanson 2014), hence it is a good setting to observe chemical mass transfer. The catchment area has a widespread abundance of silcrete, as well as weakly to strongly alkaline surface and ground-waters, at least under present conditions and regionally. In noting the occurrence of what he considered as early Cenozoic silcretes around the margins of the lake, Wopfner (1978) stated 'I suspect there may be some genetic connection attached to this circumferential occurrence …, but for the moment, I have no specific suggestions to offer'. Recently, Taylor and Eggleton (2017) proposed a model of silcrete formation by silica saturated, alkaline groundwaters encountering lower pH conditions. Could this be the connection?

In the area east of William Creek there is a low (<55 m AHD) NW-SE trending drainage divide separating Lake Eyre North from Lake Eyre South. East of this divide, the SW margin of Lake Eyre North is marked by a low-elevation (-10 to +15 m AHD) embayment bordered to the west by an irregular escarpment of breakaway terrain (Fig. 1). The breakaway margins are capped by cretes and the breakaway/mesa landforms have developed by topographic inversion of these chemically indurated zones, following physical erosion. In this area, Wopfner (1978) described two levels of capping, which he considered were related to two old landscape surfaces, which he termed the Cordillo (probably post-Eocene) and overlying Warrina (possibly Pleistocene) surfaces. More recent work (Waclawik, 2006) indicates that such superimposes surfaces reflect neo-tectonism in the Miocene and Pleistocene. The underlying Cretaceous sedimentary units include the Oodnadatta Formation, Coorikiana Sandstone, Bulldog Shale and Winton Formation (Williams & Krieg 2012). The Warrina surface is defined by gypcrete on gypsiferous sandstones and shales.

To the NW and SE, are two dune fields containing NE-trending linear dunes. The dune fields have disrupted a pre-existing drainage in which, Douglas Creek drained southeast via the area of Lake Callara, as part of the Lake Eyre South catchment (Fig. 1). The Douglas Creek channel was diverted around the NW edge of the northern dunes and appears to have had sufficient, subsequent flow to maintain this course through the northern part of the dune field. The dune fields overprint the older surfaces as well as the embayment along the SW edge of Lake Eyre. Younger

aeolian deposits, such as source-bordering dunes and larger down-wind deposits of finer sediment are associated with small playas within the ephemeral, disrupted drainage (e.g. Lake Callara).

Within the embayment flanking the present edge of the Lake Eyre playa, there is a large amount of scree, including fragments of what resembles a black silcrete, apparently shed from the eroding capping to the adjacent breakaways. This material is massive, fine-grained, hard and with a sub-conchoidal fracture. Optical and X-ray diffraction (XRD) analysis indicates that it is a ferricrete, composed mainly of goethite and lesser hematite. The only silica present is minor quartz, as small (10-120 µm), scattered grains, some veined by goethite/hematite. The scree is developing a gibber surface within the embayment. Unconsolidated alluvium/colluvium in this area contains blocks of crystalline gypsum, probably precipitated from groundwater. Currently the land surface within the embayment ranges from 20-30 m above the bed of Lake Eyre and it is likely that the lake extended into this area at around 120 Ka BP when the water level reached a depth of 25 m (Magee *et al.* 2004).

The nearby surface of Lake Eyre is covered with a salt crust (2-5 mm thick) and underlying salty mud, deposited by surface flow of suspended sediment and evaporative concentration and precipitation of dissolved salts. The surface crust exhibits areas of irregular desiccation polygons and ridges, as well as small 'igloo' structures or domes, possibly formed by swelling and shrinking of the underlying mud. XRD analysis of samples collected near Halligan Point indicates halite, as the dominant salt in the crust, with minor gypsum, calcite, quartz and clay. The underlying mud contains halite, gypsum, calcite, kaolinite, quartz, mica/illite, plagioclase and K-feldspar.

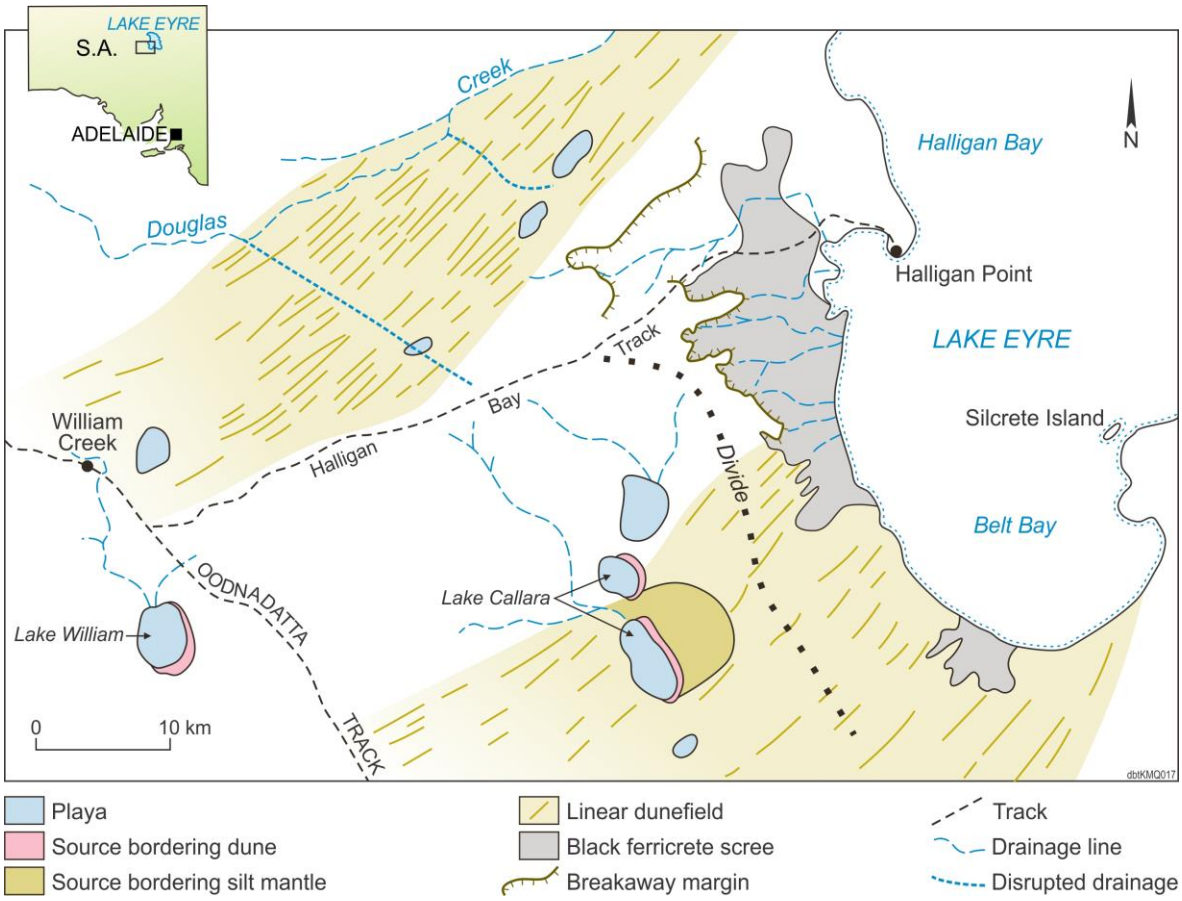

Figure 1: Schematic landform map of the Lake Eyre-William Creek area. Constructed by the author using Google Earth as the topographic base.

The Lake Eyre-William Creek area is almost a microcosm of the broader regional landscape of northern South Australia. Long-term changes in climatic conditions have led to a combination of landform associations broadly sequenced as follows.

1. During periods of marked chemical weathering accompanying wet climatic conditions (e.g. Late Cretaceous to Early Cenozoic) ferricrete and silcrete formed.
2. Progressive drying of the environment reduced chemical weathering, while continuing physical erosion led to exposure of chemically indurated zones, their topographic inversion and development of distinctive breakaway/mesa landforms and scree/gibber fields.
3. Marked aridity led to a decrease in local fluvial erosion and transport and increase in wind transport and deposition, with resulting development of dune systems and disruption of drainage. Accompanying evaporative conditions led to the development of playa-related landforms and chemical deposits, including evaporites and groundwater precipitates.

Overprinting relationships indicate that the small playas are the youngest features and that the dunes have been active less than ca.120 Ka BP (cf. Croke *et al*.,1998).

Some observations on an unusual silcrete

Near Lake Arthur, approximately 60 km east of Maree, there are silcrete exposures with low-level radioactivity (2000 c/s measured by a GR-135 Minispec scintillometer, B. Deveson pers. comm. 2006). Samples were collected at this site from about halfway up the side of a mesa on the western catchment of the lake (Fig. 2). The rock unit at the sample locality is mapped as Murnpeowie Formation (Forbes *et al*. 1965, renamed Eyre Formation, Sheard 2009), composed of sandstones and calcareous sandstones of Late Paleocene to Middle Eocene age.

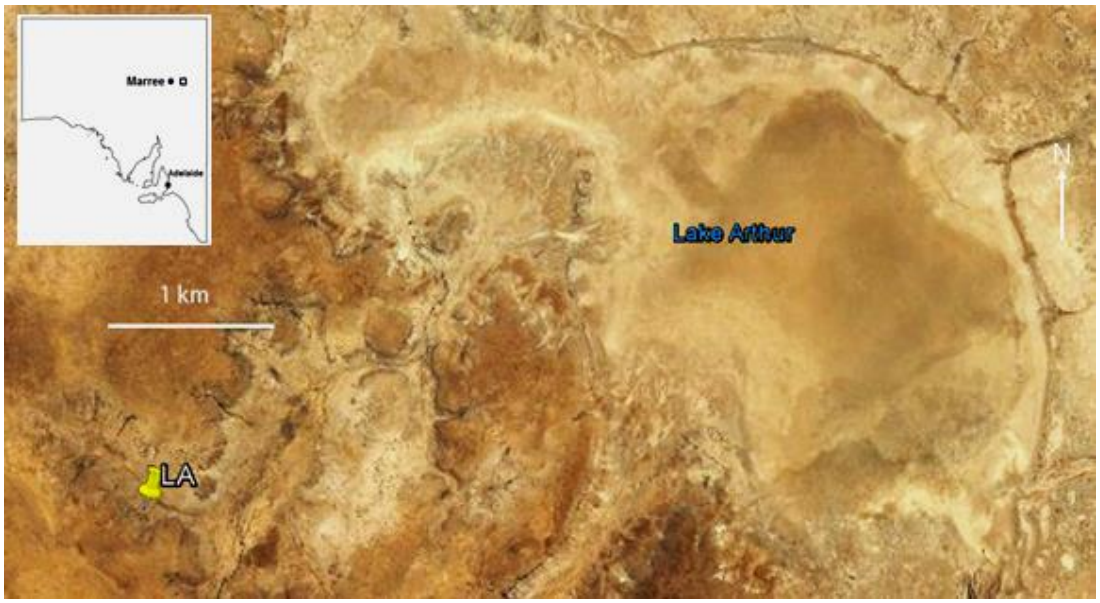

Figure 2: Google Earth image showing silcrete sample location (LA) at 138° 43' 3.15" E 29° 33' 9,6" S, west of Lake Arthur. This area is ca. 110 km southeast of Lake Eyre.

Two samples from the Lake Arthur site were examined in detail by petrographic and X-ray diffraction analysis. Both samples show similar characteristics and represent silcreted quartz-rich, fine to medium-grained sandstone. The abundance of relatively undeformed mono-crystalline quartz clasts, presence of trace amounts of detrital tourmaline, zircon and rare detrital muscovite suggest the sediment source contained abundant granite. There are also minor lithic clasts of chert and quartz-rich siltstone, indicating that smaller amounts of these rocks were present in the sediment provenance. Very minor amounts of deformed quartz and milky, fluid inclusion-rich quartz were probably derived from metamorphic rocks and quartz veins. The deposited sedimentary rock appears to have been a clean, quartz-rich sandstone, as indicated by the abundance of quartz clasts and the high degree of sorting.

In both samples, the primary sedimentary clasts are enclosed in a siliceous matrix. Textural evidence (e.g. Figs 3 & 4) indicates two stages of matrix development.

- Stage 1 matrix is composed of amorphous to poorly crystalline opal (identified as opal-A by XRD). This has a yellow brown colouration and shows colloform banding, indicating that silica was introduced in solution and sequentially deposited around the quartz grains. This type of poorly crystalline impurity-rich opaline silica is typically deposited in silcretes at a

stage when the precipitating solutions contain a high proportion of other dissolved components (e.g. when silica-bearing groundwater is first introduced into deeply weathered material, Milnes & Thiry 1992). Existing quartz grains typically act as nucleation sites. The overall fabric of both samples suggests that the introduction and precipitation of this matrix acted to displace the quartz grains so that they are now largely enclosed in the matrix.

- Stage 2 material is composed of clear, microcrystalline quartz that has in-filled cavities left in the earlier matrix. It is much less abundant than the opaline silica. Observations of other silcretes suggest that this more crystalline cement is typical of silica precipitated at a late stage from groundwaters with low levels of impurities (Milnes & Thiry 1992). This would be consistent with its later stage of development.

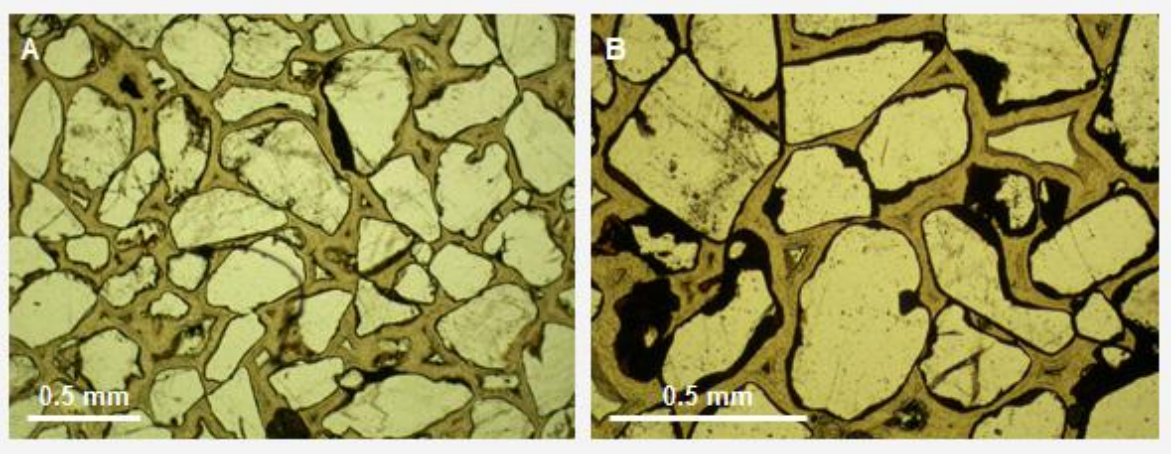

Figure 3: Photomicrographs of Lake Arthur silcrete, sample LA1. (A) showing monocrystalline, detrital quartz grains, yellowish matrix of opaline silica and scattered aggregates of opaque iron oxide/oxyhydroxide. (B) showing area from relict ferruginous mottle with iron oxide/oxyhydroxide rimming and possibly replacing detrital quartz grains.

Pale, palimpsest ferruginous mottling in one of the samples (LA1), appears to predate the silicification, as suggested by the preservation or relocation of goethite/hematite aggregates around the primary quartz clasts outside of the opaline silica matrix. This would indicate that the rocks were deeply weathered and ferruginised before they became silcreted. In some cases, the iron oxide/oxyhydroxides appear to have partially replaced the quartz or in-filled etch pits.

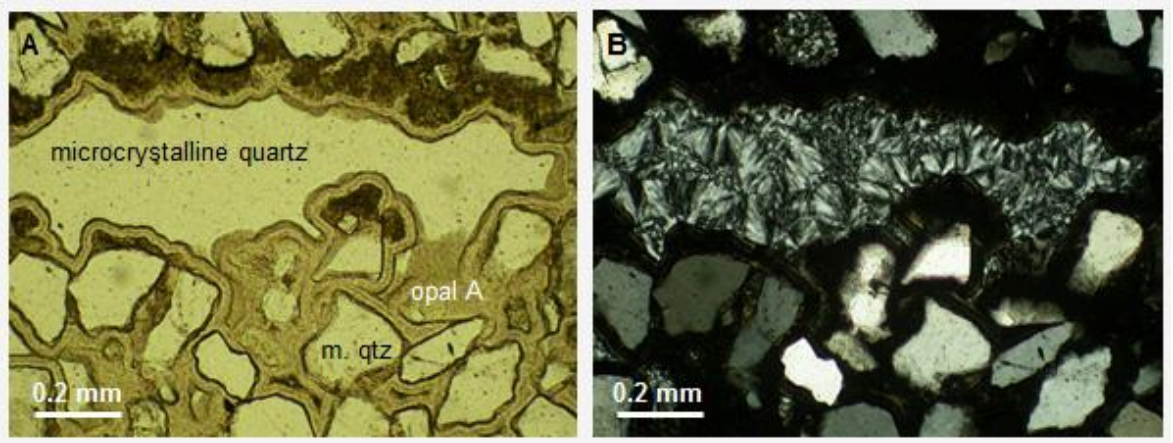

Figure 4: Photomicrographs of Lake Arthur silcrete, sample LA2. (A) showing detrital grains of mono-crystalline quartz (m. qtz), matrix of opaline silica (opal A) and cavity-filling microcrystalline quartz. Dark cloudy material near the top is possibly carnotite also identified as powdery coatings on the surface of the sample. (B) same field in cross-polarised light.

The second sample (LA2) has small surface coatings of a bright yellow, powdery mineral. X-ray diffraction analysis identified this mineral as carnotite ($K_2(UO_2)_2V_2O_8$). In thin section, the carnotite appears to be associated with the stage 1 opaline matrix (although this needs to be confirmed by *in situ* chemical analysis). This would be consistent with introduction and precipitation of carnotite with the groundwater that precipitated the early stage silica. Surface breakdown of the opaline cement during more recent weathering could have produced the surface coatings.

In semi-arid areas of Australia, carnotite is typically associated with calcrete deposits (e.g. at Yeelirrie and Lake Maitland in Western Australia, Mann & Deutscher 1978). The presence of carbonate in solution enhances the solubility range for U and V, but this does not require calcite to be present and in equilibrium with the solution, as any near surface groundwater with suitable pH in equilibrium with the atmosphere will have a similar amount of CO_3^{2-} (Mann 1974; Mann & Deutscher 1978). A decrease in pH could initiate carnotite precipitation from solution. Thus, alkaline groundwaters with U and V in solution could theoretically precipitate carnotite in the absence of calcrete. If these solutions are carrying dissolved silica, a similar change in pH could co-precipitate silcrete. Uranium-enriched silcretes have been described from Spain. Here the silcrete is associated with calcrete, including rhizomorphic forms, with calcrete-silcrete intergrades formed under pedogenic-vadose and phreatic conditions, including with calcrete replacement by silcrete (Bustillo *et al*. 2013).

Conclusions

Cretes are clearly an important component of many 'chemical' landscapes and the processes by which they form appear complex and perplexing. Evolving and fluctuating groundwater compositions and changes in the chemical environment can lead to specific or sequential formation of different cretes by precipitation and replacement. Climate change and the availability of water are key drivers.

In the Lake Eyre Basin, silcretes and ferricretes reflect periods of wetter climate and marked chemical weathering. Subsequent physical erosion has exposed these 'chemical' landscape features. The most recent 'chemical' landscape components are part of an evaporite association (predominantly halite-gypsum) developed under arid conditions, but with sporadic surface and groundwater input from monsoonal rains in the northern Lake Eyre catchment, and probably also deposition of atmospheric particulates and aerosols.

There is still much to learn about cretes and even more to understand about other formative processes of 'chemical' landscapes.

References

Bustillo M.A., Plet C. and Alonso-Zarza A.M. 2013. Root calcretes and uranium-bearing silcretes at sedimentary discontinuities in the Miocene of the Madrid Basin (Toledo, Spain). *Journal of Sedimentary Research*, **83**, 1130-1146.

Croke, J. C., Magee, J. W. and Price, D. M., 1998. Stratigraphy and sedimentology of the lower Neales River, West Lake Eyre, Central Australia: from Palaeocene to Holocene. *Palaeogeography, Palaeoclimatology, Palaeoecology*, **144**, 331-350.

Drever J.I. 1997. *The Geochemistry of Natural Waters: Surface and Groundwater Environments* 3rd Edition. Prentice Hall, Upper Saddle River N.J., 436 pp.

Forbes B.G., Coats R.P., Webb B.P. & Horwitz R.C, 1965. MAREE 1:250 000 Geological Map - First Edition, Geological Survey of South Australia.

Habeck-Fardy A. & Nanson C. 2014. Environmental character and history of the Lake Eyre Basin, one seventh of the Australian continent. *Earth-Science Reviews*, **132**, 39-66.

Mann A.W. 1974. *Chemical ore genesis models for the precipitation of carnotite in calcrete*. CSIRO Minerals Research Laboratories, Division of Mineralogy Report FP. 6, 38 pp.

Mann A.W. and Deutscher R.L. 1978. Genesis principles for the precipitation of carnotite in calcrete drainages in Western Australia. *Economic Geology*, **73**, 1724-1737.

Magee J.W., Miller, G.H., Spooner, N.A. & Questiaux, D. 2004.Continuous 150 k.y. monsoon record from Lake Eyre, Australia: Insolation forcing implications and unexpected Holocene failure. *Geology* **22**, 885-888.

Milnes A.R. & Thiry M. 1992. Silcretes. *In:* Martini I.P. & Chesworth W. eds *Weathering, Soils and Paleosols*. Elsevier, Amsterdam, pp. 309-347.

Sheard, M.J. 2009. Explanatory notes for CALLABONNA 1:250 000 geological map, sheet SH 54-6 Geological Survey of South Australia. Report Book 2009/01.

Taylor G. & Eggleton R.A., 2017. Silcrete: an Australian perspective. *Australian Journal of Earth Sciences* **64(8)**, 987-1016.

Twidale C.R. 2002. The two-stage concept of landform and landscape development involving etching: origin, development and implications of an idea. *Earth-Science Reviews* **57**, 37-74.

Twidale C.R. 2007. *Ancient Australian Landscapes*. Rosenberg Publishing Pty Ltd, Dural, NSW, 144 pp.

Waclawik V.C. 2006. Landscape evolution of the Umbum Creek Catchment, Western Lake Eyre, Central Australia. PhD Thesis (unpubl.) University of Adelaide.

Williams A.F. & Krieg G.W. 2012. Lake Eyre 1:250 000 Geological Map. Department for Manufacturing, Industry, Trade, Resources and Energy, South Australia.

Wopfner H. 1978. Silcretes of northern South Australia and adjacent regions. *In*: Langworth-Smith T. ed. *Silcrete in Australia*. New England University Press, Armidale, pp. 93-141.

Covering the bases – baseline geochemistry of South Australia's cover

A.E. Petts and C.B.E. Krapf

Geological Survey of South Australia, Department of Premier and Cabinet, PO Box 320, Adelaide SA 5000

South Australia is covered by 75% transported regolith material (Krapf *et al*. 2012). This extensive cover can be up to 100's of metres thick (Anand 2005), presenting a major exploration challenge for mineral explorers searching for basement hosted mineralisation (de Caritat *et al*. 2017). The Geological Survey of South Australia (GSSA) has recently created teams to take on the key themes of UNCOVER, the national initiative for exploration through cover (Blewett 2014). 'Characterising South Australia's Cover' is one of these key teams, and one of our key areas of focus will be on providing new and updated data compilations and innovative geoscience products to ensure that stakeholders will be able to explore with improved confidence and vigour in some of the most underexplored regions of the state.

Mineral explorers currently use a variety of sampling media (e.g. different soil fractions, lag, biota), and have often relied on previous case studies (e.g. Butt *et al*. 2005) and geochemical surveys undertaken in SA by researchers within the Cooperative Research Centre for Landscape, Environment and Mineral Exploration (CRCLEME) and later the Deep Exploration Technology Cooperative Research Centre, DETCRC such as Hill (2004), Hulme & Hill (2003), Fabris *et al* (2009a, b), and Wolff & Hill (2018). Enabling easy access to geochemical data for calcrete, biota, soil fractions, lag and other unconventional sampling media for sample sites across SA will assist explorers in determining appropriate sampling media for exploration programs and give confidence and assurance to those working in greenfield areas. The importance in establishing baseline geochemistry across all of SA's geological provinces, ideally, for each popular sampling media, cannot be overstated. This work will allow a complete update of the quality and accessibility to surface geochemical data which forms the basis for much of the early exploration work by mineral companies and environmental studies by stakeholders.

A state regolith map has been compiled by Krapf *et al*. (2012) and complements the state-wide ASTER Geoscience, geology (Cowley 2001), paleodrainage and Cenozoic coastal barrier maps (Hou *et al*. 2007; 2012) and radiometric maps. A national geochemical survey was undertaken in 2011 (de Caritat *et al*. 2011; 2016; 2017), however a state surface geochemistry map has never been attempted. Large scale surveys do not reflect regional or even local scale variations – important when exploring in such diverse geological terranes such as South Australia. We will focus on province scale to prospect scale – better data, better scale, better quality assurance which will mean better results for stakeholders, all presented in a baseline geochemistry dataset, output map and surface geochemistry atlas for South Australia.

State-based geochemical data compilations available for public use remain as a simple 'rock sample' site layer available from the South Australian Resources Information Gateway (SARIG; https://map.sarig.sa.gov.au/), however, which is a compilation of previous GSSA fieldwork as well as open file data from mineral explorers. Much of the state is covered in regional to local scale survey points (Fig. 1).

In order to fulfil the UNCOVER vision of characterising the cover, GSSA will assemble updated state-wide geochemical datasets, with layers including sampling media type and individual elements. A regional geochemistry dataset will assist mineral explorers prioritise true anomalies when looking for subtle surface variations in geochemical data, providing a background signature for many elements –gaps in this coverage will be prioritised and reconnaissance traverses planned, similar to the Eucla Basin regional biogeochemistry survey in 2014 (Dunn & Waldron 2014).

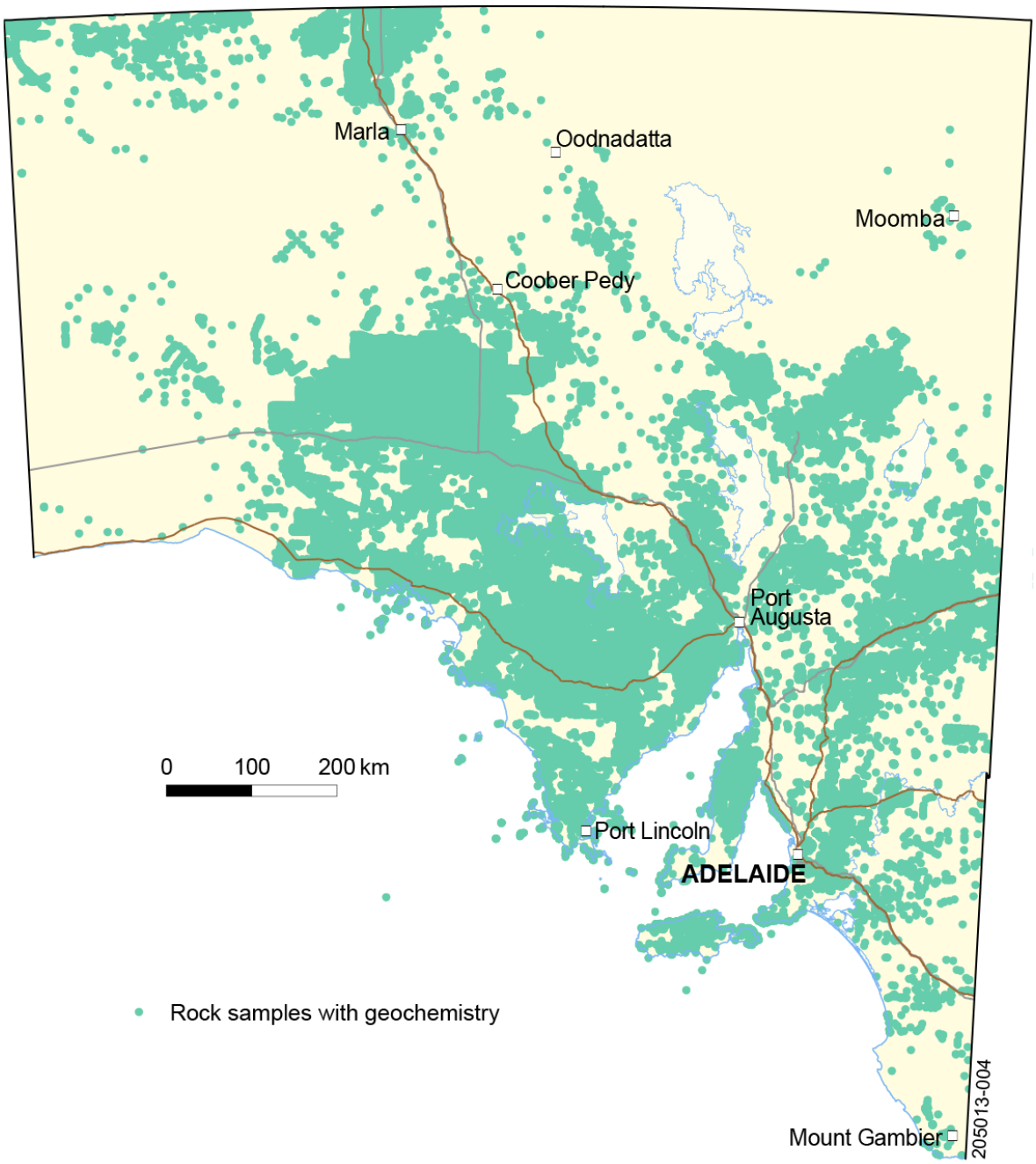

Figure 1: Rock/surface geochemical data currently available for download from SARIG.

References

Anand R.R. 2005. Weathering history, landscape evolution and implications for exploration. *In*: Anand R.R., and de Broekert P. eds. Regolith Landscape Evolution across Australia. CRC LEME, Perth, 354 pp.

Blewett R. 2014. UNCOVER: unlocking Australia's hidden mineral potential. Geoscience Australia Insights, 7 July 2014.

Butt C.R.M., Robertson I.D.M., Scott K.M. and Cornelius M. eds. 2005. *Regolith Expression of Australian Ore Systems*. CRC LEME, Perth, 431 pp.

Cowley, W.M., 2001. Geological map, South Australia. South Australian Geological Survey. Maps of South Australia Series, 1:2 000 000.

de Caritat P. and Cooper, M. 2011. National Geochemical Survey of Australia: The Geochemical Atlas of Australia. Geoscience Australia Record 2011/20, 557 pp (2 Volumes).

de Caritat P. and Cooper M. 2016. A continental-scale geochemical atlas for resource exploration and environmental management: the National Geochemical Survey of Australia. *Geochemistry: Exploration, Environment, Analysis* **16**, 3-13.

de Caritat P., Main P.T., Grunsky E.C., and Mann A.W. 2017. Recognition of geochemical footprints of mineral systems in the regolith at regional to continental scales. *Australian Journal of Earth Sciences* **64(8)**, 1033-1043.

Dunn C.E. and Waldron H.M. 2014. *Regional biogeochemical survey of the Eucla Basin, South Australia*. Department of State Development, South Australia, Report Book 2014/00025.

Fabris A.J., Keeling J.L., and Fidler R.J. 2009a. Surface geochemical expression of bedrock beneath thick sediment cover, Curnamona Province, South Australia. *Geochemistry: Exploration, Environment, Analysis* **9,** 237-246.

Fabris A.J., Keeling J.L., and Fidler R.J. 2009b. Soil geochemistry as an exploration tool in areas of thick transported cover, Curnamona Province. *MESA Journal* **54,** 32-40.

Hill S.M. 2004. Biogeochemical sampling media for regional- to prospect-scale mineral exploration in regolith-dominated terrains of the Curnamona Province and adjacent areas in western NSW and eastern SA. *In:* Roach, I.C. ed. *Regolith 2004*, CRC LEME, pp. 128-133.

Hou B., Zang W., Fabris A., Keeling J., Stoian L., and Fairclough M. 2007. *Palaeodrainage and Tertiary coastal barriers of South Australia, 1:2 000 000 Series*. 1st edn. Department of Primary Industries and Resources South Australia, Adelaide.

Hou B., Fabris AF, Michaelsen B.H., Katona LF., Keeling J.L., Stoian L., Wilson T.C., Fairclough M.C., Cowley W.M. and Zang W. (comp.) 2012. *Palaeodrainage and Cenozoic coastal barriers of South Australia, Digital Map of South Australia, 1:2 000 000 Series*. 2nd edn. Department for Manufacturing, Innovation, Trade, Resources and Energy, South Australia, Adelaide.

Krapf C.B.E., Irvine J.A., Cowley W.M. 2012. *Compilation of the 1:2 000 000 State Regolith Map of South Australia – a summary.* Department for Manufacturing, Innovation, Trade, Resources and Energy, South Australia, Adelaide Report Book 2012/16.

Hulme K.A., and Hill S.M. 2003. River red gums as a biogeochemical sampling medium in mineral exploration and environmental chemistry programs in the Curnamona Craton and adjacent regions of NSW and SA. *In:* Roach I.C. ed. *Advances in Regolith*, CRC LEME, 205-210.

Wolff K., Hill S.M., Tiddy C., Giles D. and Smernik R.J. 2018. Biogeochemical expression of buried iron-oxide-copper-gold (IOCG) mineral systems in mallee eucalypts on the Yorke Peninsula, southern Olympic Domain; South Australia. *Journal of Geochemical Exploration* **185**, 139-152.

Could rapid XRF analysis techniques provide a step change in our ability to map geochemical dispersion patterns through cover and deliver future mineral discoveries?

A.J. Fabris

Geological Survey of South Australia, PO Box 320, Adelaide SA 5000

The advent of field-portable XRF has enabled cost effective analysis of drill materials that would otherwise rarely be analysed. These include cover units over basement targets, where geochemical data may provide indications of underlying mineralisation, or, serendipitous discovery of mineralisation within cover units.

Two recent developments in the area of mineral exploration are Lab-at-Rig® and the Minalyzer CS, both of which originate from a desire for multi-element analytical results as soon after drilling as possible. Lab-at-Rig® involves X-ray fluorescence (XRF) analysis of drill cuttings returned from a Solids Removal Unit (SRU) at the drill site. This technology is a commercial product of research and development within the Deep Exploration Technologies Cooperative Research Centre (Hillis *et al*. 2014). The Minalyzer CS provides continuous XRF analysis of drill core within core trays, making it cost effective to analyse entire drill holes.

During 2015-2016, the Geological Survey of South Australia were involved in trials of Lab-at-Rig® within a regional drill program in South Australia (Fabris *et al*. 2017). Cover samples including regolith profiles were analysed at ~1 m sample resolution. Geochemical results through the regolith enabled routine mapping of depletion zones as well as regolith carbonate horizons and ferruginous- and manganiferous-rich zones, all of which can guide logging and provide context for further sampling. Variation in major element chemistry within sedimentary cover units provided an aid to lithological logging. Trace element data provided baseline values and identified elevated metal values around unconformity surfaces.

The Minalyzer CS has been trialled in the SA Drill Core Reference Library since July 2016. To date >15 000 m of selected drill core has been scanned including drill holes containing cover units to basement-hosted mineralisation. These data identified high metal values within sedimentary cover units, and provide proof-of-concept of serendipitous discovery during basement-targeted drilling.

Whether these particular technologies become routine in exploration is unknown, however, with a renewed push to characterise and map geochemical dispersion within cover across Australia as part of the national UNCOVER initiative, it is likely that these types of XRF techniques will contribute to this national endeavour.

References

Fabris A.J., Tylkowski L., Brennan J., Flint R.B., Ogilvie A., McAvaney S., Werner M., Pawley M., Krapf C., Burtt A.C., Rowe R., Henschke C., Chalmers N.C., Rechner S., Hardwick I. and Keeling J. 2017. Mineral Systems Drilling Program in the southern Gawler Ranges, South Australia. Department of the Premier and Cabinet, South Australia, Report Book 2016/00030.

Hillis R.R., Giles D., van der Wielen S.E., Baensch A., Cleverley J.S., Fabris A.J., Halley S.W., Harris B.D., Hill S.M., Kanck P.A., Kepic A., Soe S.P., Stewart G., and Uvarova Y. 2014. Coiled tubing drilling and real-time sensing - enabling prospecting drilling in the 21st century? *Society of Economic Geologists Special Publication* **18**, 243–260.

Correlations between spectral mineralogy and borehole rock properties in (and under) the Eromanga Basin

I. C. Roach

Geoscience Australia, GPO Box 378, Canberra ACT 2601

The bulk mineralogy, porosity and permeability of regolith and fresh rocks affect their petrophysical properties (rock properties). Minerals, pore water chemistry and pore space tortuosity that make up regolith and fresh rocks variably affect electrical conductivity, natural gamma-ray emission and magnetic susceptibility in a fashion that can be interpreted using lithological logs, groundwater electrical conductivity and spectral mineralogy.

The Southern Thomson Project is a collaborative project between Geoscience Australia and its partners the Geological Survey of New South Wales and the Geological Survey of Queensland. Twelve boreholes drilled as part of the Project intersected weathered and fresh rocks of the Eromanga Basin and underlying Paleozoic basement. The mud rotary chips and diamond cores obtained from these boreholes were scanned using HyLogger at the Geological Survey of New South Wales and the Geological Survey of Queensland. Wireline logging in the boreholes obtained natural gamma-ray emission, electrical conductivity and magnetic susceptibility data, and the mud rotary drill chips and diamond drill core were also logged using hand-held magnetic susceptibility meters. Groundwater was sampled for electrical conductivity in some of the boreholes, and legacy groundwater chemistry data is available for many of the waterbores in the local area.

This presentation will describe the Southern Thomson Project drilling program and illustrates some observations on the associations between spectral mineralogy, lithology, groundwater electrical conductivity and borehole rock properties data in the boreholes. The possible relationships between bulk mineralogy and groundwater chemistry, and borehole geophysical signatures in some of the boreholes, are discussed.

This paper is published with the permission of the CEO, Geoscience Australia. ICR gratefully acknowledges the staff input and resources of the GSNSW and GSQ.

Using passive seismic to estimate the thickness of the Leonora Breakaways, Western Australia

S. Jakica

Geological Survey of Western Australia, 100 Plain St., East Perth, WA 6004

Introduction

Passive seismic methods are becoming of increasing interest for defining the near-surface geology, in particular the depth of the cover. In June 2017, the Geological Survey of Western Australia carried out a passive seismic acquisition over the Leonora breakaways in the goldfields of Western Australia, to test whether the passive seismic technique can determine the thickness of the weathered granitic rocks. The acquisition was carried out using the single station HVSR Tromino® instrument. Results and interpretations are presented in this paper.

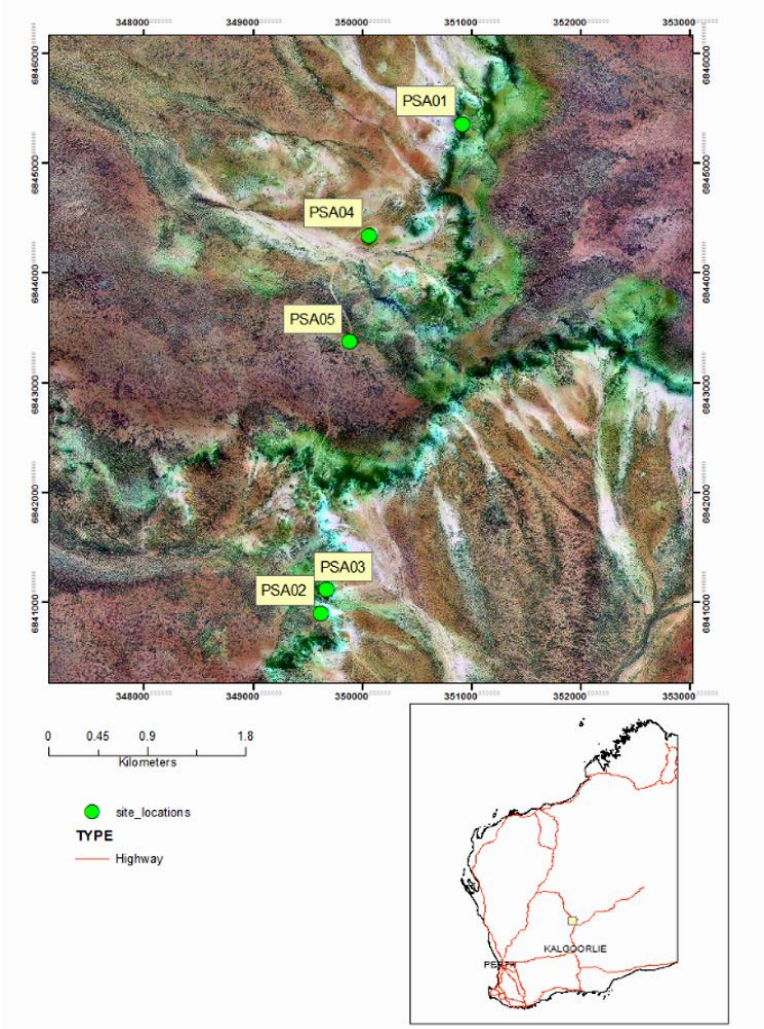

Figure 1: Location of passive seismic measurements at Leonora breakaways superimposed on the Landsat and areal images.

The Study Area

Leonora breakaways, also known as Leonora Terraces, are a popular tourist attraction located 40 km northeast from Leonora, Western Australia (Fig. 1). The south-facing breakaways are products of headward erosion of granitic and greenstone terranes (Davy & Gozzard 1995; Bradley *et al.* 1995). The breakaways have a relief of up to 30 m (Stewart, 2005). The passive seismic acquisition was designed to measure their true thickness, i.e. how far weathered granitic rock extends at depth before reaching fresh rock. Tromino® passive seismic measurements were acquired at five different locations summarised below (Fig. 1).

Breakaways are formed as a part of the relict and erosional regolith regimes. The relict surfaces over the granitic terranes are principally caprock silcretes or upland sandplains. Patches of iron-rich rubbly pebbles and duricrust are sparsely distributed on the top of breakaways by the deflation processes. Some iron-rich non-pisolithic duricrust is also present on the edges of breakaways.

Methodology

Unlike active seismic, passive seismic is a non-invasive technique, which does not require a controlled seismic source (MOHO 2015; Scheib 2014). It measures low-frequency ambient noise caused by waves, wind, deeper micro-seismic events, fracking as well as distant anthropogenic activities present in the subsurface (MOHO 2015; Lane *et al*. 2008). The passive seismic method is a horizontal-to-vertical (HVSR) method that uses three-component measurements of ambient seismic noise to determine and evaluate fundamental seismic resonance frequency.

In this study, the horizontal (east-west and north-south) components and a vertical spectral component of ambient noise have been measured using a Tromino single-station passive seismic seismometer. The acquisition duration for each site was set to 20 min. To determine the site resonance frequency, Tromino applies the Nakamura technique (or H/V method) which uses the spectral ratio of the average H and V components (Nakamura 1989).

A peak in the resulting H/V trace indicates an acoustic impedance contrast, caused by, for example, a change in the rock type. In a simple two layer earth, this acoustic impedance contrast defines the boundary between two different geological units. The resonance frequency (fz) at which the peak occurs corresponds to the thickness (h) and the shear-wave velocity (Vs) of the layer above the impedance; $Fz= Vs_1/(4*h_1)$.

Sampling

The first Tromino measurement (PSA01) was taken at the heavily weathered, silicified granite surface with only patches of very thin (2–5 cm) soil present. The breakaway was about 15 m high with a thin veneer of crystalline quartz grains set in a fine-grained, silica-rich matrix. Underlying the silica-rich weathered granite is a ~3 m-thick goethite-stained weathered profile that overlies 5–7 m of bleached, weathered granite with white quartz and fine-grained feldspathic matrix. The second Tromino measurement (PSA02) was taken at the breakaway 4.5 km south-west of PSA01. This site has the same weathering characteristics as PSA01. The site PSA03 is located ~200 m north of PSA02 and has similar weathering profile to the previous two locations with silcrete nodules being present at the edge of the breakaway. Remains of iron-rich duricrust with quartz and Fe-oxide nodules were also observed. Measurement PSA04, taken about 1.2 km south-west of PSA01, has a similar weathering profile to PSA01 except that scattered rubble and silcrete boulders were observed on the top of the breakaway. Measurement PSA05 was taken on the relict sandplain overlying the weathered granite breakaway. The site contains red-coloured, medium-grained, quartz-rich sands, with 10% other minerals such as iron-oxides and possibly kaolinites. The vegetation at this site is rich in spinifex with some small to medium bushes and small-growth eucalyptus trees.

Results and Conclusions

Figure 3 shows an example of measured H/V spectra where peaks indicate an impedance at depth. The peak gives the resonance frequency of the site. To determine whether the peak is of stratigraphic or anthropic origin, the smoothing of the H/V curve was dropped to 1% as indicated in Figure 4. For deriving depth estimates from the frequencies, shear-wave velocities were required. Although we were not able to measure the shear-wave velocity at the site, we have used the average velocity for weathered granitic rocks and sediments as indicated by Ibs-von Seht & Wohlenberg (1999) as well as Bourpie *et al*. (1987).

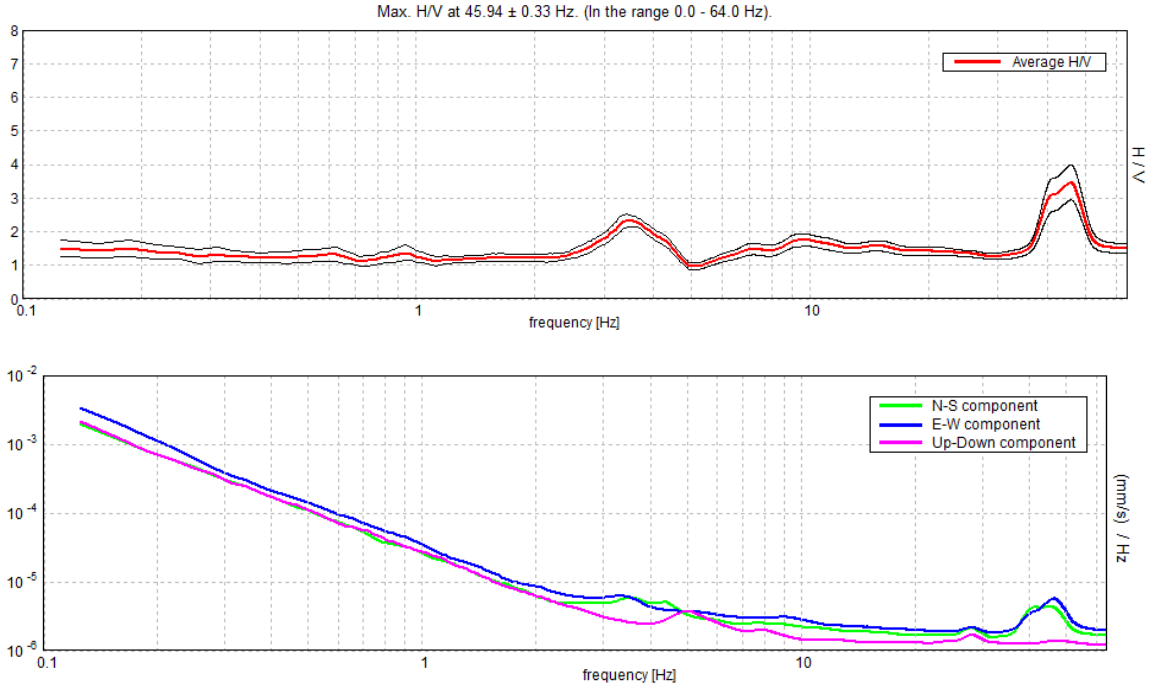

Figure 2: An example of the H/V spectra and corresponding 3-component spectra at the Leonora Breakaways, WA.

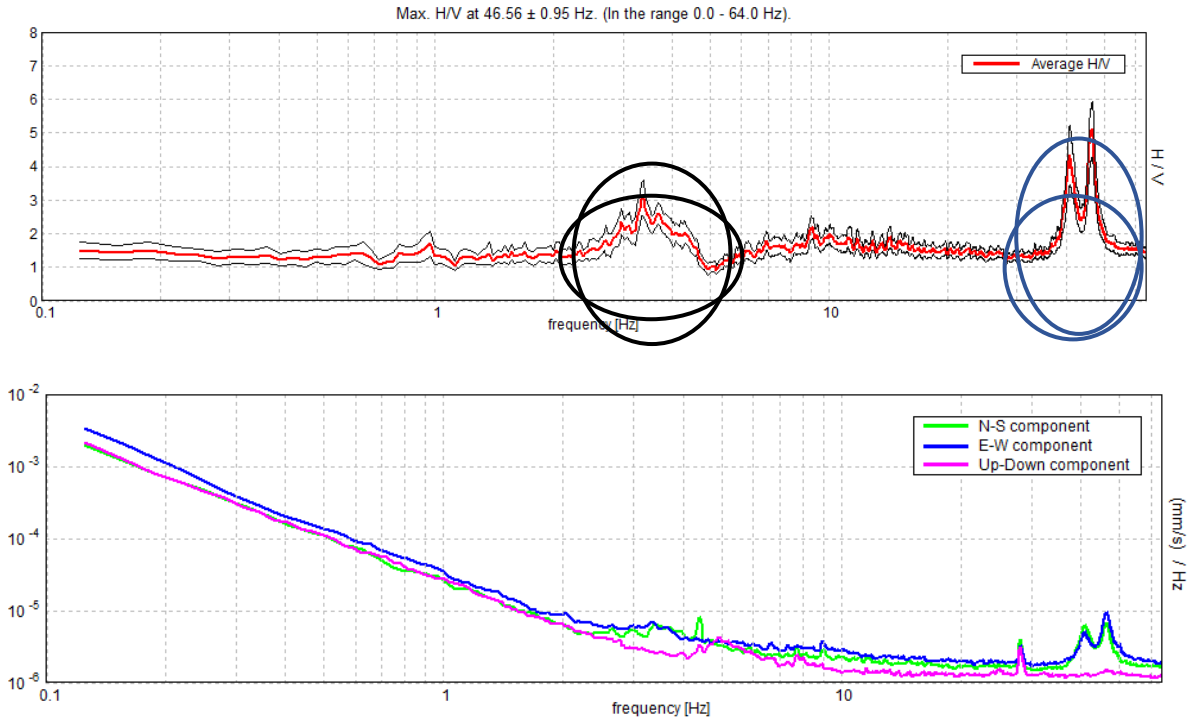

Figure 3: Smoothing dropped to 1% to check the stratigraphic origin of the passive seismic measurement. Stratigraphic peak circled in black. Anthropic peak circled in blue.

The passive seismic profiles for the first four locations PSA01–PSA04 show that the estimated interface between the weathered granite and fresh rock is at depths between ~25 and 28 m. Measurements at site PSA05 were able to pick two frequency peaks. We interpret the first peak as the interface between the relict sandplain and the weathered granite, at a depth of ~5 m. The second peak, at 33 m depth marks the interface between the weathered granite and fresh rock, which gives the thickness of the weathered granite for this location to be 28 m. From the passive

seismic data we estimated the weathering depth of granitic rocks for the Leonora breakaways to be between ~25 and 28 m.

References

Bourbie T., Coussy O. and Zinszner B. 1987. *Acoustics of Porous Media*. Institut Francais du petrole publications. Gulf Publishing Company, Book Division, The University of California, ISBN 0872010252.

Bradley J.J., Sanders A.J., Varga Z.S. and Storey J.M. 1995. Geochemical mapping of the Leonora 1:250 000 sheet. Regolith Geochemistry Explanatory Notes, Geological Survey of Western Australia, DMIRS.

Davy R. and Gozzard J.R. 1995. Lateritic duricrust of the Leonora area, Eastern Goldfields, Western Australia: A contribution to the study of transported laterites. *Geological Survey of Western Australia*, Record 1994/8.

Ibs-von Seht M., Wohlenberg J. 1999. Microtremor measurements used to map thickness of soft sediments. *Bulletin of the Seismological Society of America* **89(1)**, 250-259.

Lane Jr. J.W., White E.A., Steele G.V. and Cannia J.C. 2008. Estimation of bedrock depth using the horizontal-to-vertical (H/V) ambient-noise seismic method. *In*: Symposium on the Application of Geophysics to Engineering and Environmental Problems, April 6-10, 2008, Philadelphia, Pennsylvania, Proceedings, Denver, Colorado, Environmental and Engineering Geophysical Society, p.13.

MOHO. 2015. Tromino User's Manual. MOHO Science and Technology Firmware ver. 2015.01.

Nakamura Y. 1989. A method for dynamic characteristics estimations of subsurface using microtremors on the ground surface, Quarterly Report, RTRI, Japan **30**, 25-33.

Scheib A.J. 2014. The application of passive seismic to estimate cover thickness in greenfields area of Western Australia - method, data interpretation and recommendations. *Geological Survey of Western Australia*, Record 2014/9, 67p.

Stewart A.J. 2004. Leonora, W.A. (2nd edn.): Western Australia Geological Survey, 1:250 000 Geological Series Explanatory Notes, 46 pp.

Evaluating geomorphic and subsurface controls on surface water-groundwater interactions to contextualize a floodplain rehydration project at Mulloon Creek, NSW Southern Tablelands

L. Moore
University of Canberra

The influence of regolith configuration on hydrology and hydrogeology in the Ginini Flats Ramsar Wetland Complex, Namadgi National Park, ACT

A. Cowood
University of Canberra

Modelling initial carbonate platform formation in groundwater upwelling zones, Lake Eyre South region, South Australia

M. Keppel[1,2], V. Post[2] and A. Love[2]

[1]South Australian Government, Department of Environment, Water and Natural Resources. 81-95 Waymouth Street, Adelaide, South Australia, 5000. Australia.
[2]National Centre for Groundwater Research and Training (NCGRT), College of Science & Engineering, Flinders University, GPO Box 2100, Adelaide, South Australia, 5001

Carbonate depositional systems related to groundwater upwelling are ubiquitous around the world and form ecologically and culturally important features of many landscapes. In South Australia, the iconic mound springs, which are dome-shaped structures composed predominantly of calcium carbonate, are such an example. The upwelling and point discharge of groundwater from the Great Artesian Basin is predominantly responsible for the formation of these mounds.

To explain how these structures initially form, a carbonate-reaction hydrochemistry and water balance model, previously developed to investigate hydrochemical and spring flow processes in present-day mound spring wetlands, was adapted as a means of providing insight into this process Keppel *et al*. 2011; 2012a). Conceptually, we exploit their well-defined, circular geometry to demonstrate the existence of two size-limiting regimes: One controlled by the spring flow rate and the other by calcium carbonate concentration and precipitation (Keppel *et al*. 2012b). We found that the mound footprint predicted by the model provided a reasonable approximation of the measured footprint. Further, differences between predicted and measured mound footprints may be indicative of gross changes in discharge rate from a given spring over time.

The application of the model to past environments necessitates critical assumptions regarding past discharge and environmental conditions. This is particularly important where modelled estimates diverge notably from mapped extents. Sensitivity analysis suggests the model to be most consistently sensitive to changes in spring flow and the related value of the water column height in the mound spring wetland. Conversely, the model was consistently least sensitive to changes in evapotranspiration flux.

In most examples, the footprint of calcareous mound spring structures is conceptualised as being primarily a product of carbonate precipitation rather than spring flow, although the sensitivity of the model to discharge suggests this is also influential (Keppel 2013). This finding helps explain how active springs with reasonable variations in flow may produce mounds of comparable size and also cautions against simple correlation between spring flow and the size of resultant mound constructions.

The work presented here provides a “proof of concept” in that the acceptable similarity between the predicted footprint from carbonate-reaction modelling and the measured footprint of a spring-related structure suggests the model can be used as a basis for quantitative constraints on determinations of past spring activity. Consequently the application of carbonate-reaction hydrochemistry modelling as a means of explaining initial mound formation, combined with dating of material from calcareous spring deposits, may have application as a paleo-hydrological tool.

References

Keppel M.N. 2013. The geology and hydrochemistry of calcareous mound spring wetland environments in the Lake Eyre South region, Great Artesian Basin, South Australia. Ph.D Thesis. Flinders University, South Australia, 412 pp.

Keppel M.N., Clarke J.D.A., Halihan T., Love A.J. and Werner A.D. 2011. Mound springs in the arid Lake Eyre South region of South Australia: A new depositional tufa model and its controls. *Sedimentary Geology* **240**, 55-70.

Keppel M.N., Post V., Werner A. D., Love A., Clarke J. and Halihan T. 2012a. The use of water balance and carbonate reaction modelling to predict the initial formation of mound spring structures, central South Australia, *In*: International Association of Hydrogeologists 2012 Congress, Niagra Falls, Canada.

Keppel M.N., Post V.E.A., Love A.J., Clarke J.D.A. and Werner A.D. 2012b. Influences on the carbonate hydrochemistry of mound spring environments, Lake Eyre South region, South Australia. *Chemical Geology*, **296-297**, 50-65.

Seeing red: a history of redness in Australian landscapes

B. Pillans[1]

[1]Research School of Earth Sciences, ANU, Canberra

The iconic Red Centre of Australia broadly corresponds with the driest part of the continent - the Australian Arid Zone (AAZ) - suggesting that redness is related to aridity. However, the history of redness in Central Australia is longer than that of the AAZ. Indeed, the formation of red rocks and regolith is more constrained by atmospheric oxygen levels than by aridity.

In this talk I will briefly review the history of atmospheric oxygen, the ages of red rocks and regolith and the origins of aridity in Central Australia, to show that the history of redness may extend back to the Archean Eon (more than 2.5 billion years ago).

Introduction

Byrne *et al.* (2008) defined the AAZ as the region of Australia having a moisture index of less than 0.4 (mean annual rainfall divided by evaporation). Defined in this way, it stretches from the northwest coast of Western Australia, through the southern half of the Northern Territory and northern and central South Australia, to western New South Wales and Queensland in the east (Fig. 1). [Tourist information brochures usually refer to the 'Red Centre' as the area extending some 250 km west and south of Alice Springs, which certainly includes iconic red landforms such as Uluru, Kata Tjuta, the West Macdonell Ranges and Kings Canyon. However, equally iconic red landforms are much more widespread, including the sand dunes of the Simpson Desert and the gorges of Karijini National Park in Western Australia].

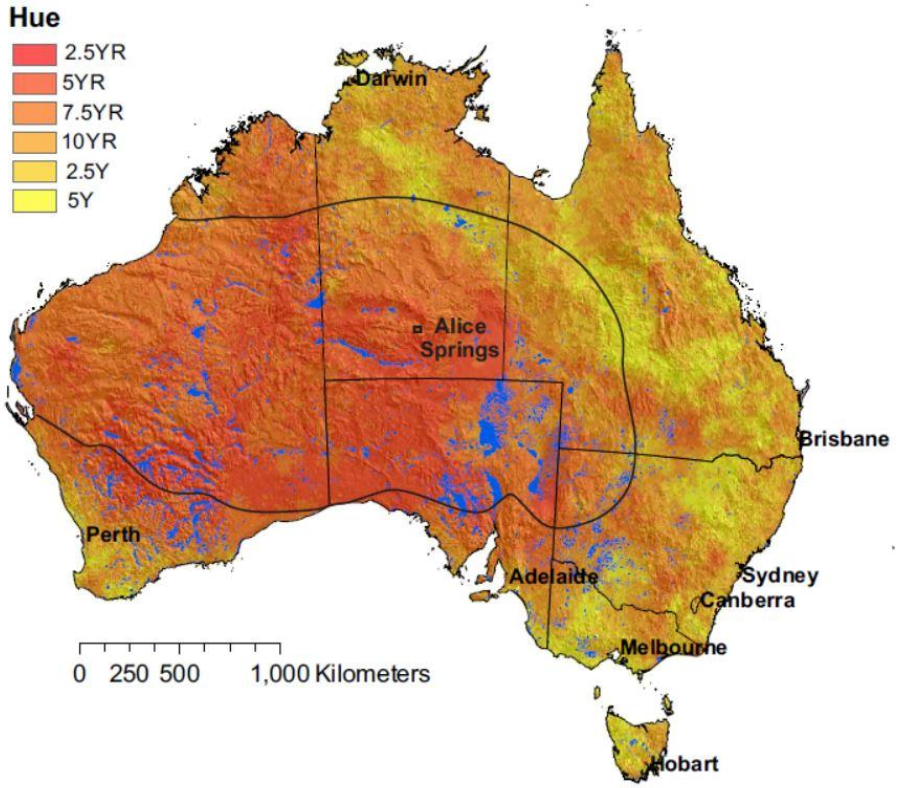

Figure 1: Spectral hue of Australian soils (after Viscarra Rossell et al. 2010), compared with the areal extent (black line) of the Australian Arid Zone (Byrne *et al*. 2008).

The redness of regolith is largely a function of iron oxide mineralogy, which varies with environmental conditions such as pH, Eh, temperature and moisture. In particular, red colours are associated with hematite. Viscarra Rossel *et al.* (2010) measured the reflectance spectra of more than 4000 surface soil samples from across Australia to generate RGB true colours that could be converted to Munsell parameters of Hue, Value and Chroma (spectral colour, lightness and

brightness, respectively). Mapped according to Hue, Figure 1 shows that the Australian Arid Zone is indeed dominated by 'red' hues.

Actually, not all hematite looks red – coarsely crystalline hematite is often a dark-grey metallic colour. Geologists have long used what is called the 'streak test' to distinguish hematite from other, similar looking minerals which involves scratching a white, unglazed porcelain surface – the resulting powder scratch or streak is characteristically red for hematite, suggesting that, in part, the red colour is dependent on the presence of fine particles, which the streak test creates. Similar links between fine grained (<2 μm) hematite and its red colour have been noted in a range of geological studies (e.g., Walker 1979; Morris *et al.* 1985; Blodgett 1988). Laboratory studies have also demonstrated a link between magnetic properties and redness (Rossman 1996).

Atmospheric oxygen

Formation of red-pigmenting hematite requires free oxygen, the primary source of which is photosynthesis. Oxygen forms some 21% of the modern atmosphere, but for much of Earth history it was much lower – low enough to inhibit oxidation of Fe to form hematite (Fig. 2). Atmospheric oxygen levels during the Archean (4 to 2.5 Ga) were extremely low, <0.001% of the present atmospheric level (PAL), as evidenced by the widespread occurrence of redox-sensitive detrital siderite ($FeCO_3$), pyrite (Fe_2S) and uraninite (UO_2) in Archean sediments (Catling & Claire 2005).

Between 2.4 and 2.1 Ga, atmospheric oxygen apparently increased dramatically - usually referred to as the Great Oxygenation Event. Red-weathered sediments (Red Beds) appear in the geological record, detrital pyrite disappears and atmospheric oxygen probably rose to around 1-3% PAL (Catling & Claire 2005). The Great Oxygenation Event could have been a response to emergence and proliferation of photosynthetic organisms, the earliest of which were probably cyanobacteria.

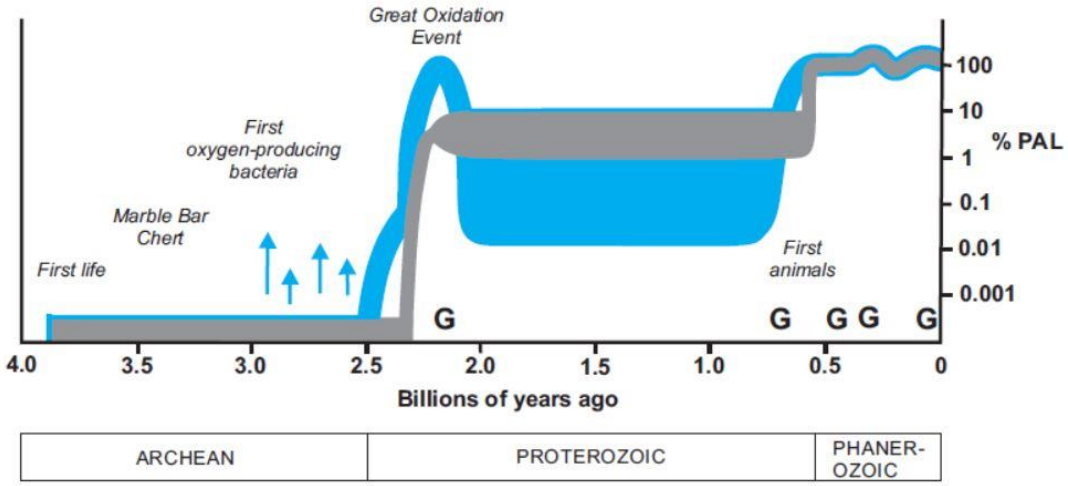

Figure 2: History of atmospheric oxygen (after Lyons *et al* 2014). Grey curve shows classic two-step view of atmospheric oxygen evolution. Blue curve is another model, with blue arrows indicating possible 'whiffs' of oxygen in late Archean. Right axis (%PAL) indicates percentage of oxygen relative to present atmospheric level. G = major glacial episodes.

During the Proterozoic, atmospheric oxygen likely remained well below modern levels, until it increased to approximately modern levels about 600 million years ago, associated with the rise of animals (Canfield *et al.* 2007; Brocks *et al*. 2017). Subsequently, atmospheric oxygen has fluctuated between about 0.75 and 1.75 PAL (between 15% and 35% oxygen in the atmosphere, respectively), which is the so called 'fire window'', constrained by the occurrence of fossil charcoal since the latest Silurian, 419 million years ago (Glasspool & Scott 2010).

Red rocks of Archean age?

Spectacular banded red rocks occur form a prominent rock bar across the Coongan River at Marble Bar, in Western Australia (Fig. 3). The rock bar gave its name to the nearby town of Marble Bar, but, despite the name, the rock is not marble, it is a type of jasper or chert. The Marble Bar Chert consists of alternating layers of silica and hematite, interpreted by Hoashi *et al.* (2009) to have been deposited in partly oxygenated ocean water 3.46 billion years ago. They suggested that the hematite crystals formed from hydrothermal fluids, rich in ferrous iron, at temperatures greater

than 60°C. According to Hoashi *et al.* (2009), the hematite is detrital, meaning that it was deposited as sedimentary particles, not formed by post-depositional weathering – in other words, it was red from the start. If correct, this represents the oldest known occurrence of red rocks in Australia, and probably the world. Subsequently, Rasmussen *et al.* (2014a) undertook a detailed petrographic study of the Marble Bar Chert, and concluded that the hematite was not primary, but rather it formed after sediment deposition. Key observations supporting a secondary origin of the hematite included the presence of magnetite cores in some hematite grains, lateral transitions in mineralogy within individual sediment layers and the occurrence of hematite in fractures and veins. In contrast, Hoashi *et al.* (2009) observed hematite crystals in the cores of many magnetite crystals, but not on the outside, indicating that the magnetite formed later than the hematite. Perhaps some of the hematite is primary, and there was a whiff of oxygen 3.46 billion years ago!

Figure 3: Marble Bar Chert (3.46 Ga) exposed on the Coongan River, near the town of Marble Bar, WA.

Other red rocks of Archean age in Western Australia, such as Banded Iron Formations, contain significant amounts of hematite, likely formed in multiple episodes of secondary mineral formation, subsequent to the Great Oxygenation Event (Rasmussen *et al*. 2014b; Abrajevitch *et al*. 2014).

Red weathering only skin-deep – but not always

The spectacular red rocks (Gidley Granophyre) on Burrup Peninsula, near Karratha are home to the world's largest gallery of rock art (Bird & Hallam 2006), but the red colour is confined to a 1 cm thick weathering rind and the unweathered interior of the rock is dark grey in colour (Pillans & Fifield 2013). A similar situation applies to Uluru, Kata Tjuta and Kings Canyon – the red colours are from surface weathering, much younger than the ages of deposition (Cambrian to Devonian) of the sedimentary rocks that comprise these landforms. However, in some places (e.g. the Tanami Desert), where deeply oxidised rocks may extend tens of metres below the surface, paleomagnetic dating has indicated the hematite pigmentation can be up 300 million years old (Pillans 2007).

Aridity in Central Australia

Major river systems characterised the Australian Arid Zone in the Cenozoic, preserved as large paleovalley systems that are buried beneath the modern arid landscape. These paleovalleys, which are important groundwater aquifers today, formed under a humid temperate climate, with higher rainfall, lower evaporation and a temperate rainforest vegetation (English *et al.* 2012).

The progressive development of the AAZ has its origins in the breakup and dispersal of the continental blocks that comprised Gondwana – India, South America, Africa, Antarctica, Australia and Zealandia. Separation of Australia from Antarctica, to enable establishment of the Antarctic Circumpolar Current around 30 Ma (Sher *et al*. 2015), reinforced the thermal isolation of Antarctica,

promoting growth of the Antarctic ice sheet, eventually leading to establishment of the modern ocean and atmosphere circulation patterns. The simultaneous northwards drift of the Australian continent and growth of the Antarctic ice sheet led to gradual juxtaposition of Central Australia with the belt of subtropical high pressure systems and increased aridity (Bowler 1982). Gradual uplift of the Maritime Continent (Indonesia), over the last 5 Ma, caused progressive constriction of warm ocean currents from the western Pacific into the Indian Ocean, resulting in cooler sea surface temperatures and seasonal aridity in northern Australia (Christensen *et al*. 2017).

Paleobotanical evidence suggests seasonal dryness from the Eocene onwards (Martin 2006), but the first truly arid landscapes, the stony deserts, did not develop until the Pliocene, some 3-4 Ma (Fujioka *et al.* 2005), while sandy desert landforms came later, starting around 1 Ma (Fujioka *et al.* 2009). The red colours that are pervasive in these landforms and regolith are therefore geologically very young (e.g. the hematitic coatings on quartz sand grains).

References

Abrajevitch A., Pillans B.J. and Roberts A.P. 2014. Haematite pigmentation events and palaeomagnetic recording: implications from the Pilbara Print Stone, Western Australia. *Geophysical Journal International* **199**, 658-672.

Bird C. and Hallam S.J. 2006. *Archaeology and rock art in the Dampier Archipelago*. A report prepared for the National Trust of Australia (WA), p. 32.

Blodgett R.H. 1988. Calcareous paleosols in the Triassic Dolores Formation, southwestern Colorado. *Geological Society of America Special Paper* **216**, 103-121.

Bowler J.M. 1982. Aridity in the late Tertiary and Quaternary of Australia, *In*: Barker W.A. and Greenslade P.J.M. eds. *Evolution of the flora and fauna of arid Australia*. Peacock Publications, Adelaide, pp. 35-45.

Brocks J.J., Jarrett A.J.M., Sirantoine E., Hallmann C., Hoshino Y. and Liyanage, T. 2017. The rise of algae in Cryogenian oceans and the emergence of animals. *Nature* **548**, 578-581.

Byrne M., Yeates D.K., Joseph L., Kearney M., Bowler J., Williams M.A.J., Cooper S., Donnellan S.C., Keogh J.S., Leys R., Melville J., Murphy D.J., Porch N. and Wyrwoll K.-H. 2008. Birth of a biome: insights into the assembly and maintenance of the Australian arid zone biota. *Molecular Ecology* **17**, 4398-4417.

Canfield D.E., Poulton S.W. and Narbonne G.M. 2007. Late-Neoproterozoic deep-ocean oxygenation and the rise of animal life. *Science* **315**, 92-95.

Catling D.C. and Claire M.W. 2005. How Earth's atmosphere evolved to an oxic state: A status report. *Earth and Planetary Science Letters* **237**, 1-20.

Christensen B.A., Renema W., Hendriks J., De Vleeschower D., Groeneveld J., Castenada I.S., Reuning L., Bogus K., Auer G., Ishiwa T., McHugh C.M., Gallagher S.J., Fulthorpe C.S., IODP Expedition 356 Scientists. 2017. Indonesian throughflow drove Australian climate from humid Pliocene to arid Pleistocene. *Geophysical Research Letters*.

English P.M., Lewis S.J., Bell J.G., Wischusen J.D.H. Woodgate M.F., Bastrakov E.N., Macphail M.K. and Kilgour P.L. 2012. *Water for Australia's arid zone - identifying and assessing Australia's palaeovalley groundwater resources: Project summation*, Waterlines Report Series No 86, August 2012, Canberra, p. 147.

Fujioka T., Chappell J., Honda M., Yatsevich I., Fifield K. and Fabel D. 2005. Global cooling initiated stony deserts in central Australia 2-4 Ma, dated by cosmogenic ^{21}Ne-^{10}Be. *Geology* **33**, 993-996.

Fujioka T., Chappell J., Fifield L.K. and Rhodes E.J. 2009. Australian desert dunes initiated with Pliocene-Pleistocene global climatic shift. *Geology* **37**, 51-54.

Glasspool I.J. and Scott A.C. 2010. Phanerozoic concentrations of atmospheric oxygen reconstructed from sedimentary charcoal. *Nature Geoscience* **3**, 627-630.

Hoashi M., Bevacqua D.C., Otake T., Watanabe Y., Hickman A.H., Utsonomiya S. and Ohmoto H. 2009. Primary haematite formation in an oxygenated sea 3.46 billion years ago. *Nature Geoscience* **2**, 301-306.

Lyons T.W., Reinhard C.T. and Planavsky N.J. 2014. The rise of oxygen in Earth's early ocean and atmosphere. *Nature* **506**, 307-315.

Martin H.A. 2006. Cenozoic climatic change and the development of arid vegetation in Australia. *Journal of Arid Environments* **66**, 533-563.

Morris R.V., Lauer Jr H.V., Lawson C.A., Gibson Jr E.K., Nace G.A. and Stewart C. 1985. Spectral and other physicochemical properties of submicron powders of hematite (α-Fe_2O_3), maghemite (γ-Fe_2O_3), magnetite (Fe_3O_4), goethite (α-FeOOH) and lepidocrocite (γ-FeOOH). *Journal of Geophysical Research* **90**, 3126-3144.

Pillans B. and Fifield L.K. 2013. Erosion rates and weathering history of rock surfaces associated with Aboriginal rock art engravings (petroglyphs) on Burrup Penisnsula, Western Australia, from cosmogenic nuclide measurements. *Quaternary Science Reviews* **69**, 98-106.

Rasmussen B., Krapež B. and Muhling J.R. 2014. Hematite replacement of iron-bearing precursor sediments in the 3.46-b.y.-old Marble Bar Chert, Pilbara craton, Australia. *Geological Society of America Bulletin* **126**, 1245-1258.

Rasmussen B., Krapež B. and Meier D.B. 2014. Replacement origin for hematite in 2.5 Ga banded iron formation: Evidence for postdepositional oxidation of iron-bearing minerals. *Geological Society of America Bulletin* **136**, 438-446.

Rossman G.R. 1996. Why hematite is red: Correlation of optical absorption intensities and magnetic moments of Fe^{3+} minerals, *In*: Dyar M.D., McGammon C. and Schaefer M.W. eds. *Mineral Spectroscopy: A Tribute to Roger G. Burns*. The Geochemical Society, Special Publication No. **5**, pp. 23-27.

Scher H.D., Whittaker J.M., Williams S.E., Latimer J.C., Kordesch W.E.C. and Delaney M.L. 2015. Onset of Antarctic Circumpolar Current 30 million years ago as Tasmanian Gateway aligned with westerlies. *Nature* **523**, 580-583.

Viscarra Rossel R.A., Bui E.N., de Caritat P. and McKenzie N.J. 2010. Mapping iron oxides and the color of Australian soil using visible-near-infrared reflectance spectra. *Journal of Geophysical Research* **115**, F04031.

Walker T.R. 1979. Red color in dune sand. *In*: McKee, E.D. ed. *A Study of Global Sand Seas*. US Government Printer, Washington, pp. 61-81.

Beneath the sand of the Tanami Desert

N.de Souza Kovacs

Geological Survey of Western Australia, Mineral House, 100 Plain St, East Perth WA 6004

The Ngururrpa area is located in the Tanami Desert, in the northeast of Western Australia. In 2013 the Ngururrpa traditional owners (Parna Ngururrpa) invited the Geological Survey of Western Australia (GSWA) to conduct gravity and geochemistry programs on their country. As a result, the Ngururrpa regolith landform map was produced as part of GSWA's 2015 regional regolith geochemistry program (Morris *et al*. 2018, Fig. 1). The Ngururrpa regolith-landform map has been compiled using remotely-sensed data (e.g. ASTER, Landsat), geophysics, Google Earth imagery, existing geological maps, and ground observations made during the regolith sampling program, as well as data from existing GSWA's databases. The mapping revealed diverse regolith landforms, and regolith thicknesses varying from a few metres to over 90 meters. The classification of regolith and approach to regolith-landform mapping has been discussed in the Geological Survey of Western Australia record 2013/7 (Geological Survey of Western Australia 2013).

Regolith and geology

The geology of the Ngururrpa area includes parts of the Proterozoic Granites-Tanami and West Arunta Orogens, the Neoproterozoic Murraba Basin, and the Paleozoic to Mesozoic Canning Basin. The landscape is flat, with variably weathered, low-lying rock outcrops, and extensive eolian dune fields, sandplain and lacustrine - playa terrain. The climate is semi-arid, soils are sandy, and the vegetation is composed mostly of spinifex grass with sparse, small shrubs and scattered small trees. The major topographic feature is the west-dipping sandstone and siltstone cuestas on the eastern margin of the Canning Basin forming the Stansmore Range (Fig. 2). The Range rises along the west side of the northwest-trending Stansmore Fault, a major regional tectonic structure. The Stansmore Fault runs mostly through the Canning Basin, but at the southern end of the Range the fault separates the Phanerozoic Canning Basin in the west from the Neoproterozoic Murraba Basin in the east (Fig. 2).

Regolith in the Ngururrpa area is extensive (>87%) and mostly depositional (>71%). The regolith layer varies in thickness, from a thin cover of quartz rich sand less than one metre thick near areas of outcrop and residual regolith, to more than 90 m thick over paleovalleys and paleochannels. Residual and relict regolith is varied, ranging from ferruginised lag a few centimetres thick to 70 m of weathered rock underlying paleovalleys. Regolith and bedrock show a broad compositional relationship. For example, Canning Basin rocks are ferruginised at the surface and the regolith formed from them is generally quartz-rich and ferruginous; whereas regolith developed over the Murraba Basin is generally quartz-rich and calcareous, and characterised by playa-lacustrine terrain and longitudinal dune fields.

Paleodrainage Network

Two paleodrainage networks have been identified, a deep network of broad calcrete-filled paleovalleys and a shallow network of paleochannels infilled with magnetic material. Four broad and deep calcrete-filled paleovalleys numbered 1–4 in Figure 3, occupy topographic depressions, as part of an internal drainage network into Lake Mackay (English 2016).At the surface, paleovalleys are delineated by lacustrine-playa landforms. Shallow stratigraphic drilling conducted in the Granites-Tanami Region by the Bureau of Mineral Resources revealed that these paleovalleys are filled with up to 15 m of calcrete and up to 90 m of unconsolidated alluvial sediments (Blake 1974).

A shallow network of dendritic buried paleochannels is visible in the aeromagnetic RTP 1VD image (Fig. 4). These paleochannels have minimal surface expression in areas of eolian cover, and their aeromagnetic response can be attributed to a high content of magnetic minerals including maghemite-rich gravel lenses (Mackey *et al*, 2000). In addition to aeromagnetic data, the extent of these paleochannels can also be traced using a variety of imagery. Moderate to high gamma-ray radiometric response for Th and U indicates relatively high concentrations of residual minerals in, and surrounding, the channels. The ASTER Ferric Oxide Content image maps the relative amounts of hematite and magnetite in these channels, whereas on the Landsat AGSO ratio image, paleochannels at the surface appear bright yellow, reflecting higher contents of clay and iron-rich

minerals. To be visible in the aeromagnetic images, the maghemite-rich gravel lenses in paleochannels have to be at least 0.4 to1 m thick, and at depths between 1.5 to 4.5 m (Mackey *et al*. 2000; Anand 2005). These paleochannels appear to be tributaries of the calcrete-filled paleovalleys. In the Stansmore Range area, the surface paleochannels and surrounding ferruginous duricrust are eroding to form Fe-rich sheetwash fans containing magnetic lag. In parts of the Stansmore Range area, paleochannels appear to be continuous but displaced vertically across the Stansmore Fault indicating the possibility of Cenozoic fault movement (Fig. 4).

Conclusion

Regolith cover can be characterised by combining regolith-landform mapping, drillhole data and geophysics, as exemplified by the mapping of the Ngururrpa area. Maghemite-filled paleochannels are possibly tributaries of the larger calcrete filled paleovalleys, as part of a regional paleodrainage system draining into Lake Mackay. Paleochannel displacement may indicate neotectonism along the Stansmore Fault.

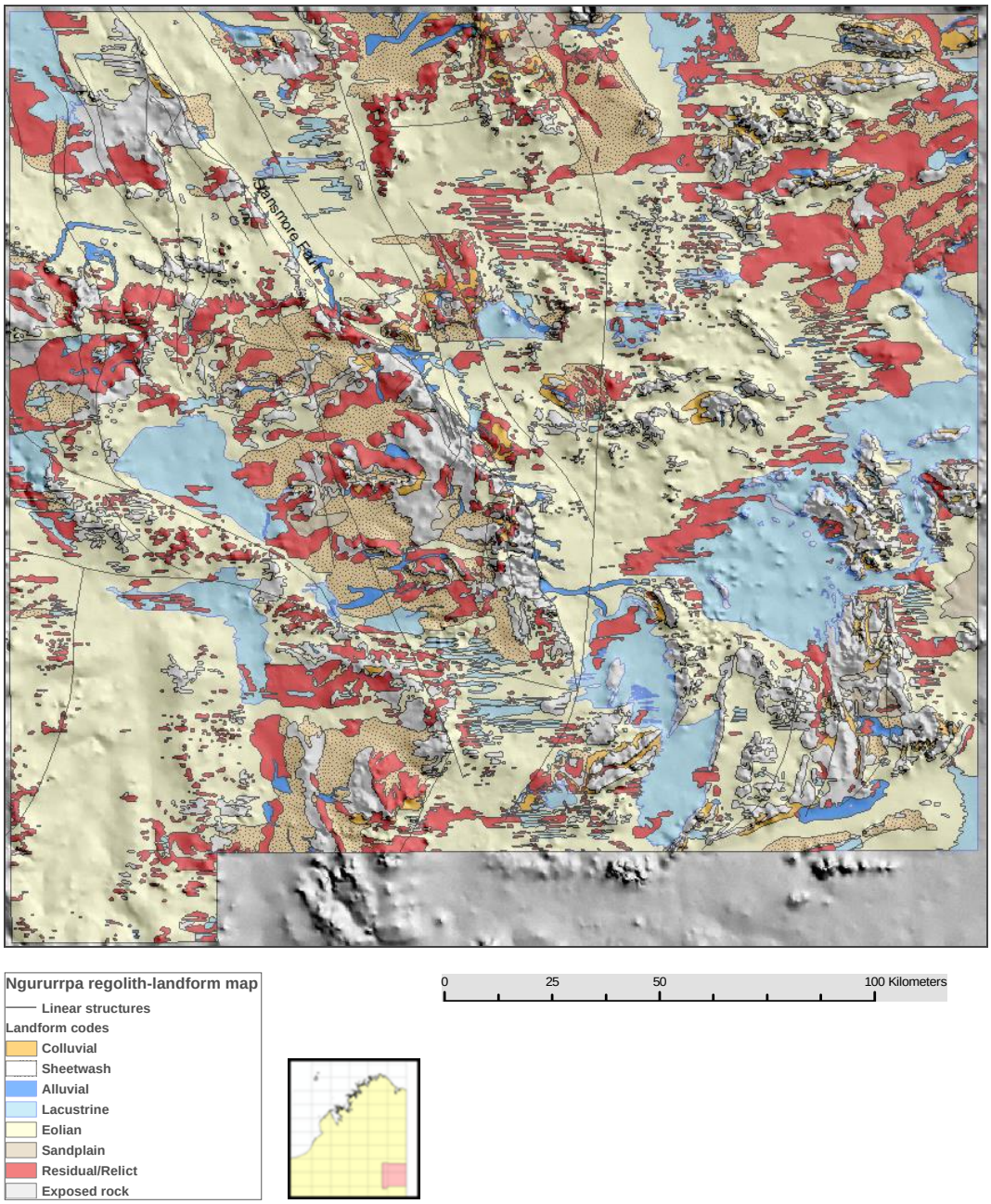

Figure 1: Simplified regolith-landform map of the Ngururrpa area, showing regolith-landform units according to the landform code only, and location of major faults and lineaments. The map is draped on digital elevation model image. Inset map shows the location of the Ngururrpa regolith and geochemical soil sampling program shown in red, NE of Western Australia.

Figure 2: West dipping cuestas of the Stansmore Range are the major topographic features in the area reaching up to 510 m (a.s.l). The range rises along the west side of the NW-SE trending Stansmore Fault. At the southern end of the ranges the fault separates hills of the Phanerozoic Canning Basin in the west from aeolian dunefields overlying the Neoproterozoic Murraba Basin in the east

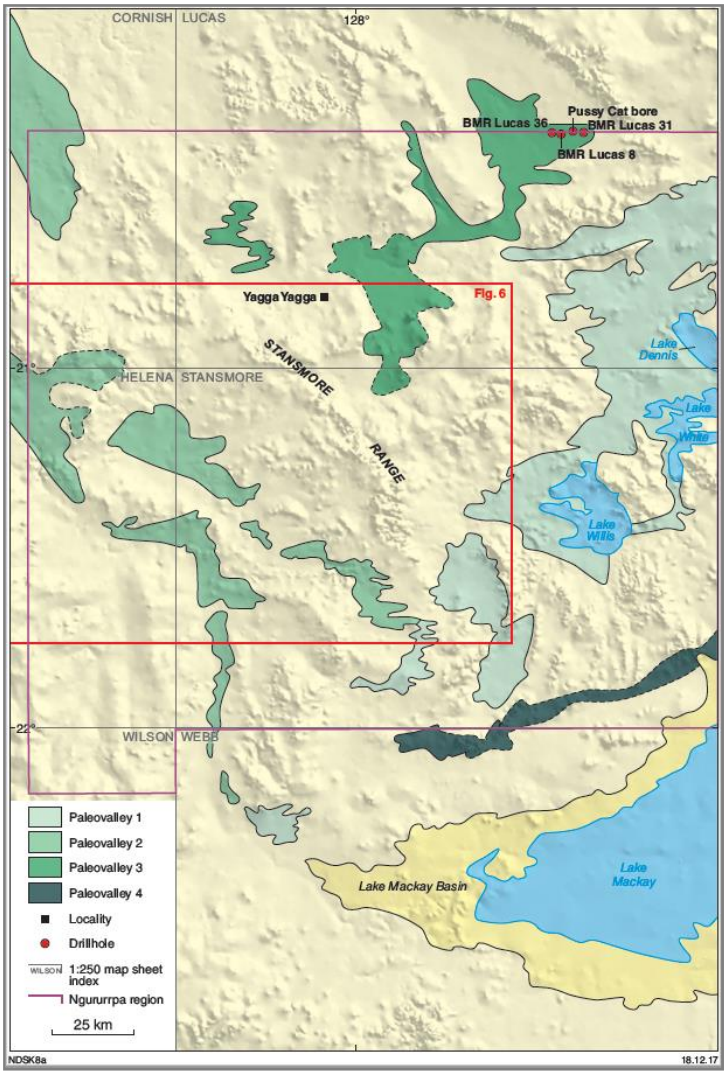

Figure 3: Distribution of four inset paleovalleys as part of an internal drainage network into Lake Mackay. The figure is drapped on digital elevation model image. Three stratigraphic drillholes are shown intersecting Paleochannel 3 which reached the 91 m deep in drillhole BMR Lucas 36. Potable water was encountered between 14-16.5 m, below 4 m of calcrete and 10 m of sand in drillholes BMR Lucas 8 (paleochannel is 49 m deep) and BMR Lucas 31 (paleochannel is 88 m deep). Pussy Cat bore contained potable water between 14-16.5 m deep (Blake 1974).

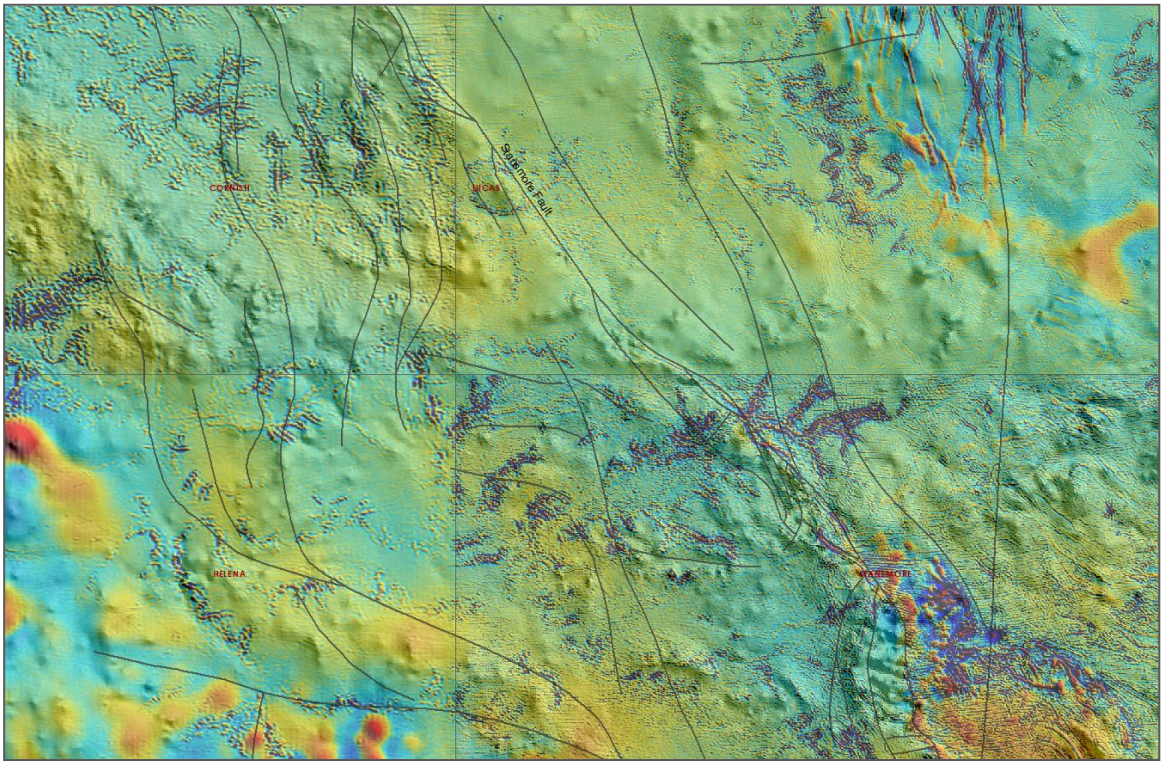

Figure 4: Magnetic RTP 1VD image draped on Digital Elevation Model. Dendritic network of paleochannels is visible in purple-red colour. A major paleochannel appears to cross the Stansmore Fault. Image source: Geological Survey of Western Australia.

References

Anand R.R. 2005. Weathering history, landscape evolution and implications for exploration. *In*: Anand R.R. and de Broekert P ed. *Regolith landscape evolution across Australia*. CRC LEME, Perth. 2-40.

Blake D.H. 1974. Shallow stratigraphic drilling in the Granite-Tanami Region, Northern Territory and Western Australia, 191 – 73. Bureau of Mineral Resources, Record BMR 1974/104.

English P. 2016. Ancient origins of some major Australian salt lakes: geomorphic and regional implications. *In*: Thomas M. ed. *Fourth Australian Regolith Geoscientists Association Conference Proceedings*, February 2016, Thredbo NSW.

Geological Survey of Western Australia 2013. Revised classification system for regolith in Western Australia, and the recommended approach to regolith mapping: Geological Survey of Western Australia, Record 2013/7.

Mackey T., Lawrie K., Wilkes P., Munday T., de Souza Kovacs N., Chan R., Gibson D., Chartres C. and Evans R. 2000. Palaeochannels near West Wyalong, New South Wales: a case study in delineation and modelling using aeromagnetics. *Journal of Exploration Geophysics*, June 2000**, 31, 1/2**: 1-7.

Morris P.A., De Souza Kovacs N. and Scheib A.J. 2018, Regolith geochemistry of the Ngururrpa area, northeastern Western Australia: Geological Survey of Western Australia, Record 2018/3.

Aeolian dust in vineyard soils in Australia and New Zealand: how their properties may influence wine quality

R.Greene[1], R. Gibson[2], P.Fogarty[3], C. Strong[1] and D. Freundenberger[1]

[1]Fenner School of Environment and Society, ANU, Canberra, ACT, 0200
[2]Vigneron, Central Otago, New Zealand
[3]Soil and Land Conservation Consulting Pty Ltd

Introduction

Terroir is a term used to define the features of a wine growing region that reflect the region's physical qualities such as climate, geology, topography, and soils. There is an increasing interest in understanding the overall role of soil properties in determining the quality of wine from vineyards (Bramley *et al*. 2011).

This paper discusses the importance of aeolian dust in determining soil properties that influence the quality of wines. The soils from vineyards in two wine regions are discussed; one is the Murrumbateman wine region situated in the Yass River Valley of New South Wales, Australia, and the other region is in the Cromwell Basin, Central Otago, and New Zealand. Both of these regions have soils that contain deposits of aeolian dust (referred to as parna in the Australian context, and loess in New Zealand). Figures 1a) and 1b) depict the two of the soil profiles from the Yass Valley and Cromwell Basin respectively discussed in this paper.

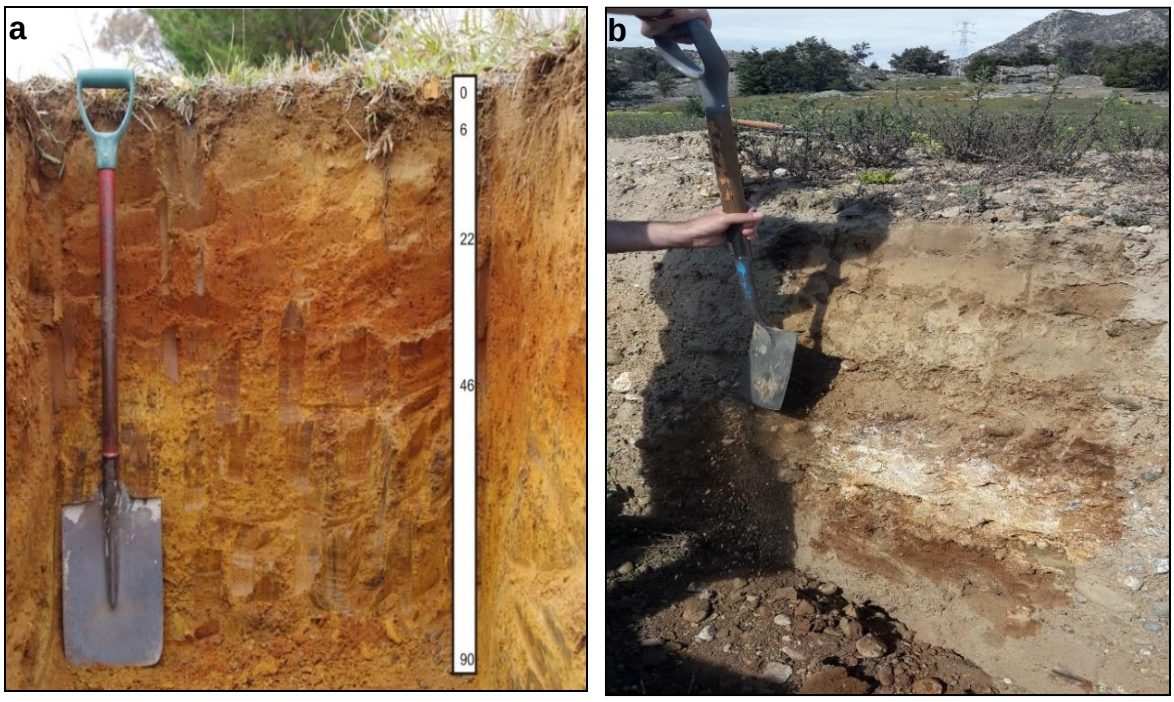

Figure 1: a) Soil profile Yass Valley containing parna material 25-40 cm. b) Soil profile in Cromwell Basin, Central Otago NZ containing loess material 0.5-60 cm.

The key hypothesis put forward in this paper is that the particle size and aggregation of the parna/loess component of these soils confers advantages to the quality of the wine produced on them. It does this through the moisture retention properties of the soil: i.e. by creating appropriate tensions during the key periods in vine ripening to create the right amount of stress for optimal production of secondary metabolites (e.g. tannins).

This paper presents a description of the soils in the two regions, plus some preliminary data from two soil profiles in the Yalley Valley, NSW.

Background to study sites

Study Site 1, Murrumbateman, Yass Valley, NSW

The Murrumbateman region in the Yass Valley is a well-established "cool climate" wine region having a relatively dry temperate climate, with an average yearly rainfall 652 mm, and average high and low temperatures of 21° C and 7° C respectively. It is situated approximately 50 km north of Canberra (Fig. 2). During the relatively hot summers the water requirements of the vines are supplemented by irrigation.

Vineyard soils in this area are largely derived from dacite geology. The rocks have weathered to form soils ranging from well drained deep red chromosols through to imperfectly drained yellow chromosols and tenosols. There is also evidence for a contribution of windblown (aeolian) fine silt to the development of vineyard soils in the region. These aeolian deposits (also named "parna" by Butler & Hutton 1956) which overlay the parent geology are thought to improve the water holding capacity, drainage and fertility of vineyard soils. Previous studies (Melis & Ackworth 2001, Walker *et al*. 1988) have also highlighted the presence of discrete aeolian deposits in soils of the Yass Valley.

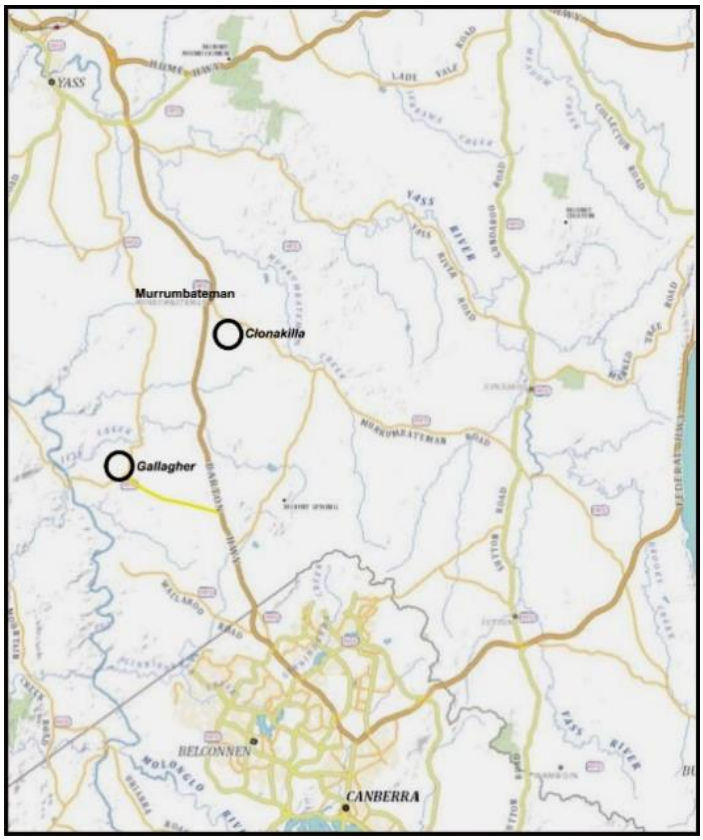

Figure 2: Map of Murrumbateman wine region, Yass Valley, NSW.

Study Site 2, Cromwell, Central Otago New Zealand

Central Otago is a rapidly growing wine region gaining significant international recognition particularly for the quality of its Pinot Noir (Fig. 3). Although New Zealand is considered Oceanic in its climate, Central Otago is located in an inland basin surrounded by mountains protecting it from the weather from all directions. Its climate is better described as continental-like.

It is very dry and is the hottest and coldest part of mainland New Zealand, with an average yearly rainfall of 391 mm, and average high and low temperatures 17° C and 5° C respectively. Because the rainfall is low and vast water supplies are available from high in the adjacent Southern Alps, perfect moisture control is achieved through careful irrigation.

The landscape of the Cromwell Basin has been significantly shaped through the glacial advances and retreats of the Pleistocene, the last million years of which has seen a series of major advances each being smaller than the previous. Each advance has been accompanied by a melt phase and

massive deposition of glacial outwash material filling the valley up to a level not as high as the previous event and thus creating a series of terraces. The oldest terrace we find vineyards on can be dated back to circa 650,000 years (Q16), whereas the youngest surfaces are post glacial and a mere few thousand years old. There is of course everything in between.

Loess deposition is a feature of soils of the entire eastern side of New Zealand. The predominantly and at times very strong westerly winds pick up the sediment from the geologically active mountains and from the many river beds, spreading the sediment across the eastern side of both main islands. The amount of loess encountered in a soil profile is a function of time and local topography. Exposed ablation surfaces may have none at all whereas parts of the landscape favoring deposition (e.g. protected terraces) can easily have 0.5-60 cm. Greater depths can be encountered in some locations.

Soil textures in Central Otago are also influenced by the accumulation of pedogenic/illuvial clay in a Bt horizon typically at a depth of 0.5-70 cm. The level of clay accumulation is a function of the age of the surface and on the older surfaces can exceed 20% within the Bt horizon. Pedogenic lime also accumulates as a Bk or on mature profiles as a Bkm horizon underneath this.

What results is a landscape with vineyards growing on glacial outwash or river gravels with no silt and no clay accumulation through to relatively young surfaces, which may have significant silt deposition then to older surfaces, which may have both silt and clay. The water retention and release properties of these soils differ very significantly even though the soils may be geographically located very close to each other.

Figure 3: Map of Cromwell Basin, Central Otago, New Zealand.

Laboratory Measurements

During 2017 as part of a preliminary investigation into the role of soil properties in determining wine quality, a range of undisturbed and disturbed samples were taken from various horizons at soil profiles the Yass Valley site. The undisturbed samples included a core of an A2 horizon (non parna) and a core of a B2 horizon (parna) from the profile in Figure 1a. The disturbed samples came from (i) a soil horizon of parna material occurring in the soil profile at the Clonakilla vineyard (shown in Fig. 2) and (ii) a soil horizon of non-parna material from another soil profile (Gallagher vineyard in Fig. 2).

The undisturbed samples were applied to pressure plates for determination of their moisture retention curves, while the disturbed samples were subjected to measurements of particle size analysis (psa) using a Mastersizer.

Results and Discussion

Moisture retention curves from two soil cores at the Yass Valley site; i.e. one from a parna horizon and the other a non-parna horizon were investigated. The results from the moisture retention release curves from the two horizons were fitted to the van Genuchten water retention model (1980) that allows the hydraulic properties of the soils to be tested for any statistically significant differences.

The results of the psa measurements on the 25-40 cm horizon of parna material from the Yass Valley depict a very clear bi-modal distribution, which changes after the application of ultrasonics to show a very strong peak at 20-30 µm and therefore provides strong evidence for the occurrence of strongly aggregated clay material referred to as “parna” by Butler and Hutton (1956) (Fig. 4a). However, at the other profile the psa measurements of non-parna material from 40-90 cm showed very little evidence after ultrasonics of a strong peak that would indicate strongly aggregated clay, thus confirming the absence of parna (Fig. 4b).

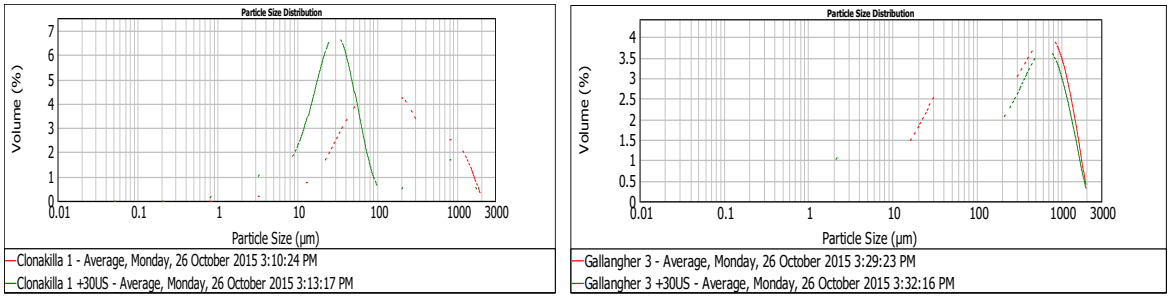

Figure 4: a) Mastersizer psa results of parna horizon b). Mastersizer psa results from non-parna horizon

The cause and effect link between soil texture and wine character comes through the degree of moisture stress the plant may encounter during the growing season. As texture or particle size determines the size of the micro-pores gaps and the size of the micro-pore determines how hard a plant needs to work it will set the level, or at least the range, of stress levels the plant will encounter when extracting water from the soil depending on irrigation management. Stress in plants is well known to trigger production of all sorts of secondary metabolites many of which can affect the character of wine, some of the best known being tannins. Hence there is a direct logical link between texture (influenced by parna/loess deposition and clay accumulation) and wine character. Despite statements that sometimes gets bandied about within the international wine industry which suggest irrigation destroys expression of terroir it’s not so – irrigation used wisely may simply enhance the expression, an expression that is determined by the soil texture.

Acknowledgements

The authors acknowledge the co-operation of the owners and staff at the Clonakilla and Gallagher Yass Valley wineries.

References

Bramley R.G.V., Ouzman J. and Boss P.K. 2011. Variation in wine vigour, grape yield and vineyard soils and topography as indicators of variation in the chemical composition of grape wine and wine sensory attributes. *Australian Journal of Grape and Wine Research* **17**, 217-227.

Butler B.E. and Hutton J.T., 1956. Parna in the Riverine Plain of south-eastern Australia and the soils thereon. *Australian Journal of Agricultural Research* **7**, 536–553.

Melis M.I. and Acworth R.I. 2001. An aeolian component in Pleistocene and Holocene valley aggradation: evidence from Dicks Creek catchment, Yass, New South Wales. *Australian Journal of Soil Research* **39**, 13–38.

Van Genuchten, M Th., 1980. A closed-form equation for predicting the hydraulic conductivity of unsaturated soils. *Soil Science Society of America Journal* **44**, 892-898.

Walker P.H., Chartres C.J. and Hutka, J., 1988. The effect of aeolian accessions on soil development on granitic rocks in south-eastern Australia. I. Soil morphology and particle-size distributions. *Australian Journal of Soil Research* **26**, 1–16.

Distribution of transported regolith along the Skeleton Coast Erg of Namibia: a complex story of fluvio-aeolian interaction

C.B.E. Krapf

Geological Survey of South Australia, PO Box 320, Adelaide SA 5000

The Skeleton Coast Erg forms a prominent 6–22 km wide NNW-trending dune belt comprising dunes up to 50 m high, subparallel to the southern Atlantic coastline of Namibia. The dune belt dams WSW-wards flowing ephemeral river systems on their route towards the ocean. The interactions between these two systems have not only significant implications for the geomorphology of the landscape (Krapf *et al*. 2003; Bullard & Livingstone 2002), but also for the distribution of various transported regolith materials preserved in such environments (Fig. 1; Langford 1989; Langford & Chan 1989; Stanistreet & Stollhofen 2002).

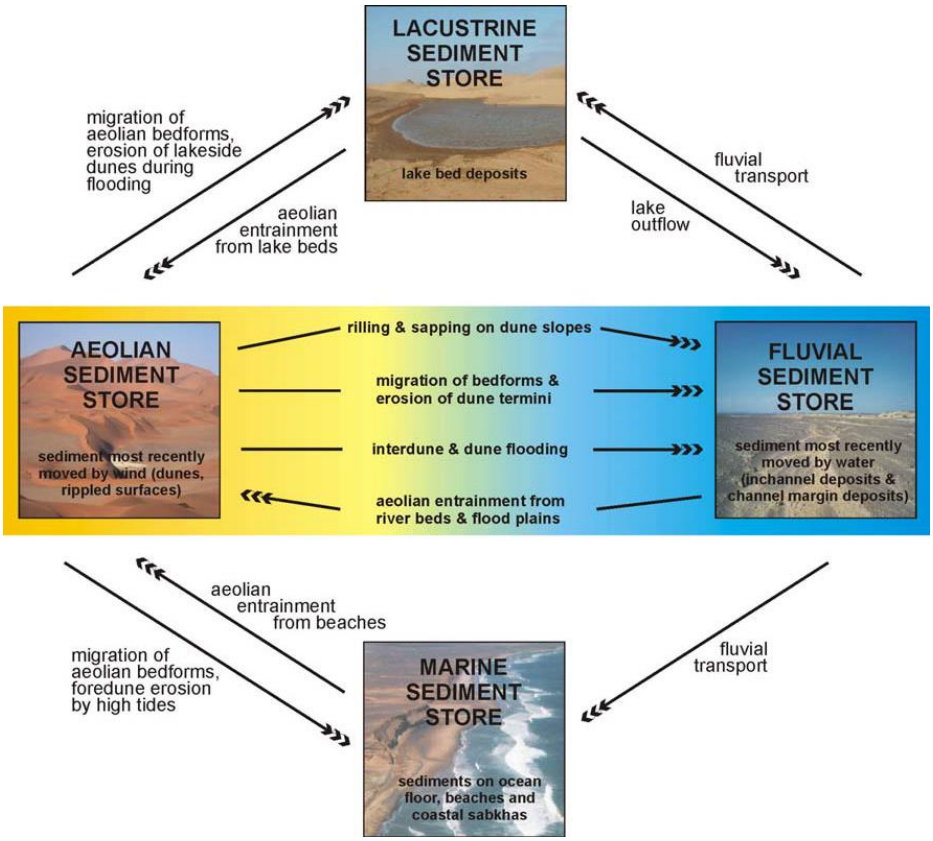

Figure 1: The linkage between the four main sediments stores for sand-sized material in dryland environments (from Krapf 2002; modified after Bullard & Livingstone 2002).

Five ephemeral rivers (Fig. 2), which variously interact with the Skeleton Coast Erg, were chosen for the purpose of this study to consider the variability of parameters within these fluvio-aeolian systems and resultant regolith material distribution and preservation. The styles of fluvio-aeolian interactions between the rivers and the dune field are controlled by the climate and the geology of the river catchment areas, the sediment load of the rivers, their depositional architecture, the longitudinal river profiles, as well as the 3D architecture of the Skeleton Coast Erg.

Resulting processes are: 1) aeolian winnowing of fluvially derived material and sediment transfer into and deposition within the erg; 2) dune erosion during break-through resulting in hyperconcentrated flow and intra-erg mass flow deposits (Svendsen *et al*. 2003); 3) the development of extensive flood-reservoir basins caused by dune damming of rivers during flood; 4) interdune flooding causing stacked mud-pond sequences; and 5) the termination of the erg by more frequent river floods.

The southernmost river, the Koigab River, plays an important role providing sand for the southern end of the erg (Krapf *et al*. 2005). North of the Koigab River a chain of low basement hills provides a localized trap for sand deflated off the fan surface through flow separation. This trap feeds sand into the downwind edge of the erg, representing a major sand input area (Lancaster 1982). In contrast, the Hoarusib River flows sufficiently often to prevent a northward migration of the erg. Hence, it forms the northern boundary of the erg by flushing aeolian sand into the Atlantic Ocean, in a manner akin to the effects of the Kuiseb River as the northern boundary of the southern Namib Sand Sea (Ward 1987). Between these two, the remaining rivers provide a spectrum of types of interaction with the dunes of the erg.

Figure 2: Landsat TM5 image 181-074 (741 RGB) of the Skeleton Coast Erg/NW Namibia, taken on August, 22nd, 1984. Dominant in the Skeleton Coast Erg are simple and locally compound, barchanoid and transverse dunes arranged into a 6 to 22 km wide belt that parallels 2 to 5 km inland the southern Atlantic coastline. The main wind direction is from south-southwest.

References

Bullard J.E. and Livingstone I. 2002. Interactions between aeolian and fluvial systems in dryland environments. *Area* **34.1**, 8-16.

Krapf C.B.E., Stanistreet I., Stollhofen H. 2005. Morphology and fluvio-aeolian interaction of the tropical latitude, ephemeral braided-river dominated Koigab Fan, north-west Namibia. *In:* Blum M.D., Marriott S.B. and Leclair S.F. eds. Fluvial Sedimentology VII. *IAS Special Publication* **35**, 99-120.

Krapf C.B.E., Stollhofen H., Stanistreet I. 2003. Contrasting styles of ephemeral river systems and their interaction with dunes of the Skeleton Coast erg (Namibia). *Quaternary International* **104**, 41-52.

Langford R.P. 1989. Fluvial-aeolian interactions: Part I, modern systems. *Sedimentology* **36**, 1023-1035.

Langford R.P. and Chan M.A. 1989. Fluvial-aeolian interactions: Part II, ancient systems. *Sedimentology* **36**, 1037-1051.

Stanistreet I.G. and Stollhofen H. 2002. Hoanib River flood deposits of Namib Desert interdunes as analogues for thin permeability barrier mudstone layers in aeolianite reservoirs. *Sedimentology* **49**, 719-736.

Svendsen J, Stollhofen H., Krapf C., Stanistreet I. 2003. Mass and hyper-concentrated flow deposits record dune damming and catastrophic breakthrough of ephemeral rivers, Skeleton Coast Erg, Namibia. *Sedimentary Geology* **160 (1-3)**, 7-31.

Oxygen isotope dating the Australian regolith: A review and new applications

A. R. Chivas[1,2] and R. P. Bourman[1,3]

[1]School of Earth and Environmental Sciences, University of Wollongong NSW 2522
[2]Department of Earth Sciences, University of Adelaide SA 5005
[3]Department of Geography, Environment and Population, University of Adelaide SA 5005

There is a strong correlation between the isotopic composition of meteoric waters and geographical factors such as latitude, altitude and continental position so that, since the onset of continental fragmentation of Gondwana and the northward drift of the Australian continent, the $\delta^{18}O$ values of meteoric waters have become progressively higher since the Permian and that this change has been recorded in weathering minerals such as kaolinite and gibbsite (Bird & Chivas 1988; 1989; 1993). With increasing age, these minerals are progressively more depleted in ^{18}O and, by correlating the samples with independent age constraints, it has been possible to establish a time scale, which allows application of the dating method to profiles of unknown ages. Accordingly, samples from known-age weathering profiles in eastern and central Australia, provide a chronology wherein Permian kaolinites have $\delta^{18}O$ values of +6 to +10‰, Jurassic-early Cretaceous +10 to +15‰, late Cretaceous-Paleogene +15 to +17.5‰ and Neogene +17.5 to +21.3‰ (Bird & Chivas 1988; 1989; 1993). That such a range of $\delta^{18}O$ values (15‰ variation) is still faithfully preserved at Earth's surface is testament to the lack of later oxygen isotopic exchange, as all profiles have been subject to rain- and ground-waters with progressively changing (increasing) $\delta^{18}O$ values.

The oxygen-isotope values of kaolinite are little affected by their temperature of formation at Earth-surface temperatures, unlike several other mineral-water systems, such as for carbonates, quartz and phosphates.

In Western Australia, the lack of volcanic horizons intercalated with weathering profiles precludes the establishment of a similar independent chronology, although a broadly similar range of $\delta^{18}O_{kaol}$ values must apply, given similar continental drift histories, particularly during the Cenozoic, as Australia accelerated northwards across 40 degrees of latitude. In any case, the isotopic distinction among Permian, Mesozoic and Cenozoic weathering profiles should be straightforward. Chivas & Atlhopheng (2010) applied these techniques to some 58 weathered profiles across the Yilgarn Craton of Western Australia, concluding that kaolinite from the majority of partially dissected weathering profiles displays Neogene $\delta^{18}O$ values, with older profiles in the north and east of the craton producing inferred pre-late Mesozoic ages. Similar investigations were performed on the kaolinitic clays from "The Pound" profile at Burringurrah (Mount Augustus), which lies ~320 km NNE of Meekatharra, the most northerly site of Chivas & Atlhopheng (2010).

The down-profile raw $\delta^{18}O$ values for kaolinite-rich samples from a 30 m-thick weathering profile form a clear downward progression of +11.6, +13.9, +17.6 and +18.2‰, respectively. Some samples have minor residual igneous quartz impurities, although these do not significantly change the calculated pure kaolinite $\delta^{18}O$ values. For example, if the quartz had a $\delta^{18}O$ value of +8‰, typical of I-type granitic rocks (O'Neil & Chappell 1977), and at the low end of plausible $\delta^{18}O$ values for igneous quartz, the adjusted $\delta^{18}O$ values for the same progression would be 12.3, 14.3, 17.6 and 18.4‰, respectively; a change barely outside the analytical precision of the data. Similarly, a $\delta^{18}O$ value for quartz of +12‰, typical of S-type granitic rocks, would adjust the down-profile calculated kaolinite values to 11.5, 14.0, 17.6 and 18.3‰. In either case or, indeed, with any reasonable estimate of the $\delta^{18}O$ value for quartz, the calculated $\delta^{18}O$ values for pure kaolinite remain very similar to the raw $\delta^{18}O$ data. In the discussion that follows, we steer a mid-course, and hereafter refer to the $\delta^{18}O_{kaol}$ values down-core, in sequence, to have approximate values of +12.0, +14.0, +17.6 and +18.3‰.

Analysis of the kaolinite exposed in "The Pound" profile revealed two distinct $\delta^{18}O$ groups. Samples 4 ($\delta^{18}O$ value +12.0‰) and 2 ($\delta^{18}O$ value +14.0‰) suggest an age of weathering of Jurassic to early Cretaceous, while samples 9 ($\delta^{18}O$ value +17.6‰) and 8 ($\delta^{18}O$ value +18.3‰) are indicative of a Neogene age of deep weathering (Chivas & Atlhopheng, 2010). These results also suggest a

reduction in the age of the kaolinitic clays in the profile as weathering proceeded in a downward direction, and the results fill in part of the hiatus between the Mulka Tectonic Event at c. 570 Ma and the Neogene, supplying critical information on both the evolution and age of Mount Augustus. Our samples do not have $\delta^{18}O$ values low enough to be confidently assigned to a Permian age of weathering.

The oxygen isotope data suggest that weathering of the monzogranite beneath the Mount Augustus Sandstone occurred during Jurassic to early Cretaceous (~200 to 100 Ma) time, an age broadly coincident with that derived from the application of denudation rates. This suggests that Burringurrah was partly exhumed at least in the Late Cretaceous, ~100 Ma ago. The younger $\delta^{18}O$ ages with increasing depth suggest continuing weathering and scarp retreat into the Neogene (23 Ma), during which time the surrounding, now dissected planation surface was also weathered.

That two principal ages of weathering and, perhaps a long continuum, are reported from a seemingly single weathering profile is unusual, particularly one of such antiquity. Previous $\delta^{18}O$ data on weathered products from Australia have found a variety of ages but, almost always, only an apparent single age per profile where multiple samples are analysed in each location. We suggest that the recorded long duration of weathering at “The Pound” relates to the protracted protection from erosion afforded by the topographically enclosing and highly resistant Mount Augustus Sandstone.

More recent work has aimed at coupling the oxygen-isotope values of the iron-rich portions of weathering profiles with those of the kaolinite-rich part. This is aimed at addressing the long-standing uncertainty as to whether these portions formed coevally. Accordingly, we have measured the $\delta^{18}O$ values of goethite and hematite from many weathering profiles in both southern and northern South Australia. With few exceptions, we find little relative differences in their ages and can also infer that these minerals are seemingly largely retentive of their original oxygen-isotope values.

References

Bird M.I. and Chivas A.R. 1988. Oxygen isotope dating of the Australian regolith. *Nature* **331**, 513-516; **332**, 568.

Bird M.I. and Chivas A.R. 1989. Stable-isotope geochronology of the Australian regolith. *Geochim. Cosmochim. Acta* **53**, 3239-3256.

Bird M.I. and Chivas A.R. 1993. Geomorphic and palaeoclimatic implications of an oxygen isotope chronology for Australian deeply weathered profiles. *Australian Journal of Earth Sciences* **40**, 345-358.

Bourman R.P., Ollier C.D. and Buckman S. 2009. Mount Augustus geology and geomorphology. *Geographical Research* **48**, 111-122.

Bourman R.P., Ollier C.D. and Buckman S**.** 2015. Inselbergs and monoliths: A comparative review of two iconic Australian landforms, Uluru (Ayers Rock) and Burringurrah (Mount Augustus). *Zeitschrift für Geomorphologie* **59**, 197-227.

Chivas A.R. and Atlhopheng J.R. 2010. Oxygen isotope dating of the Yilgarn regolith. *In*: Bishop P. and Pillans B. eds. *Australian Landscapes*. Geological Society of London, Special Publications **346**, 309-320.

O’Neil J.R. and Chappell B.W. 1977. Oxygen and hydrogen isotope relationships in the Berridale Batholith. *Journal of the Geological Society London* **133**, 559-571.

Mineralogy Maketh Snowy Mountains Too

T. Eggleton

Research School of Earth Sciences, Australian National University, Canberra, ACT

The rates at which different granitoids of a batholith erode depend on their mineralogy. Where tectonics is not a factor, the landscapes of such granite batholiths show variations in average pluton elevation which follow each pluton's composition very closely (Fig. 1, Eggleton 2017). The granitoids of the Kosciusko and Maragle Batholiths, on the other hand, have clearly been influenced by tectonics (Webb 2017; Braun *et al.* 2009 and references therein). Examination of the relation between composition and mean pluton elevation reveals the presence of three fault-bounded regions, each of which in its own way shows a linear relation between mean pluton elevation and pluton mineralogical composition (Figs 2, 3).

Other workers have found other factors implicated in granitic pluton topography, notably grain size, foliation and joint spacing. Grain size shows some correlation with composition for these granites, in that the mafic plutons are finer grained than felsic plutons (Fig. 4a). Foliation either shows no relation to elevation, or there is possibly the suggestion that more foliated granites are more resistant to erosion (Fig. 4b). Joint spacing appears to be related to grain size, coarser plutons having, on average, more widely spaced joints (Foudoulis & Eggleton this conference). When these three factors are combined with composition, it appears that more felsic plutons erode more slowly, are coarser, have more widely spaced joints, are more foliated and are higher in the landscape than mafic plutons (Fig. 5). Just how much each of these factors really determine pluton regolith and topography is discussed in this talk.

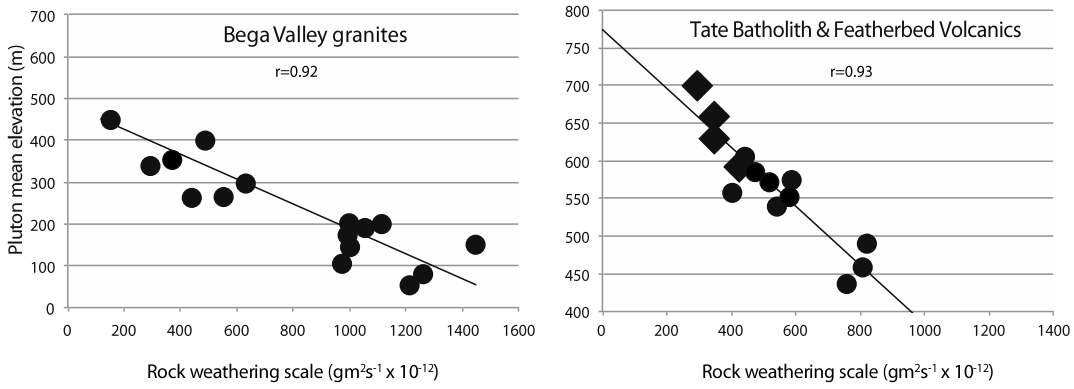

Figure 1: Rock Weathering Scale *vs* mean pluton elevation for the Bega and Tate Batholiths. Diamond symbols are volcanics (Eggleton 2017).

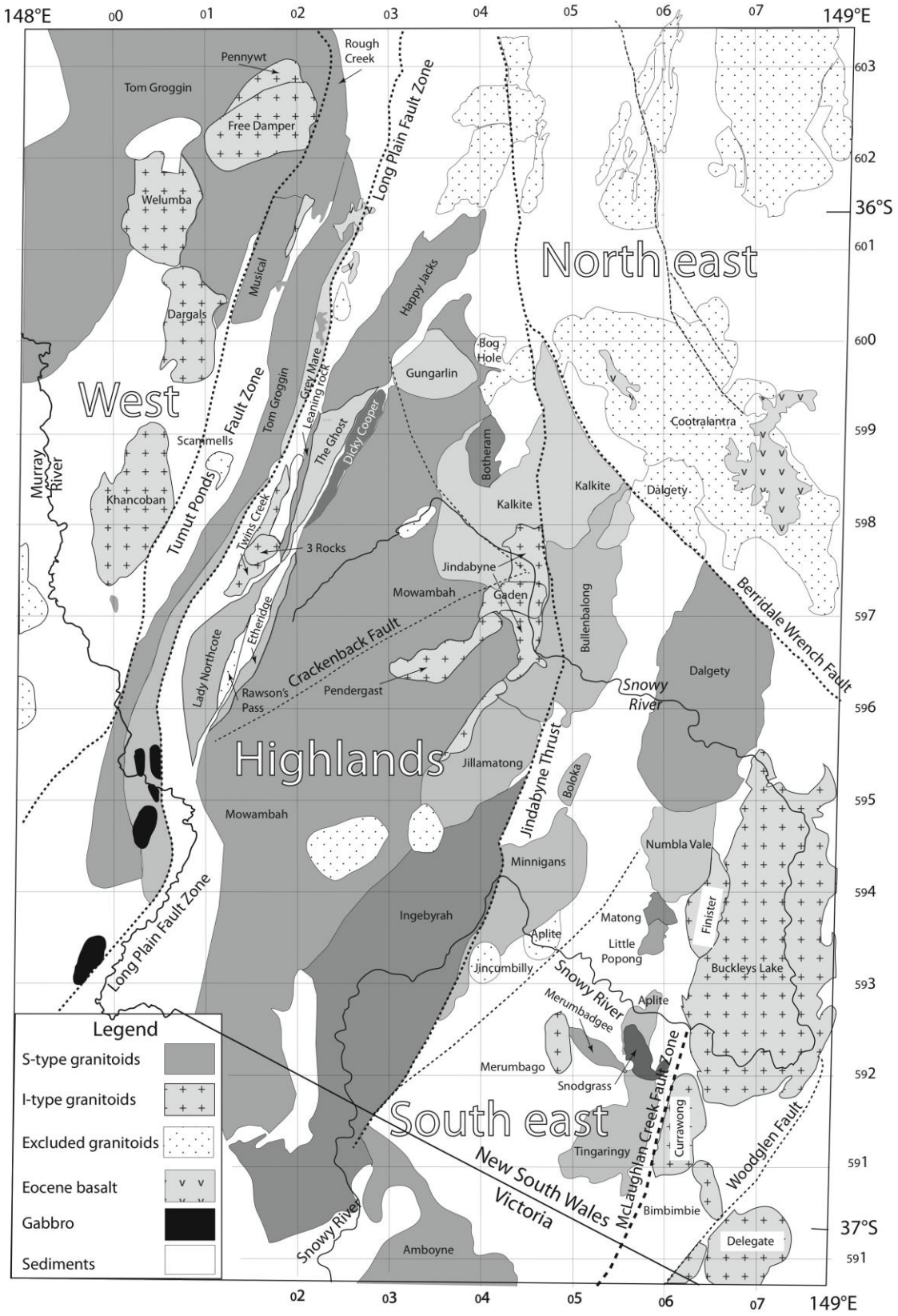

Figure 2: Simplified regional geological map of the Kosciusko region (after Wyborn *et al*. 1990).

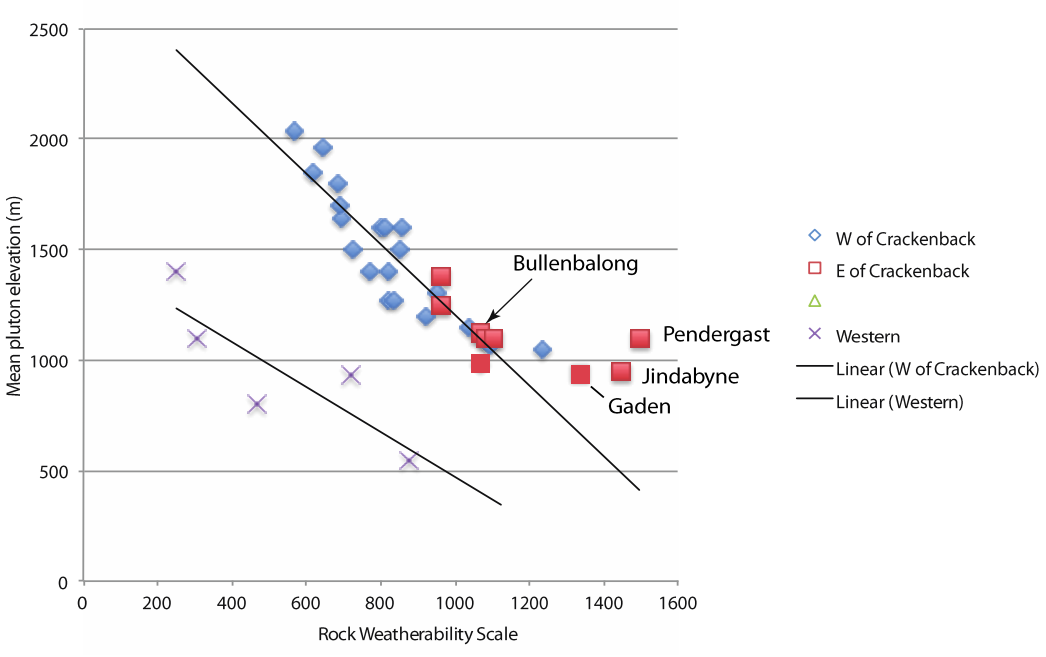

Figure 3a: RWS vs height for the Highlands northwest of the Crackenback Fault (blue), southeast of the Crackenback Fault (red) and west of the Tumut Ponds Fault Zone (X). The Pendergast, Jindabyne and Gaden Tonalites are all part of the Snowy River catchment and are upstream of the more resistant Bullenbalong and cannot erode significantly below it.

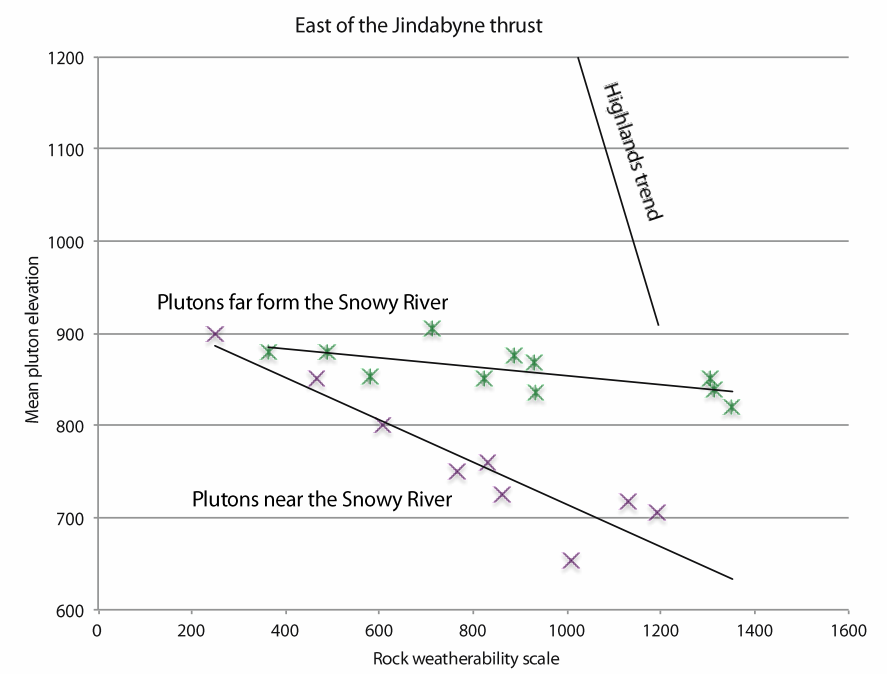

Figure 3b: Plutons of the Berridale Batholith southeast of the Jindabyne Thrust. Note the much narrower elevation range than seen among the Highlands plutons - 200 m compared with 1,000 m, and that plutons near the path of the Snowy River show greater relief than the others.

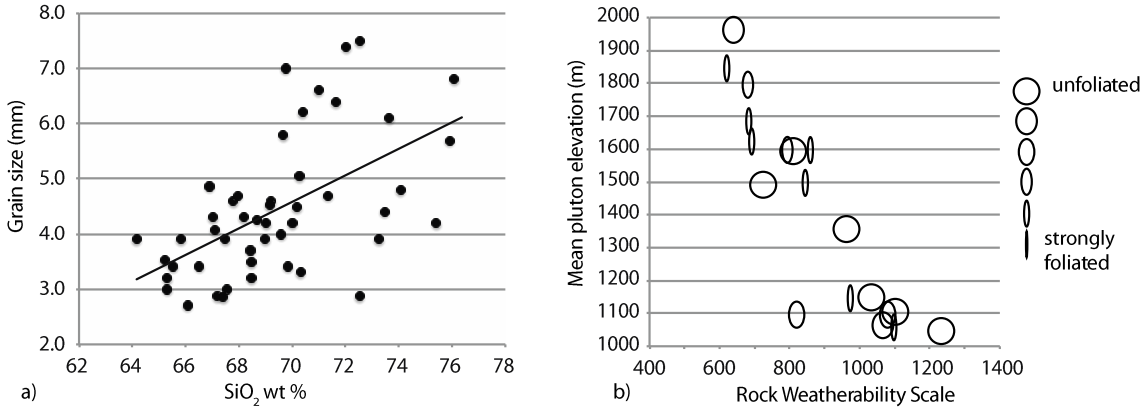

Figure 4a: Composition vs. grainsize for 50 plutons of the Kosciusko, Maragle and Berridale Batholith. Grainsize measured as the mean diameter of the 50 largest grains in an 11x16 cm stained slab. b: RWS vs. elevation for the Highlands region with degree of foliation shown by symbol width.

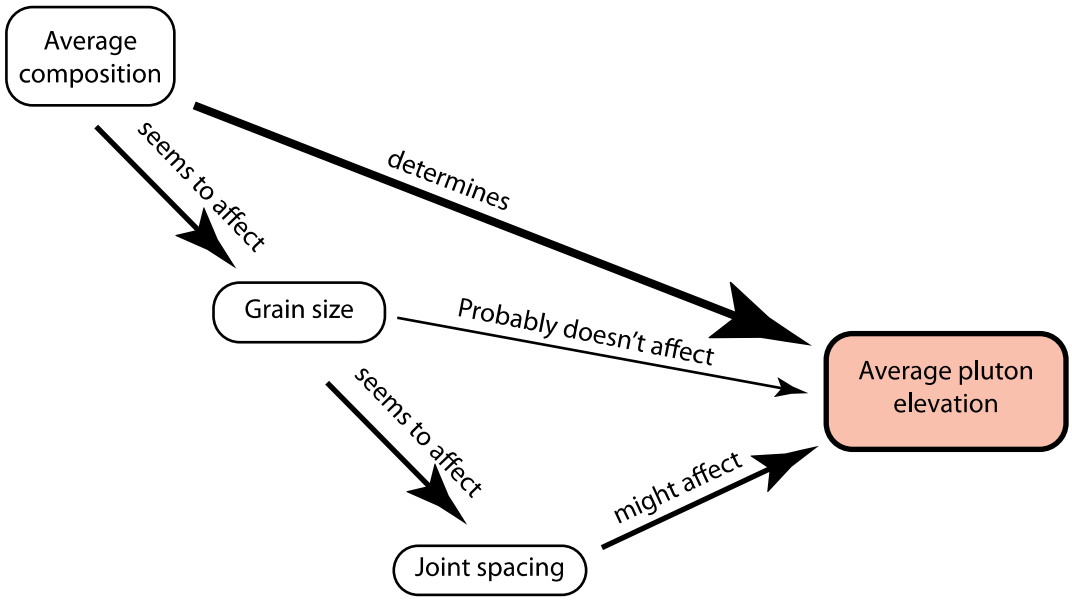

Figure 5: Summary of factors possibly affecting pluton elevation.

References

Braun J., Burbidge D.R., Gesto F.N., Sandiford M., Gleadow A.J.W., Kohn B.P., and Cummins P.R. 2009. Constraints on the current rate of deformation and surface uplift of the Australian continent from a new seismic database and low-T thermochronological data. *Australian Journal of Earth Sciences* **56(2)**, 99-110.

Eggleton R.A. 2017. Mineralogy maketh mountains: Granitic landscapes shaped by dissolution. *Geomorphology* **285,** 363-373.

Webb J.A. 2017. Denudation history of the Southeastern Highlands of Australia. *Australian Journal of Earth Sciences* **64(7),** 841-850.

Wyborn D., Owen M., and Wyborn L. 1990. Geology of the Kosciusko National Park 1: 250 000 scale map. *Bureau of Mineral Resources, Canberra*.

Atypical alteration of biotite to celadonite and nontronite, southern Eyre Peninsula: timing and environmental factors

J.L Keeling[1], H. Zwingmann[2], M.D. Raven[3], P.G. Self[3]

[1]Geological Survey of South Australia, PO Box 320, Adelaide SA 5000
[2]Kyoto University, Division of Earth and Planetary Sciences, Kyoto-shi, Japan 606-8502
[3]CSIRO Land and Water, Waite Road, Urrbrae, SA 5064

Introduction

Metasedimentary rocks of the Paleoproterozoic Hutchison Group on southern Eyre Peninsula, South Australia contain zones of high-grade flake graphite, distributed along a north-south belt of tightly folded upper amphibolite to granulite facies biotite-quartz schist and quartz-feldspar-biotite-garnet gneiss, immediately west of the Kalinjala shear zone (Fig. 1). During early 1990s, open-cut mining for graphite at the Uley mine, 18 km southwest of Port Lincoln, exposed extensive patches of nontronite (Fe-rich smectite) alteration, with minor celadonite (Fe-rich white mica), in weathered biotite-graphite schist and amphibolite (Keeling *et al*. 2000). Quartz-biotite-graphite schist in coastal cliffs at Clem Cove on Sleaford Bay, 7 km south of Uley mine, is also intensely altered with veins and patches of celadonite, Fe-oxy/hydroxides, silica and Mn-oxides.

Alteration of biotite to nontronite or celadonite is unusual and was concluded to result from low temperature, saline hydrothermal fluids circulating within shear zones (Keeling *et al*. 2000). This was based on the persistence of alteration with depth, increased intensity near prominent shear zones, and environmental conditions most commonly associated with nontronite/celadonite formation (i.e. conditions of hydrothermal alteration of basalt in mid-ocean ridge spreading centres).

Celadonite samples from Uley and Sleaford Bay were dated subsequently using K-Ar method, which indicated early Eocene to early Miocene ages of crystallisation. The timing is not linked to any recorded thermal event in the region but corresponds broadly with episodes of Cenozoic deep weathering. The timing and apparent restriction of this style of alteration to zones with high graphite content suggests an alternative explanation is required that involves some local modification of weathering processes.

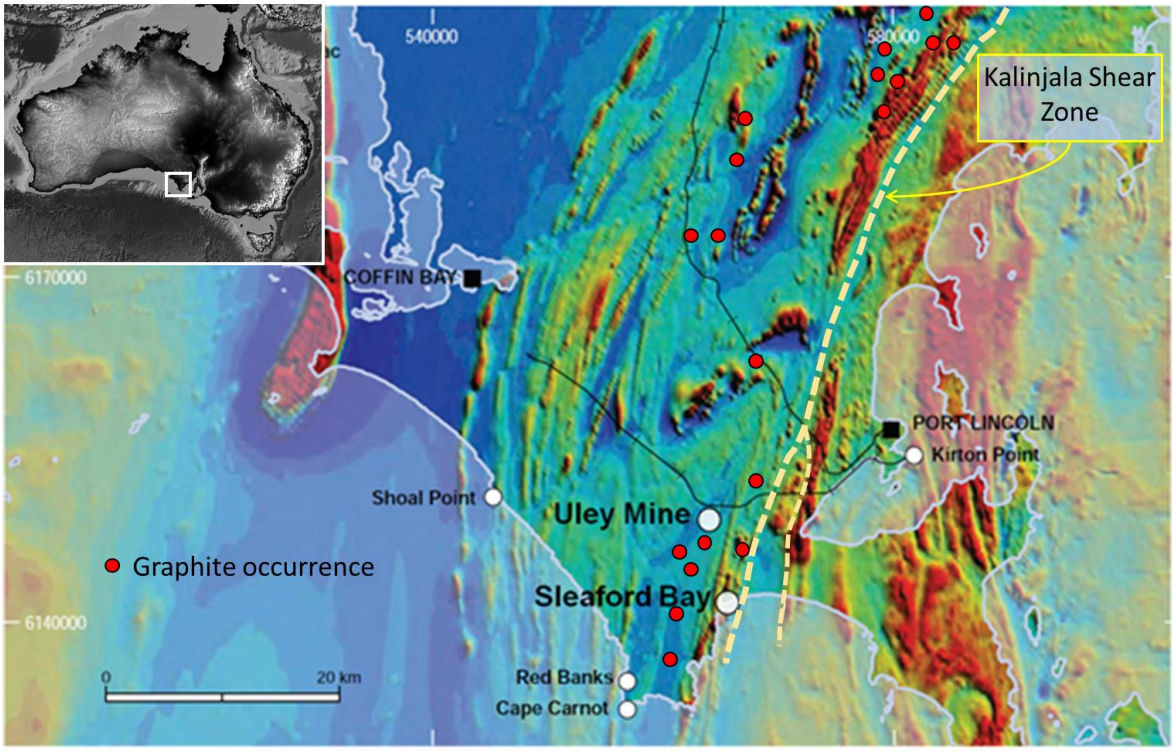

Figure 1: Uley mine and Sleaford Bay nontronite/celadonite localities, southern Eyre Peninsula, including graphite occurrences and structural features on regional total magnetic image (TMI).

Geological Setting

Uley graphite mine is in granulite facies metamorphic rocks equated with Paleoproterozoic Hutchison Group metasedimentary rocks, originally deposited as marine, fine-grained clastic and chemical sediments between 2000 and 1850 Ma. Graphitic beds, averaging 13% graphitic carbon, are interpreted as organic-rich facies in marine clays and silts. The sediments were intruded by mafic dykes and sills and were deformed and metamorphosed during the Kimban Orogeny, with peak metamorphic conditions estimated at 1000 Mpa and 730°C (Dutch *et al*. 2008). The Uley open pit mine is on the hinge of an anticlinorium that plunges to the north-northwest with graphitic schist and gneiss folded in a series of minor isoclinal folds, overturned to the east, with the synclinal limbs strongly attenuated by shearing along graphitic layers (Keeling *et al*. 2000). Depth of weathered bedrock at Uley mine exceeds 60 m. A thin capping of Bridgewater Formation aeolian calcarenite (0-5 m) on sandy soil (0.3-0.7 m) overlies the weathering profile which is comprised of a 0.5-3 m-thick kaolinitic/Fe-oxide mottled zone with carbonate concretions, 5-15 m-thick plasmic zone overprinted by a groundwater calcrete zone (0.5-3 m thick), grading into saprolite, 25-40 m thickness, over saprock and fresh rock, recorded in drill hole samples at >50 m below surface.

Nontronite alteration is present in the plasmic zone at around 15 m below surface, and is patchily distributed in weathered biotite-graphite schist and interlayered amphibolite, with thicker development proximal to an obvious north-south fault. Traces of nontronite alteration persist into the saprock. Celadonite is less common but was identified, along with nontronite, from small green alteration patches and veinlets in weathered, kaolinitic, high-grade graphitic schist in the eastern pit wall, and in drill core (MD 210) at 38-39 m depth (Keeling *et al*. 2000).

The celadonite occurrence at Sleaford Bay is near the western end of Clem Cove in a 12 m-thick zone of sheared and highly altered graphitic schist and gneiss that strikes north-south, with schistosity dipping at 65-70° W. The alteration is a mixture of celadonite, goethite, silica and manganese oxides. Bluish-green celadonite forms as thin stringers and as veins and patches, several centimetres across. The 20 m high cliff section at Clem Cove and adjoining Lone Pine Beach is a key exposure of Hutchison Group stratigraphy on southern Eyre Peninsula.

Methods

Celadonite-altered rocks were examined in thin section and by scanning and transmission electron microscopy. Handpicked samples of nontronite and celadonite were separated into size fractions <0.2 µm, 0.2-1 µm, and 1-2 µm by gentle hand grinding, ultrasonification and centrifugation. Goethite in celadonite from Sleaford Bay was removed by cold sodium dithionite treatment. Mineralogy was determined using XRD on pressed powders with Co Kα radiation. Chemical composition of purified samples was by X-ray fluorescence (XRF) analysis of fused discs. The FeO content was determined by colorimetric method. Selected samples of celadonite were dated by K-Ar method.

Results

Nontronite from alteration of biotite at Uley Mine was reported previously in Keeling *et al*. (2000) and samples lodged subsequently with the Clay Minerals Society, Source Clay Repository (labelled NAu-1) have been the subject of several hundred investigations described in the literature. Replacement of biotite by nontronite was observed with scanning electron microscopy (SEM) (Fig. 2a) but was not investigated using high-resolution transmission electron microscopy. Celadonite samples from Uley mine were not effectively separated from intimately associated kaolinite (Fig. 2b). Sleaford Bay celadonite was observed in optical microscopy to replace crenulated mica interleaved with graphite (Fig. 3a). The alteration was associated with chalcedony, cherty quartz and iron oxide. Remnant primary minerals were K-feldspar, garnet, magnetite and possibly pyroxene. Under SEM, celadonite appeared as masses of thin laths and as layers with cryptomelane ($K(Mn_6^{4+}Mn_2^{3+})O_{16}$) or silica lepispheres, on graphite (Fig. 3b). Celadonite was confirmed by XRD, probably 1M polytype, with (060) reflection corresponding to d-spacing of 1.510 Å. Structural formula for Uley nontronite and Sleaford Bay celadonite are given below.

- Nontronite Uley (NAu-1) $Ca_{0.5}K_{0.04}\ (Fe^{3+}_{3.61}Al_{0.36}Mg_{0.04})\ (Si_{6.98}Al_{0.95}Fe^{3+}_{0.07})\ O_{20}(OH)_4$
- Celadonite Sleaford Bay: $K_{0.82}Na_{0.03}\ (Fe^{3+}_{1.08}Al_{0.06}Fe^{2+}_{0.20}Mg_{0.55})\ Si_4O_{9.9}\ (OH)_{1.98}\ (H_2O)_{0.12}$.

(a) (b)

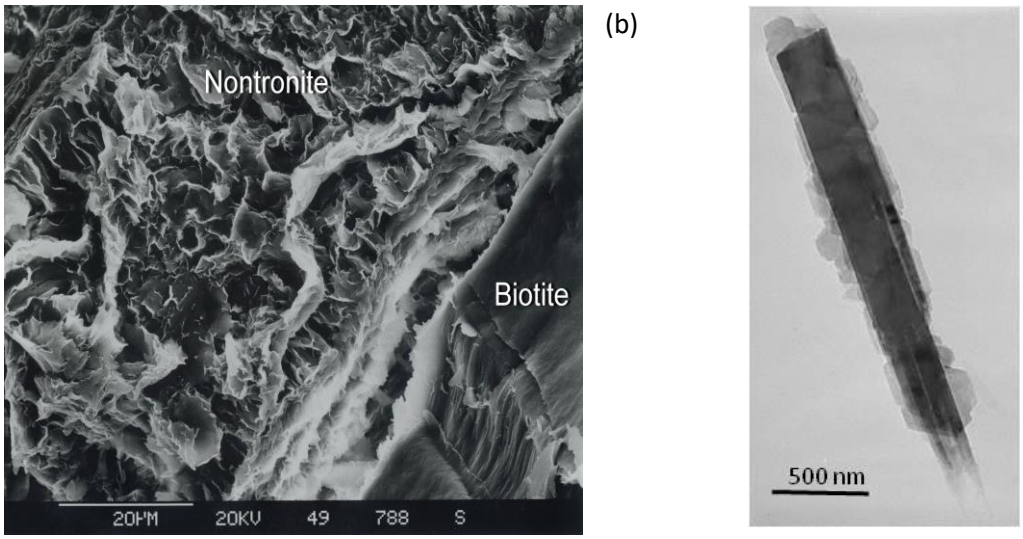

Figure 2: (a) Uley mine, biotite, lower right, with expanded crystal interlayer infilled with nontronite – SEM image, scale bar 20 µm. (b) Uley mine - celadonite lath partly altered to kaolinite (pseudo-hexagonal overgrowths) – TEM image, scale bar 500 nm.

(a) (b)

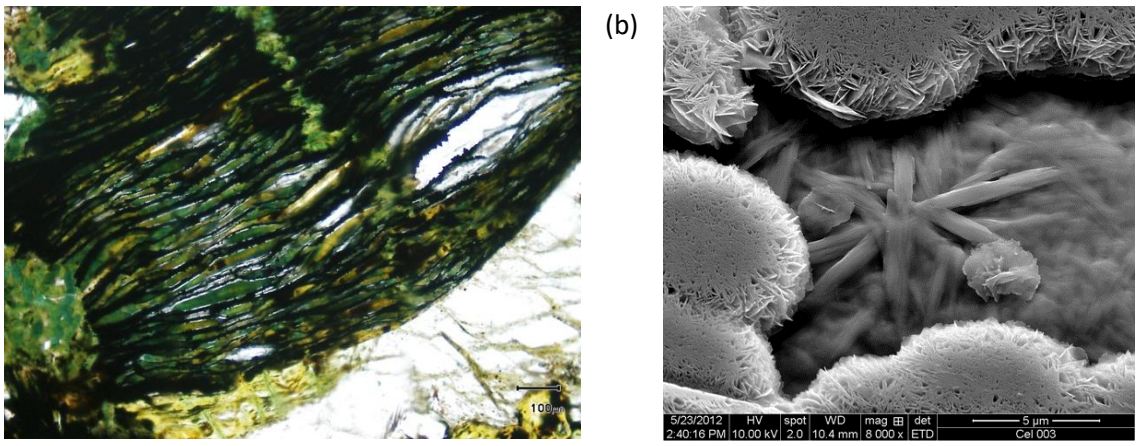

Figure 3: (a) Sleaford Bay celadonite (green) replacing mica, interleaved with graphite (black), and as veinlets, with granular K-feldspar (white) - thin section with crossed nicols, scale bar 100 µm. (b) Radiating celadonite laths coated by silica lepispheres as alteration products interleaved with flake graphite – SEM image, scale bar 5 µm.

Timing of crystallisation of celadonites from K-Ar dating:

- **Uley mine**: (2-5 µm samples) UGCE1 [20.9±0.7 Ma]; UGCE4 [16.7±0.4 Ma]; UGCZ [15.4±0.6 Ma] (early Miocene),

- **Sleaford Bay**: (0.2-2 µm) [48.9±1.1 Ma]; (1-3 µm) [46.1±1.0 Ma] (early Eocene)

Environment of bioite alteration and celadonite/nontronite crystallisation

Biotite alteration to celadonite and nontronite under conditions of supergene weathering or hydrothermal alteration is unusual. Biotite weathering typically commences with loss of K^+ ions from the interlayer and oxidation of Fe^{2+} to Fe^{3+} in octahedral sites to form hydrobiotite, an interstratified biotite and vermiculite, progressing to vermiculite and then kaolinite-vermiculite and ultimately to kaolinite and goethite (e.g. Gilkes and Suddhiprakarn 1979, Banfield and Eggleton 1988, Fordham 1990, Taylor and Eggleton 2001, Wilson 2004). Fe/Mg smectite may form locally where conditions are more alkaline or where dissolution and recrystallization activity modifies cation dispersion (Aspandiar and Eggleton 2006). Halloysite precipitation in voids created during biotite weathering sometimes accompanies kaolinite crystallites that nucleate on dissolving silicate surfaces. In hydrothermal settings, biotite is stable at high temperatures but may be recrystallised or altered to chlorite (e.g. Eggleton and Banfield 1985), or directly to halloysite at temperatures <100°C (e.g. Papoulis *et al*. 2009).

Low temperature hydrothermal activity is widely cited as the cause of combined celadonite and nontronite alteration, generally in mafic igneous rocks or their metamorphic equivalents, with most reported occurrences being alteration of oceanic basaltic crust by heated seawater (e.g. Odin *et al*. 1988, Marescotti *et al*., 2000; Mas *et al*. 2008). The alteration minerals infill voids and fractures and result from dissolution of volcanic glass and groundmass forming the basalt, with possibly some cation contribution from the circulating fluid. The fluids responsible for alteration vary from oxidising to reducing, are saline and slightly alkaline, with temperatures generally <40°C (Marescotti *et al*. 2000). Celadonite/nontronite form in preference to saponite when Fe and K activity is high and Al availability is low (Mas et al. 2008).

Graphitic rocks facilitate shearing and tend to concentrate fracturing during deformation. This can produce zones of high permeability that focus fluid flow, resulting in increased depth of weathering and higher flux of meteoric water. Anomalous heat flow together with high sea levels at the time of celadonite formation may have combined to produce warm saline fluid circulation in the fault zones. If this was the case, however, occurrences of celadonite and nontronite might be expected also in non-graphitic biotite-rich rocks in faulted structural settings.

While graphite is essentially inert at temperatures <300°C, the presence of graphitic carbon may still modify the local environment during weathering. The relative high conductivity of graphitic zones is suggested as a probable factor. Chemical weathering and oxidation creates a spontaneous potential between the weathered zone and fresh rock that induces gradual movement of negatively charge-carrying species towards the zone of oxidation. Graphitic shear zones can act as conductive bodies that focus the flow of negative charge leading to increased consumption of oxidising agents around the upper part of the conductor. This results in a more reduced environment in the area around the top of the conductor, relative to adjacent areas. The effect is a natural electrochemical negative 'self-potential' that can be measured using non-polarizing electrodes connected to a voltmeter. Under conditions of saline groundwater, a weathering environment is envisaged where relative reducing conditions were such that Fe^{2+} in biotite was not oxidised immediately to Fe^{3+} and was therefore available to substitute in silicate structures to form celadonite and nontronite, prior to partial or complete oxidation to Fe^{3+}.

References

Aspandiar M.F. and Eggleton R.A. 2006. Weathering of biotite: micro to nano scale reactions in the regolith. *In*: Fitzpatrick R.W. and Shand P. eds. *Regolith 2006 – Consolidation and Dispersion of Ideas*. Cooperative Research Centre for Landscape Environments and Mineral Exploration, Perth, pp. 5-8.

Banfield J.F. and Eggleton R.A. 1988. TEM study of biotite weathering. *Clays and Clay Minerals* **36**, 47-60.

Dutch R., Hand M. and Kinny P.D. 2008. High-grade Paleoproterozoic reworking in the southeastern Gawler Craton, South Australia. *Australian Journal of Earth Sciences* **55**, 1063-1081.

Eggleton R.A. and Banfield J.F. 1985. The alteration of granitic biotite to chlorite. *American Mineralogist* **70**, 902–910.

Fordham A.W. 1990. Weathering of biotite into dioctahedral clay minerals. *Clay Minerals* **25**, 51-63.

Gilkes R.J. and Suddhiprakarn A. 1979. Biotite alteration in deeply weathered granite. I. Morphological and chemical properties. *Clays and Clay Minerals* **27**, 349-360.

Keeling J.L., Raven M.D. and Gates W.P 2000. Geology and characterization of two hydrothermal nontronites from weathered metamorphic rocks at Uley graphite mine, South Australia. *Clays and Clay Minerals* **48**, 537–548.

Marescotti P., Vanko D.A. and Cabella R. 2000. From oxidising to reducing alteration: mineralogical variations in pillow basalts from the east flank, Juan De Fuca ridge. *In:* Fisher A., Davis E.E. and Escutia C. eds. *Proceedings of the Ocean Drilling Program, Scientific Results*, v **168**, 119-136.

Mas A., Meunier A., Beaufort D., Patrier P. and Dudoignon P. 2008. Clay minerals in basalt-Hawaiite rocks from Mururoa Atoll (French Polynesia). I. Mineralogy. *Clays and Clay Minerals* **56**, 711-729.

Odin G.S., Desprairies A., Fullagar P.D., Bellon H., Decarreau A., Frohlich F. and Zelvelder, M. 1988. Nature and geological significance of celadonite. *In* Odin G.S. ed. Green Marine Clays. *Developments in Sedimentology* **5**, Elsevier, Amsterdam, pp. 337–398.

Papoulis D., Tsolis-Katagas P., Kalampounias A.G. and Tsikouras B. 2009. Progressive formation of halloysite from the hydrothermal alteration of biotite and the formation mechanisms of anatase in altered volcanic rocks from Limnos Island, northeast Aegean Sea, Greece. *Clays and Clay Minerals* **57**, 566-577.

Taylor G. and Eggleton R.A. 2001. *Regolith Geology and Geomorphology*. John Wiley & Sons, Chichester, England, 375p.

Wilson M.J. 2004. Weathering of the primary rock-forming minerals: processes, products and rates. *Clay Minerals* **39**, 233-266.

Are critical zone observatories materially advancing regolith science?

Lisa Worrall

Landscape Evolution in the Albany-Fraser Orogen and South Yilgarn Craton, Western Australia

S. Pernreiter[1,2], I. González-Álvarez[1,3], J. Klump[1], G. Smith[1] and T. Ibrahimi[1]

[1]CSIRO, Mineral Resources, Discovery Program, Kensington 6151, Western Australia,
[2]Institute of Geology, University of Innsbruck, Innrain 52, A-6020 Innsbruck, Austria
[3]Centre for Exploration Targeting, University of Western Australia, Crawley, Western Australia

Landscape evolution is the result of the interaction of climatic conditions, geological characteristics and sedimentary dynamics through time (Ollier and Pain 1996; Ollier 2001; Goudie 2006; Fujioka and Chappell 2010; Pain *et al.* 2012). In regolith-dominated terrains (RDT), landscape morphologies and their stratigraphy record the 3D architecture of the overburden, and capture the relation of the surface and cover to basement geology (e.g., Butt and Zeegers 1992; Pain *et al.* 2012; Anand 2015; González-Álvarez *et al.* 2016a, Butt *et al.* 2017).

Remote sensing datasets such as Digital Elevation Models (DEM) image the geomorphological features of the land surface. Combining of different surface geometrical features can be used to classify landscape types. Therefore, DEMs can be employed to map landscapes over large geographic areas (e.g., geological province, country or continental scale).

In this study we tested the conceptual variability of landscape types in the Albany-Fraser Orogen and South Yilgarn Craton, using machine learning algorithms, DEM data and DEM-derived products (e.g., DEM Hillshade, Flatness Map), Google Earth and Bing images and field observations to assess how landscapes can be classified based on their specific surface geometric features.

Six different conceptually surface landscape patterns were defined using DEM products (Figs. 2A and 3). A statistical analysis on the surface features of these six landscape types was carried out to test whether the surface features of each landscape type were significantly different and to determine which geometric features characterize each landscape type. A landscape map was generated based upon this classification (Fig. 2C).

The south of Western Australia is subdivided into two main regional geological provinces: the Yilgarn Craton (YC) and the Mesoproterozoic Albany-Fraser Orogen (AFO; Spaggiari *et al.* 2017). The YC dominantly comprises rocks of Archean age (3.0-2.6 Ga), i.e. metavolcanic and metasedimentary rock suits, granites and granitic gneisses in a SE-NW trend (Cassidy *et al.* 2006 and references therein; Spaggiari *et al.* 2017). The AFO comprises Archean to Proterozoic rocks (2.8-1.1 Ga), i.e. (meta-) granites and metamafic rocks, orthogneisses, metagabbros and hybrid rock suits in a SW-NE trend (Kirkland *et al.* 2015; Spaggiari *et al.* 2017). The Cundeelee Shear Zone forms the sharp boundary between the YC and the AFO (Spaggiari *et al.* 2017). Outcrops in these regions are rare due to intense weathering and the presence of widespread transported cover, increasing in thickness inland from the coast (González-Álvarez *et al.* 2016b).

Australia's plate movement through humid paleolatitudes have resulted in deep weathering profiles that reach depths of up to 200 m (e.g., Ollier and Pain 1996; Hill 2004; Twidale 2007; Fujioka and Chappell 2010). The present climate is arid to semiarid. In arid landscape plateaus, stony deserts and dune fields form under strong aeolian influence (Twidale 2007). However, in contrast to its present-day environment, the YC displays landscape features consistent with a system that was dominated by fluvial processes, whereas the AFO displays a more complex stratigraphy that strongly suggests a landscape dominated by marine transgression-regression sedimentary dynamics (Figs. 2A and B; González-Álvarez *et al.* 2016b).

In this geological context, a 4,000 km traverse was conducted to compare a landscape computer generated map based on geometric surface features, with field observations (Fig. 1). Using the computer-generated landscape map as a reference, different landscape type boundaries were ground truthed in the field. Google Earth imagery and mapping/recording of stratigraphic sequences associated with the diverse landscape types were also used. The observations will be linked to geochemical surface data.

In the field, observations were collected mainly along paleovalley systems, as well as fluvial and lacustrine environments. Variations within the frequency and amplitude of the wavelength of the landscape were confirmed from the road, but the landscape classification based purely on DEM products (computer map) was not able to capture all of the landscape variability observed in the field, such as in the Bremer Region and southernmost part of the YC (Stirling Range National Park).

For the conceptual definition of the six landscape types, surface DEM patterns were selected in the YC and AFO (Fig. 2C). However, in the Bremer Region landscape variability and DEM patterns are unique as compared to other regions in the YC and AFO. The Stirling Range was not displayed as a distinct landscape type. Several landscape elements in the field had the same geometric features but for different genetic reasons. For example, flat areas may represent valley bottoms or high plateaus, lacustrine environments or the top of a paleovalley fill sequences. Field observations are crucial in accurate interpretation of similar geometric features that have unique geneses.

Field observations of specific landscape type boundaries (defined by computer algorithms) was challenging. At the ground observation scale, it was not possible to detect the defining features of specific landscape types described by the machine learning algorithms (Fig. 2C). However, landscape changes at large scale pattern were recorded. Scale and dimensions observed become critical factors when comparing the observations made in the field to those generated by remote sensing. This approach can detect changes in geomorphology that are too subtle for the human observer in the field to identify. Algorithm interpretations need to be linked with field observations to map landscape types that are not evident via direct observation nor on Google Earth and hence the classification of the landscape types in the model (Fig. 2C) needs to be revised. An important aspect to be improved upon is the introduction of a category for landscapes that cannot be classified into one of the six defined categories.

The approach applied in this project can be generalised to assist landscape mapping in RDT by the use of DEM surface geometry. This will be a powerful tool to map and feature landscape types in similar contexts such as West Africa, India, Brazil and large parts of China. Landscape mapping can provide a solid reference in mineral exploration for a better understanding of geochemical dispersion of the basement geochemical signatures through cover by linking stratigraphic units to dispersion processes and surface geometries.

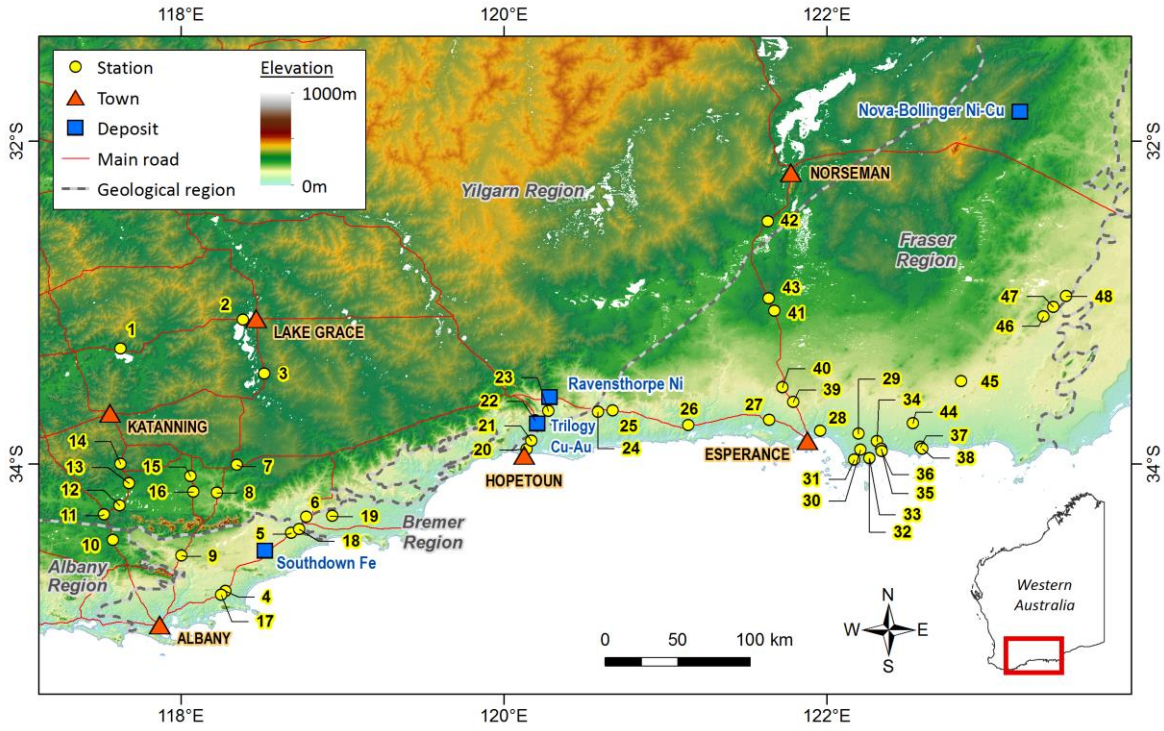

Figure 1: DEM of area of interest including fieldtrip stops (1-48), towns and ore deposits (DEM source: Geoscience Australia 2009).

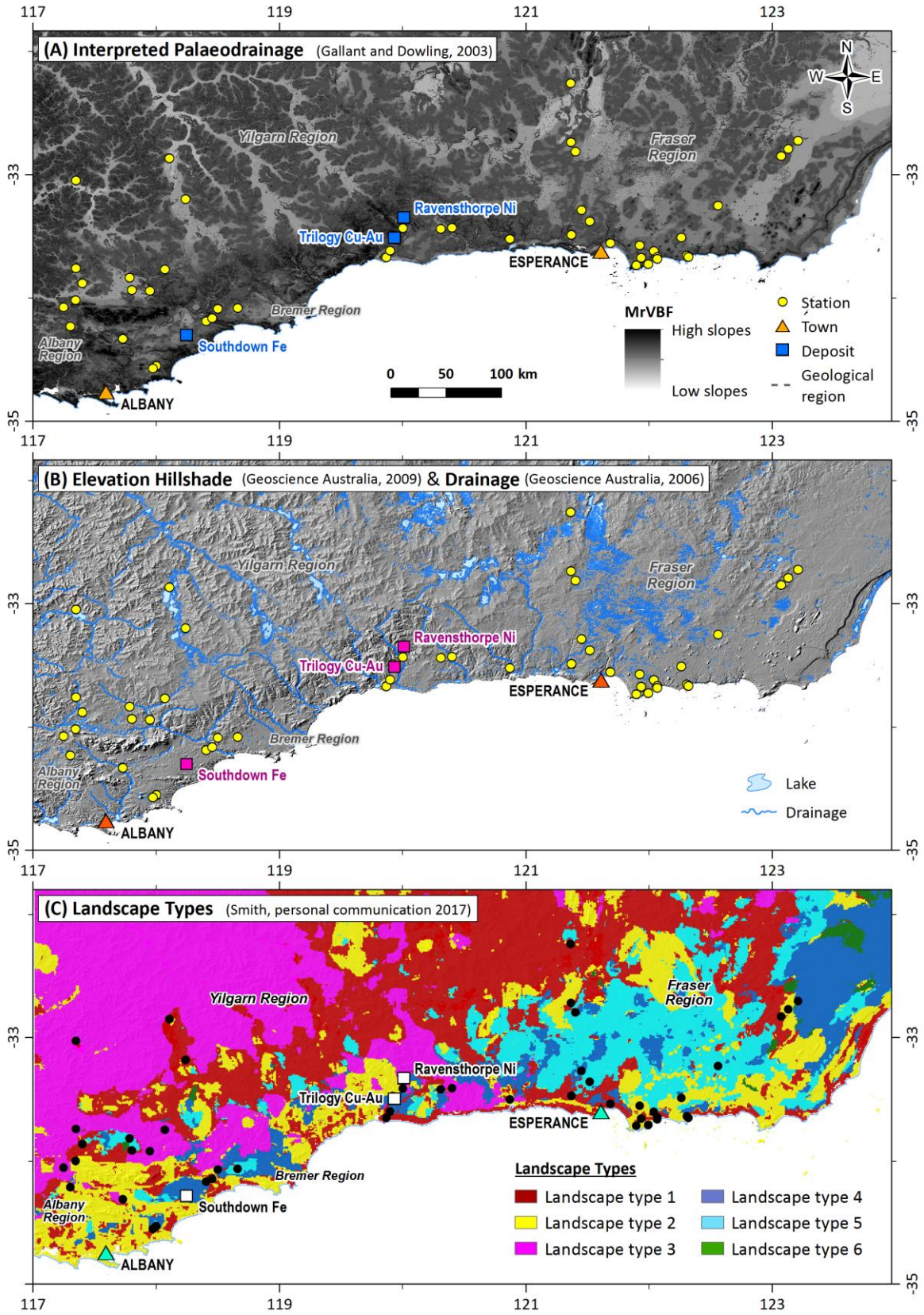

Figure 2: (A) Interpreted Palaeodrainage (Gallant and Dowling 2003); (B) Elevation Hillshade and Drainage (Geoscience Australia 2006 & 2009); and (C) Landscape Types (Smith, personal communication 2017).

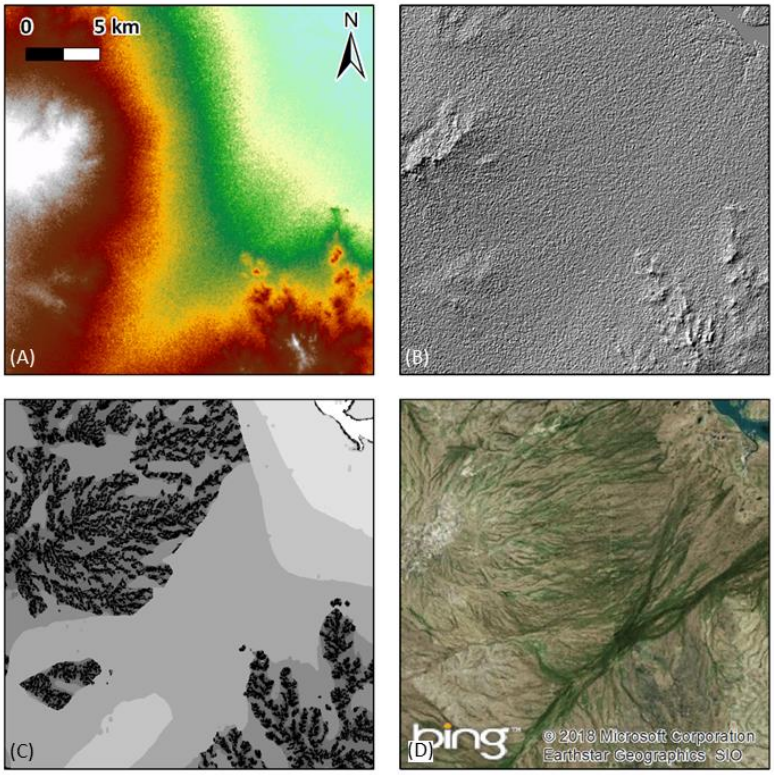

Figure 3: Example for use and comparison of DEM products for landscape type 1 (Location: 374,487E; 6,689,572N 51H): (A) DEM (colours according to legend for Fig. 2C, Geoscience Australia 2009); (B) DEM Hillshade (Geoscience Australia 2009); (C) Flatness map (MrVBF; Gallant and Dowling 2003); and (D) Satellite Image of Bing ©2018.

References

Anand R.R. 2015. Importance of 3-D regolith-landform control in areas of transported cover: implications for geochemical exploration. *Geochemistry: Exploration, Environment, Analyses* **16**, 14-26.

Butt C.R.M. and Zeegers H. 1992. Regolith Exploration Geochemistry in Tropical and Subtropical Terrains. *In:* Butt C.R.M, Zeegers H. eds. *Handbook of Exploration.* Geochemistry 4 Elsevier, Amsterdam, 607p.

Butt C.R.M., Anand R.R. and Smith R.S. 2017. Geology of the Australian regolith. *In:* Phillips N. ed. *Australian Ore Deposits.* AusIMM Monograph **32**, 27-34.

Cassidy K.F., Champion D.C., Krapež B., Barley M.E., Brown S.J.A., Blewett R.S., Groenewald P.B. and Tyler I.M. 2006. A revised geological framework for the Yilgarn Craton, Western Australia. *Western Australia Geological Survey,* **Record 2006/8**.

Fujioka T. and Chappell J. 2010. History of Australian aridity: chronology in the evolution of arid landscapes. *In*: Bishop P. ed. *Australian Landscapes.* Geological Society Special Publications, **346**, 121-139.

Gallant J.C. and Dowling T.I. 2003. A multiresolution index of valley bottom flatness for mapping depositional areas. *Water Resources Research* **39**, 1347.

Geoscience Australia 2006. GEODATA TOPO 250K Series 3. Bioregional Assessment Source Dataset. http://data.bioregionalassessments.gov.au/dataset/a0650f18-518a-4b99-a553-44f82f28bb5f.

Geoscience Australia 2009. Digital Elevation Model of Australia. SRTM-derived 1 Second Digital Elevation Models Version 1.0. http://www.ga.gov.au/scientific-topics/national-location-information/digital-elevation-data.

González-Álvarez I., Boni M. and Anand R.R. 2016a. Mineral Exploration in Regolith-Dominated Terrains. Global considerations and challenges. *Ore Geology Reviews Special Issue,* **73**, 375-379.

González-Álvarez I., Salama W. and Anand R.R. 2016b. Sea-level changes and buried islands in a complex coastal palaeolandscape in the South of Western Australia: Implications for greenfield mineral exploration. *Ore Geology Reviews Special Issue* **73**, 475-499, http://dx.doi.org/10.1016/j.oregeorev.2015.10.00 2

Goudie A.S. 2006. *Encyclopaedia of Geomorphology*. Routledge Ltd, New York, USA, 1202pp.

Hill R.S. 2004. Origins of the southeastern Australian vegetation. *The Royal Society* **359**, 1537-1549, doi:10.1098/rstb.2004.1526

Kirkland C.L., Spaggiari C., Smithies R.H., Wingate M.T.D., Belousova E.A., Gréau Y., Sweetapple M.T., Watkins R., Tessalina S. and Creaser R. 2015. The affinity of Archean crust on the Yilgarn-Albany-Fraser Orogen boundary: implications for gold mineralisation in the tropicana zone. *Precambrian Research* **266**, 260-281.

Ollier C.D. 2001. Evolution of the Australian landscape. *Marine Freshwater Research* **52**, 13-23, doi: 10.1071/MF00032.

Ollier C. and Pain C. 1996. *Regolith, Soils and Landforms*. John Wiley & Sons, Chichester, 316pp.

Pain C., Pillans B., Worrall L. and Roach I. 2012. Old, flat and red: Australia's distinctive landscape. *In*: Blewett R. ed. *Shaping a Nation: Geology of Australia*. ANU ePress, Canberra, 228-275.

Spaggiari C.V., Kirkland C.L. and Smithies R.H. 2017. Regional geology and metallogeny of the Albany-Fraser Orogen. *In:* Phillips N. ed. *Australian Ore Deposits.* AusIMM Monograph **32**, 385-388.

Twidale C.R. 2007. *Ancient Australian Landscapes*. Rosenberg, NSW, 144pp.

Inverted dune swales, Hunder Dunes, Ladakh, India

J. D. A. Clarke[1] and S. L. McGuirk[1, 2]

[1]Mars Society Australia, c/o 43 Michell St Monash, ACT 2904
[2]Fenner School, Australian National University, ACT 0200

Abstract

The Hunder dunes are one of a series of small dune fields in the Shyok and Nubra valleys of the Ladakh region in north-western India. Comprised of three separate dunefields, the Hunder dunes are primarily barchanoid and transverse in form and composed of sand reworked from the seasonally exposed channel beds of the Shyok and Nubra Rivers. Wind direction is strongly uni-modal in orientation and controlled by valley orientation (McGuirk 2017). At an altitude of 3083m, the Hunder dunes cover an area of about 1500 x 700m in the Shyok Valley. The area is a popular tourist location because of the visual impression of the dunes against the background of the Ladakh and Karakoram Range, which rise to over 6000m, and the presence of a small herd of Bactrian camels. No scientific investigation of the dunes have been previously made. During our 2016 expedition to the area, we noticed the presence of numerous inverted swale deposits. Inverted swales have not, to our knowledge, been described in the literature. We here present a brief description of them, and discuss their formation and possible significance.

Location

The Hunder dune field occurs in the Nubra Valley and are centred at 77°29'47.60"E and 34°34'49.00"N. The dune fields at the present time are composed primarily of barchanoid dunes, although the evidence from Google Earth imagery shows a dominance of transverse bedforms in the past. Lying on the southern bank of the Shyok River at 3083 m asl the dunefield surrounding the swale described in this study covers an area of about 1500 x 700 m (Fig. 1).

Figure 1: Hunder dunes.

Climate

The Hunder dunes lie in an area of arid climate with warm summers and cold winters, where winter temperatures commonly remain below zero. The area corresponds to the geomorphic and climatic Zone IV of the Karakoram region described by Hewitt (1989). In Zone IV, valley floors experience strong winds and the dominant wind vector responsible for dune formation is from the northwest. No rainfall data exists for Hunder, but the city of Leh in the nearby Indus Valley to the south, has an annual rainfall of 104 mm (Climate data 2018).

Figure 2: Concave upward 'wedding cake' mesas formed by inversion of flooded swale deposits at Hunder dunes.

Morphology and stratigraphy

The features interpreted as inverted swales consist of small (10-20 m long, 5-10 m wide, and up to 1.5 m high), ellipsoidal mesas exposed in the swales between active dunes. Most of the mesas have a tiered, 'wedding cake' appearance, due to the presence of stacked cycles of deposited sediment (Fig. 2). These range from 40 to 50 cm in thickness, and are composed of a repeated succession of lithologies (Table 1), forming cycles. Not all units are present in each cycle. Unit A is only present at the base of the mesa, and is not always exposed. Only one of the rippled units - B and C may be present, and rarely the muddy unit D is absent. Some swales are partly buried by dune migration, others are being exposed by the same process.

Table 1: Repeating cyclic units in mesas

Unit	Grainsize	Structures	Interpretation	Figure
D	Mud	Mud drape over ripples, desiccation cracks, vertebrate footprints	Desiccated pond	Figure 3
C	Sand	Symmetrical ripple cross-laminae	Pond	Figure 4
B	Sand	Asymmetrical ripple cross-laminae	River flooding	Figure 4
A	Sand	Parallel bedding, slightly concave upwards	Aeolian dunes	Figure 4

Figure 3: Unit 4 desiccation-cracked mud (unit A) at top of swale flood cycle showing cloven hoof footprints.

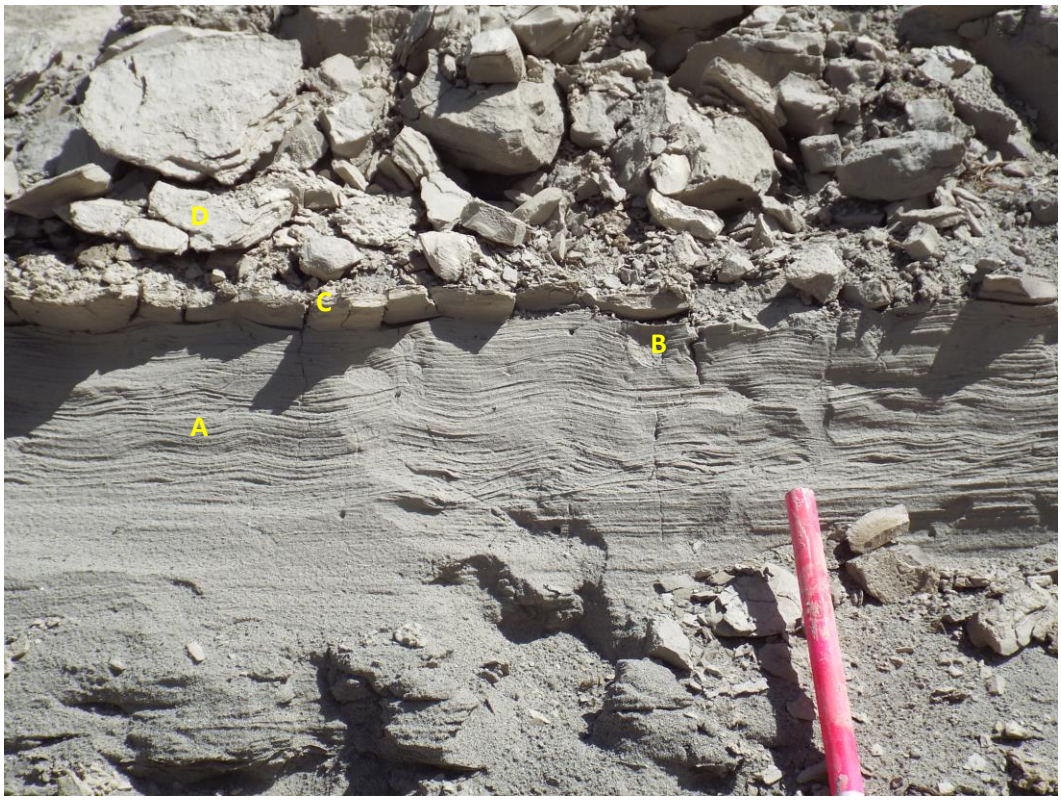

Figure 4: Complete cycle exposed in side of mesa, units A, B, C, and D shown.

Interpretation

As shown in Table 1, the cyclic units are interpreted as showing the flooding of dune swales by muddy river waters, followed by their desiccation. The convex-upward basal unit A represents aeolian swale deposits. The convex upward geometry of the swale is propagated through each cycle. The asymmetric cross-laminated unit B represents the influx of river flood water, carrying sand and mud. The symmetric cross-laminated unit C represents wind-driven, wave sand deposition, and sand deposited by the (water) flood recession, which is deposited into ponds. Interference patterns between ripple sets are visible on the upper surfaces of the topmost cycles exposed in the mesas. The uppermost unit in the swales; C represents settling out of suspended mud in the final phases of pond drying. The muddy unit is often cracked by desiccation and may preserve vertebrate footprints. Multiple cycles of flooding and desiccation form the swale deposits.

The deposits are very weakly indurated following deposition by the precipitated carbonate. This allows them to withstand deflation, and form the mesas. The muddy unit C is also slightly more resistant than the sands to erosion, and forms overhanging caps. The mesas are small scale landforms showing wind erosion, including polished surfaces and ventifacts (Fig. 5).

Discussion

Several swales in the Hunder dunes were flooded at the time of our visit. These ponds lacked mud, however, we interpret the water as being due to either a raised groundwater table, or rainfall runoff, or both. The flooding from the river would carry mud, as the suspended sediment load of the Shyok River is substantial.

While dune swales can be flooded by the Shyok River, we expect the deposits to accrete to the height of the river flood. When isolated from the river by dune migration, erosion of the swale deposits can begin, leading to formation of the concave upward wedding cake inverted mesas.

Figure 5: Complex ventifact formed by wind erosion of mud drape (unit D)

Acknowledgements

The data from Hunder was collected during Mars Society Australia's NASA Spaceward bound India expedition in August 2016. The expedition was funded in-part by a grant from Tata Motors, India. We also acknowledge the support of the Birbal Sahni Institute of Palaeosciences, the Department of Science and Technology, the Chief Wildlife Warden of Ladakh, and Inspired Journeys Ltd. Craig Strong and Frank Mills ANU supervised the project at ANU.

References

Climate Data.org 2018. Leh. Address when accessed https://en.climate-data.org/location/24802/

Hewitt K. 1989. The altitudinal organization of the Karakorum geographic processes and depositional environments. *Zeitshschrift fur Geomorphologie* Supplement **76,** 9-32.

McGuirk S. 2018. Do synoptic scale atmospheric processes drive surface winds in the valleys of Ladakh, in the northern Himalaya? Thesis submitted in partial requirement for the degree of Bachelor of Science with Honours in the Fenner School of Environment and Society, Australian National University, Canberra, unpublished, 68p.

Cover and UNCOVER: an update on new science at Geoscience Australia

I. C. Roach, Y. Ley-Cooper, J. R. Wilford, K. Czarnota and A. A. McPherson

Geoscience Australia, GPO Box 378, Canberra ACT 2601

Geoscience Australia is mandated to engage in research into exploration through cover as part of the Council of Australian Government's National Mineral Exploration Strategy (COAG, 2012). This strategy adopted the recommendations of the Australian Academy of Science's UNCOVER Initiative (Australian Academy of Science, 2012), which recognised that future mineral discoveries must be made through increasing thicknesses of regolith and sedimentary basin cover.

Stavely and Thomson stratigraphic drilling

Geoscience Australia is engaged in a range of new exploration-through-cover activities in the Stavely region of western Victoria, in collaboration with the Geological Survey of Victoria, and the southern Thomson Orogen of northwest New South Wales and southwest Queensland, in collaboration with the Geological Survey of New South Wales and the Geological Survey of Queensland. In both projects, we worked closely with our state geological survey partners to collect new pre-competitive geological, geochemical, geophysical and geochronological data to determine the thickness and nature of cover, and also the character of basement rocks in the two regions through new stratigraphic drilling.

Exploring for the Future

Geoscience Australia leads the Exploring for the Future program (EFTF; http://www.ga.gov.au/eftf), which is investigating the potential mineral, energy and groundwater resources in northern Australia and South Australia, in areas where the resource potential is relatively poorly known. Exploring for the Future is the most intensive pre-competitive geoscience acquisition program ever undertaken in Australia. The program aims to reduce exploration risk and renew the appetite for investment to identify new resources. Three disciplines at Geoscience Australia (mineral systems, energy systems and groundwater) are being combined to build a holistic picture of the resource potential across key areas of northern Australia. To support this work, Geoscience Australia is acquiring new pre-competitive data, and is engaged in the creation of new machine learning codes to map regolith and basin cover and provide more accurate estimates of cover thickness to explorers. These projects are described below.

Coompana stratigraphic drilling

The Geological Survey of South Australia (GSSA) and Geoscience Australia performed pre-drilling geophysical data acquisition to characterise the thickness of cover and reduce risk for drilling operations. This supported new stratigraphic drilling, managed by the GSSA, which seeks to characterise the thickness and nature of cover and provide new information on the basement rocks and put the region into a mineral systems framework.

AusAEM survey

Geoscience Australia, in collaboration with state and territory government geoscience agencies, is conducting a series of TEMPEST® airborne electromagnetic (AEM) surveys of a large region of northern Australia (the AusAEM Program). The first in the series of surveys is being undertaken in the Tennant Creek-Mount Isa region (approximately 1,117,000 km^2). The regional survey consists of 20 km-spaced reconnaissance lines over the onshore parts of the Newcastle Waters, Alice Springs, Normanton and Cloncurry 1:1,000,000 standard map sheets. The AEM data collected will contribute to mapping regional features of the regolith, the geology and the hydrogeology and to the understanding of mineral and groundwater resource potential of the survey area. As part of the acquisition program Geoscience Australia invited exploration companies holding tenements in the survey area to subscribe to the survey and fly higher resolution infill over their tenements. This is in order to increase the understanding of mineral exploration prospects at both tenement- and regional-scales, and complement the objectives of the regional survey. The EFTF AusAEM program is acquiring data over extents never previously attempted. It comes from a long-lasting tradition at Geoscience Australia of delivering precompetitive data to stimulate mineral and energy exploration, and acquiring AEM data in areas with a paucity of data, as a way of promoting exploration in new frontiers. At its current stage of acquisition the Tennant Creek-Mount Isa AusAEM survey preliminary data have already proven useful in mapping the cover and basement interface. The new AEM data will provide explorers with insights to areas of thick cover and areas with potential targets for further investigation. Conductivity-depth sections derived from the flight

lines acquired at 20 km spacing have shown they provide enough detail to map cover thickness and basement topography.

Machine learning codes

Machine learning algorithms are computer programs that have the ability to learn and predict without being explicitly programmed (see https://en.wikipedia.org/wiki/Machine_learning). Geoscience Australia is developing a sophisticated machine learning resource called uncoverML (https://github.com/GeoscienceAustralia/uncoverml) in partnership with CSIRO Data61 (https://www.data61.csiro.au). Machine learning facilitates the integration and modelling of large and diverse geoscientific datasets (e.g. satellite imagery, geophysical data, terrain attributes, climate surfaces) to predict properties of the Australian continent including surface geochemistry and models of cover thickness. It provides new opportunities to quantitatively map the nature of the Australian regolith not previously possible. Current research involves generating national predictive models (with uncertainties) of weathering intensity, major element abundance (Si, Al, Ca, Mg, Na, K, Ti, Fe, Mn and P), cover thickness and interpreted AEM sections.

Estimates of Geological and Geophysical Surfaces database

Geoscience Australia is developing databases, methodologies and predictive models mentioned above to facilitate more effective exploration in buried landscapes to better understand the nature of the cover. We aim to generate 3-dimensional surfaces of the depths to major chronostratigraphic interfaces including the bases of Cenozoic, Mesozoic, Palaeozoic and Proterozoic packages. Drilling provides the most reliable source of depth information. Geophysical depth estimates derived from, for example, depth to magnetic basement techniques and seismic reflection profiles also provide important constraints on cover thickness. These point measurements are stored in a new national database, the Estimates of Geological and Geophysical Surfaces (EGGS). Depth information centrally stored in EGGS will be used to underpin the generation of chronostratigraphic depth surfaces using point interpolation methods such as kriging or machine learning that establishes predictive relationships between the depth estimates and other geological or geophysical information (e.g. distance from outcrop, gravity).

Groundwater

In northern Australia, groundwater resources and water banking/aquifer storage provide significant opportunity to underpin economic expansion due to the limitations posed by the seasonal nature of surface water, the limited availability of surface dam sites, and high evaporation rates that rapidly deplete surface storages. However, there are major gaps in our knowledge of groundwater systems and resources in northern Australia. The groundwater component of the EFTF program will therefore focus on addressing these knowledge gaps, to underpin future opportunities for irrigated agriculture, mineral and energy development, and community water supply. The program will comprise both targeted regional investigations and analysis of groundwater prospectivity more broadly across northern Australia. Five regional areas have been selected for new targeted geoscience studies in East Kimberley, Northern Stuart Corridor (Howard East and Daly River Basin), Southern Stuart Corridor (Tennant Creek to Alice Springs), Upper Burdekin, and the Surat and Galilee basins. The groundwater investigations will involve the collection, interpretation and delivery of a range of new pre-competitive hydrogeological, geophysical, geospatial and remote sensing datasets to map the near-surface geology and groundwater systems in selected regions, as well as assessing any potential salinity hazards potentially associated with resource development. Geoscience Australia is working with a range of stakeholders, including state and territory government agencies, local councils, pastoral leaseholders, local indigenous groups, and Land Councils to deliver the program.

Acknowledgements

This paper is published with the permission of the CEO, Geoscience Australia. The authors gratefully acknowledge the staff input and resources of the state and territory agencies involved in the various programs including the Geological Survey of Victoria, Geological Survey of South Australia, Geological Survey of Queensland, Northern Territory Geological Survey, and Geological Survey of Western Australia.

References

Australian Academy of Science, 2012. Searching the Deep Earth.
Retrieved from: http://www.science.org.au/sites/default/files/user-content/searchingthedeepearth.pdf.

COAG, 2012. Council of Australian Governments National Mineral Exploration Strategy.
Retrieved from https://scer.govspace.gov.au/files/2012/12/National-Mineral-Exploration-Strategy.pdf.

POSTER ABSTRACTS

Establishment of geochemical exploration criteria in mineral phases within basement and cover sequences

A. Brotodewo[1, 2], C. Tiddy[1], D. Giles[1], A. Fabris[3] and D. Plavsa[1]

[1]Future Industries Institute, University of South Australia, Mawson Lakes Campus, Mawson Lakes, 5095
[2]School of Natural and Built Environments, University of South Australia
[3]Geological Survey of South Australia, 101 Grenfell St, Adelaide SA 5005

With the increase in population, technology and rising standards of living, an increase in deposit discovery is necessary to meet growing global metal demand. The challenge for mineral exploration companies is therefore to discover new large (Tier 1 or Tier 2) mineral deposits. However, this challenge is amplified by decreasing rates of deposit discovery as the exploration frontier is moving to progressively deeper terranes at increased cost and risk. The development of new technologies and exploration techniques is therefore becoming a necessity in decreasing exploration risk and increasing discovery rates.

Many mineral exploration programs use geophysical techniques to target areas at the surface or buried by thin/shallow cover, but are dampened when applied to areas with a thick cover (De Cartitat et al., 2016). This is challenging as the majority of the mineralised basement rocks in South Australia are overlain by a sedimentary cover sequence that can range from centimetres to several hundred metres depth. Consequently, there has been a shift towards understanding how the cover can be used to maximise the recognisable footprint of mineral deposits through understanding geochemical signatures related to mineral deposits and how they may be transported into the overlying sedimentary cover (e.g. Forbes et al., 2015; De Cartitat et al., 2016).

Geochemical signals related to underlying mineralisation have been recognised within cover sequence materials (e.g. Forbes et al. 2015). However, our understanding of where pathfinder elements related to mineral systems reside is limited. For instance, they may be incorporated into the lattice of specific minerals (e.g. Ce and La in monazite: Forbes et al. 2015; Se, Cu, Bi, Ni in pyrite: Belousov et al. 2016), or they may be adsorbed to clays (e.g. Öhlander et al. 1996). Resistate mineral phases (e.g. zircon, monazite) that may host pathfinder elements related to old mineralising systems are particularly useful targets in exploration as they may undergo minimal alteration during weathering and transport processes. This has the potential to allow dispersion of geochemical signatures related to a mineralising system throughout cover sequence materials that overlie the mineralising system.

This project aims to develop geochemical criteria for exploration using zircon in potentially mineralised basement rock packages and overlying sedimentary cover. The project will investigate the broad differences in zircon chemistry across hydrothermal, igneous and metamorphic environments through mapping out distinct textural and chemical characteristics. This information will then be used to identify geochemical anomalies in zircon grains over selected mineral deposit case study areas. Focus will be placed on mapping the geochemical footprint of zircon within the basement rocks that host mineralisation, and how this signature may be translated into overlying, younger cover sequence materials. This will be combined with assessment of the palaeogeography and landscape processes active at the time of deposition of sedimentary cover to understand the potential effect of weathering and transport. A final synthesis will lead to the establishment of an exploration criteria using the zircon chemistry , which would be applicable within basement and cover sequences to target deeper exploration in South Australia.

References

Belousov I., Large R.R., Meffre S., Danyushevsky L.V., Steadman J. and Beardsmore T., 2016 'Pyrite compositions from VHMS and orogenic Au deposits in the Yilgarn Craton, Western Australia: Implications for gold and copper exploration' *Ore Geology Reviews,* 79, pp. 474-499.

De Caritat P., Main P.T., Grunsky E.C. and Mann A.W. 2016, 'Recognition of geochemical footprints of mineral systems in the regolith at regional to continental scales' *Australian Journal of Earth Sciences*, pp. 1-11.

Forbes C., Giles D., Freeman H., Sawyer M. and Normington V., 2015, 'Glacial dispersion of hydrothermal monazite in the Prominent Hill deposit: An exploration tool' *Journal of Geochemical Exploration,* vol. 156, pp. 10-33.

Öhlander B., Land M., Ingri J. and Widerlund A. 1996, 'Mobility of rare earth elements during weathering of till in northern Sweden', *Applied Geochemistry,* 11(1), pp. 93-99.

G-FLOWS – Hidden water, innovation exploration

A. Costar and M. Keppel

Groundwater Team, Water Science & Monitoring Branch Science & Information Group
Department of Environment, Water & Natural Resources, South Australia

The Goyder Institute for Water Research's Finding Long-term Outback Water Solutions (G-FLOWS) research project will develop new techniques to interpret airborne geophysical electromagnetic (AEM) data to identify groundwater resources buried by deep sediments, which is a constraint to identifying water sources in the northern parts of South Australia, which also impedes mineral discovery.

The G-FLOWS Stage 3 project is a partnership between the SA Department of Environment, Water and Natural Resources (DEWNR), CSIRO, Flinders University of SA with in-kind support from the Geological Survey of SA. The project is utilising new AEM data collected in late 2016 under the PACE program (co-funded by DEWNR) to undertake a targeted program of data acquisition, interpretation and mapping of groundwater resources in the Musgrave geological Province (Musgrave Province) located in the in the Anangu Pitjantjatjara Yankunytjatjara (APY) Lands. The research is applying the new and innovative geophysical techniques developed in previous G-FLOWS Stage 1 and 2 projects combined with field evaluation techniques to map the groundwater resources.

Stage 3 will undertake a targeted program of data acquisition, interpretation and mapping of groundwater resources in the Musgrave Province that will specifically:

1. Extend the AEM geophysical interpretation process by establishing a hydrogeological control test site (in the vicinity of the Kaltjiti (Fregon) community) which is expected to reduce uncertainty in using AEM data to identify potential groundwater resource in the palaeovalley system, and
2. Characterise the groundwater resources, including the potential water in storage in the systems and their capacity to provide viable water supplies.

Completion of the project will result in an improved understanding of the groundwater resource potential in remote, data poor areas of South Australia (such as the APY Lands). The project will validate, refine and improve on geophysical interpretation techniques for groundwater hydrology with integrated hydrogeophysical conceptualisation, characterisation and modelling.

Importantly G-FLOWS Stage 3 will place an emphasis on collaboration and information sharing with the APY Lands community.

Granite joints and granite regolith

T. Eggleton[1] and C. Foudoulis[2]

[1]Research School of Earth Sciences, ANU, Canberra ACT
[2]Waniassa, ACT

It is well known that granitic regolith develops as water and organisms initially penetrate the granite along joints. Since Linton's 1955 study of the Dartmoor granite it has been accepted that more closely spaced joints allow greater access to the regolith profile, which leads to enhanced weathering and ultimately to relatively more erosion than occurs where the joints are more widely spaced, leading to a hill and valley topography (Fig. 1, from Linton 1955).

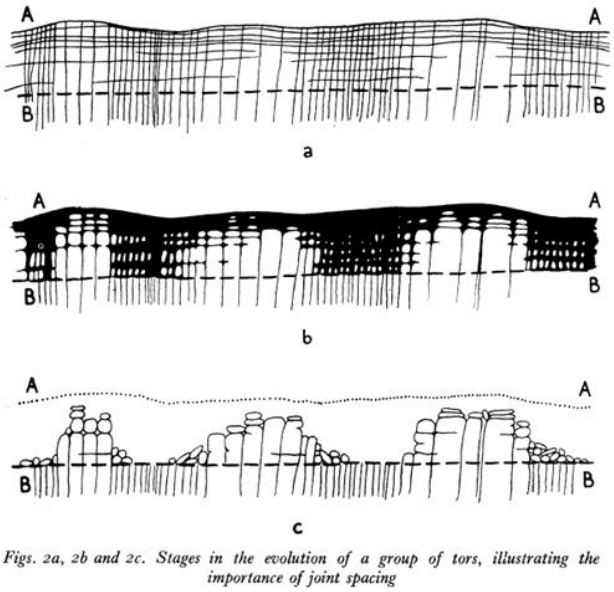

Figs. 2a, 2b and 2c. Stages in the evolution of a group of tors, illustrating the importance of joint spacing

Figure 1: How joint spacing in granites controls topography. From Linton (1955).

The aim of our study is to assess the Linton hypothesis across the granites of the southern Lachlan Fold Belt. To do this we need answers to a series of questions.

Q: What is a joint in granite? A. A fracture dividing the rock into two sections, generally planar and with no evidence of lateral displacement.
Q: Is any crack a joint? A: In the strict sense, yes. However it is commonly seen that joints in granites occur in roughly orthogonal sets dividing the rock into rectangular boulders, and that individual joint planes extend across several rows of jointed boulders. We have restricted our definition to penetrative joints extending across at least two rows of jointed boulders and having a common strike.
Q: What does "joint spacing" mean? A: The average of the distance between adjacent joints.
Q: How is joint spacing measured? A: By measuring all such spacings along a series of transects and constructing a frequency distribution.
Q: Is there one characteristic joint spacing for a pluton: A: Yet to be determined but early results suggest "No".
Q: Does joint spacing vary from place to place across a pluton? A: Yet to be determined but early results suggest "Yes".
Q: If there is a characteristic value within an area, what determines that value? A: Yet to be determined but grain size seems to be a factor.
Q: Why should joint spacing be worth measuring: A: The geomorphologically received wisdom is that joint spacing affects weathering extent and hence erosion rate and so modifies the topography of the granite. Joint spacing is just one of several factors thought to affect granite weathering and erosion and so in any study of granite geomorphology it needs to be evaluated as much as the other factors such as composition, grain size and foliation. Observations of joints in granites from

southeastern New South Wales and of those on Magnetic and Montague Islands allow us to explore the Linton hypothesis.

Firstly we find evidence that joint spacing in the Buckley's Lake Adamellite varies with the size of the K-feldspar phenocrysts (Fig. 2), which themselves vary linearly with average grain-size of the rock. Hence joint spacing does vary across this pluton.

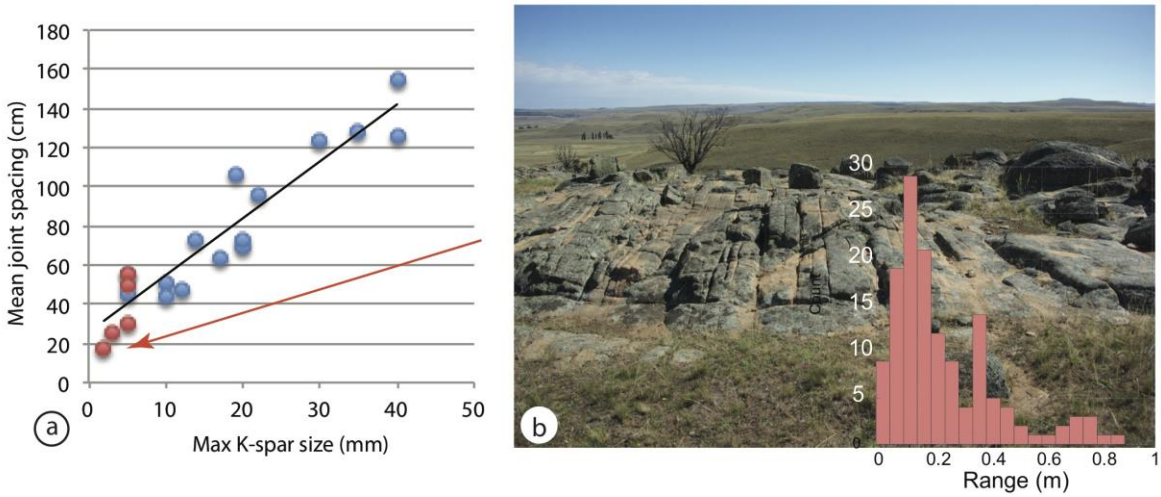

Figure 2: a) Relation between grain-size and joint spacing in the Buckley's Lake Adamellite. b) Closely spaced joints (17 cm average) in fine-grained adamellite, histogram inset. Red spots in a) are from a part of the pluton shown in b) mapped as Buckley's Lake but of much finer grain-size than the majority of the pluton.

Secondly we find that in many places (Fig. 3) outcrops of unjointed granite lie beside patches of closely jointed granite with no change in topographic position.

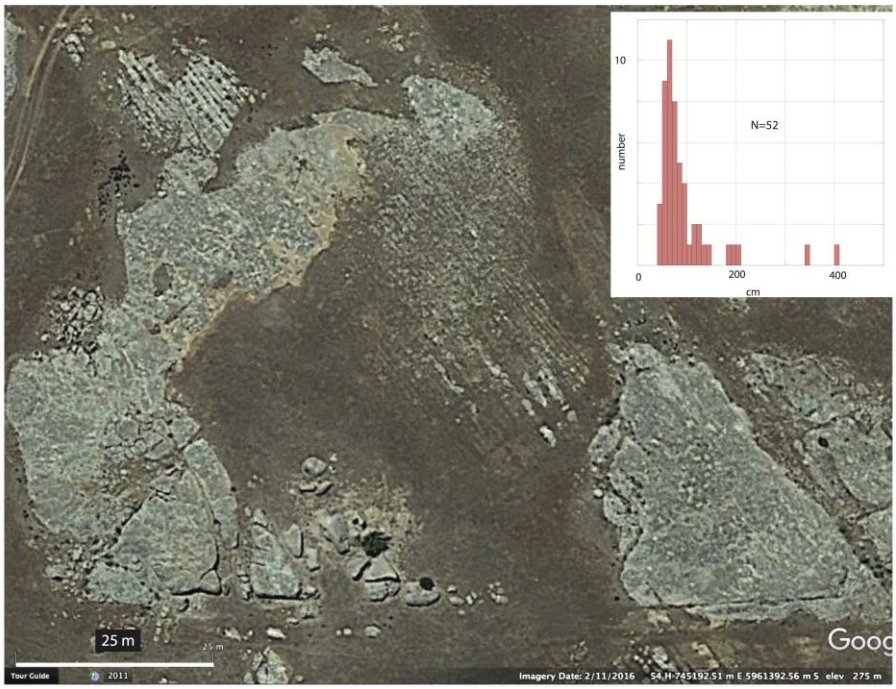

Figure 3: Wedderburn Granodiorite hillcrest showing both parallel finely jointed and unjointed expanses of granite. The finely jointed granite in the centre is in a small depression, the unjointed patch at the left is on the flank of the ridge, total relief across the image is 4 m. Histogram of joint spacing inset is taken from the closely spaced joints centre and upper left; mode at 80 cm. GR 745200E, 5169400N. Image Google Earth, 30 cm resolution.

Thirdly we observe that more widely spaced joints are common on steeper slopes as well as hill tops, and that closely spaced joints are not uncommon on ridge crests (Fig. 4).

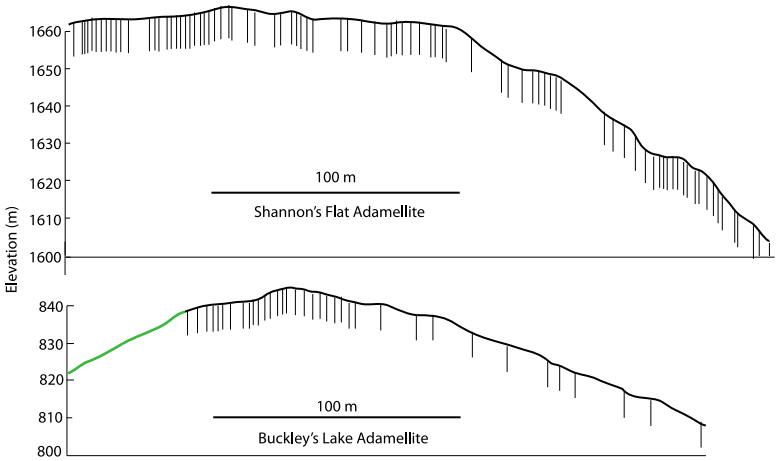

Figure 4: Positions of joints shown as short lines along a transect across two ridges of plutons. Note wide spacings on some steeper slopes, close spacings on crests and slopes. Green line no outcrop. Joints taken from Google Earth images at 1 m resolution.

Fourthly we note that at the margins of the plutonic intrusions of Magnetic and Montague Island the joints are closely spaced whereas on the slopes and crests of the islands the joint spacing is very wide (Fig. 5). This pattern continues all around both islands and also around other granites such as Gabo Island. We think it unlikely that oceanic erosion has acted preferentially on primary peripheral closely space joints, but been defeated by the parts of the islands where the joints are widely spaced or that these islands all had a ring of closely spaced joints just at the level of the latest Holocene sea-level rise.

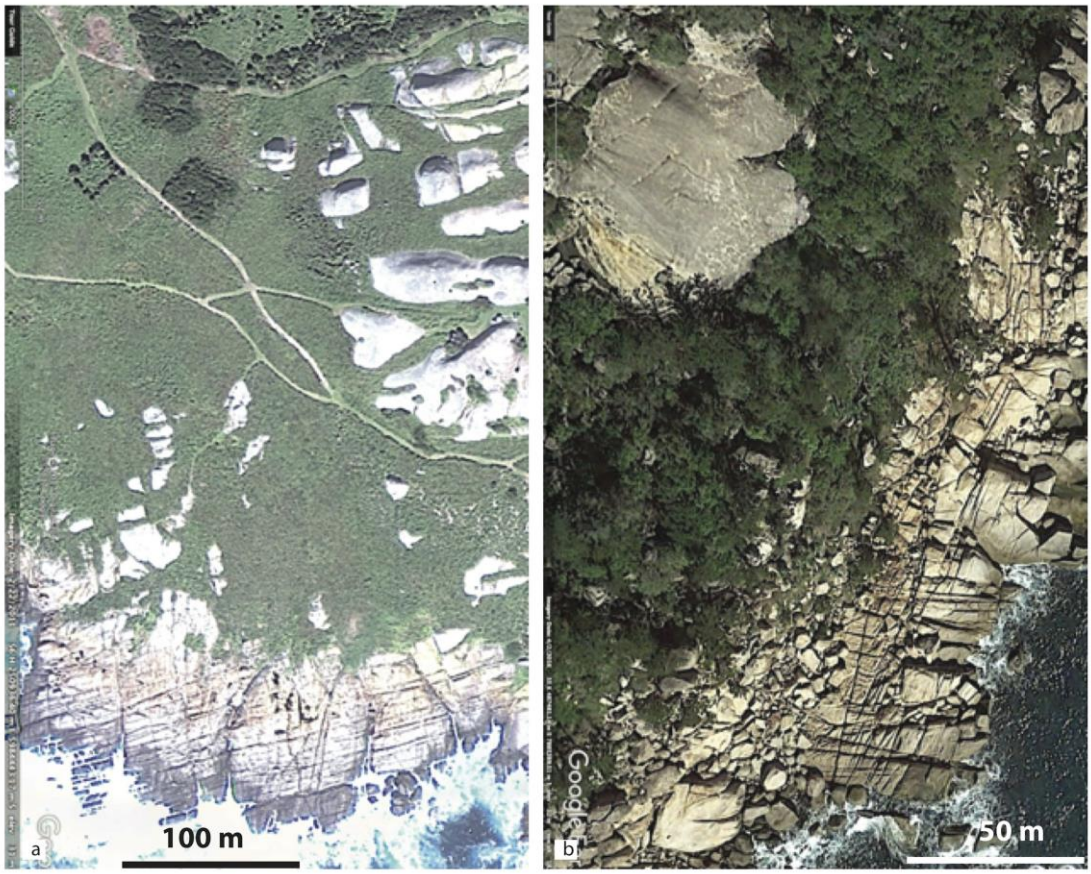

Figure 5a: Barunguba (Montague Island) Syenite, NSW and b: Magnetic Island Granite, Queensland, showing widely jointed rock above the shore-line and closely jointed rock at the shore-line. Google Earth images.

Fifthly, we see that in very local settings, sloping outcrops are relatively joint free compared to adjacent flatter or concave outcrop (Figs 3 and 6).

Figure 6: Joints in the Buckley's Lake Granodiorite. Spacings are wider at left where the water sheds, closer at the right where the ground remains saturated longer. Black-marked scale length 1 m.

These observations lead us to conclude that the Linton hypothesis is inverted. Micro-cracks (incipient-, or proto-joints) having developed from unloading, only become visible when they are sufficiently weathered. Below, the regolith joints are not observed (Fig. 7).

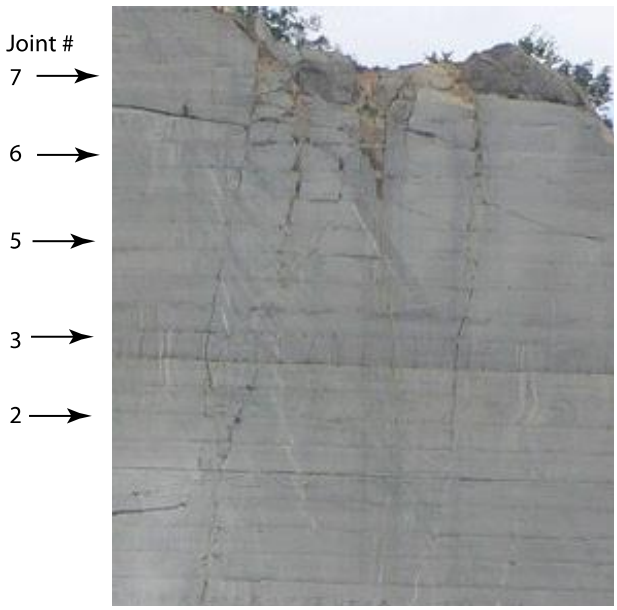

Figure 7: Joints in a Chinese monzonite quarry and the number of discernable vertical joints at several levels shown by the arrows. Note that the number of open joints decreases with depth, evidence that the joints at depth are not open pathways ready to admit water. Horizontal lines are quarry bench levels. Photo Hans Hensel.

Permanently water saturated regions such as valleys or seashores, allow constant access to weathering solutions and biota, increasing the probability that an incipient joint will become invaded. Thus the association of close joint spacing with valleys is a *consequence* of weathering and erosion, not a *cause*.

Reference

Linton D.L. 1955. The problem of tors. *The Geographical Journal* **121(4)**, 470-487.

Author Index

Baudet	E.	5	Klump	J.	1, 48
Bourman	R.P.	37	Krapf	C.B.E.	12, 35
Brønner	M.	1	Ley-Cooper	Y.	56
Brotodewo	A.	5, 58	Love	A.	22
Chivas	A.R.	37	McGuirk	S.L.	52
Clarke	J.D.A.	52	McPherson	A.A.	56
Costar	A.	59	McQueen	K.G.	7
Cowood	A.	21	Moore	L.	21
Custance	K.M.	5	Normington	V.	5
Czarnota	K.	56	Pernreiter	S.	1, 48
de Souza Kovacs	N.	27	Petts	A.E.	12
Eggleton	A.	39, 60	Pillans	B.	23
Fabris	A.J.	15, 58	Plavsa	B.	5, 58
Fogarty	P.	31	Post	V.	22
Freundenberger	D.	31	Raven	M.D.	43
Foudoulis	C.	60	Roach	I.C.	16, 56
Gibson	R.	31	Self	P.G.	43
Giles	D.	5, 58	Smith	G.	1, 48
González-Álvarez	I.	1, 48	Strong	C.	31
Greene	R.	31	Tiddy	C.J.	5, 58
Hill	S.	5	van der Hoek	B.	5
Hill	R.L.	5	Wilford	J.R.	56
Ibrahimi	T.	1, 48	Wolff	K.	5
Jackia	S.	17	Worrall	L.	47
Keeling	J.L.	43	Zwingmann	H.	43
Keppel	M.	22, 59			
King	A.R.	1			